JOURNAL OF MATHEMATICAL SCIENCES AND MODELLING

ISSN: 2636-8692

VOLUME VII
ISSUE III

VOLUME VII ISSUE III
ISSN 2636-8692

December 2024
http://dergipark.gov.tr/jmsm

JOURNAL OF MATHEMATICAL SCIENCES AND MODELLING

Language Editor

Technical Editor

Contents

Research Article

Journal of Mathematical Sciences and Modelling, 7(3) (2024) 112-120
Research Article

Journal of Mathematical Sciences and Modelling

Journal Homepage: www.dergipark.gov.tr/jmsm
ISSN: 2636-8692
DOI: https://doi.org/10.33187/jmsm.1475322

Radius Model for Some Cells in Human Body on Multiplicative Calculus

Zeynep Altay[1], Emrah Yılmaz[2*], Meryem Uşen[1] and Fadime Demirbağ[1]

[1]*Fırat University, Graduate School of Natural and Applied Sciences, Mathematics, 23200, Elazığ, Türkiye*
[2]*Fırat University, Department of Mathematics, Faculty of Science, 23200, Elazığ, Türkiye*
[*]*Corresponding author*

Article Info

Keywords: *Cell, Multiplicative Analysis*
2010 AMS: *11N05, 92C37*
Received: *29 April 202*
Accepted: *7 December 2024*
Available online: *17 December 2024*

Abstract

The cell is the basic structure and process unit that carries all the living characteristics of a living thing and has the ability to survive on its own under suitable conditions. The relationship of cell size with nutrient absorption and nutrient consumption in the cell membrane has been examined with the current model using the theory of differential equations in classical analysis. During these examinations, the cell considered was assumed to be spherical. In fact, the shapes of cells vary depending on their functional properties. Many have long appendages, cylindrical parts or branch-like structures. However, in this study, a simple global cell will be discussed, leaving all these complex situations aside. In the current model, the relationship between the change in the radius of the cell and the nutrient absorption and consumption in the cell membrane is detailed using classical differential equations. The answer to the question for which cell size is the consumption rate exactly balanced with the absorption rate was found in classical analysis. The current model consists of first-order differential equations. In this model, the dependent variables are the radius of the cell and the mass of the cell. The classical solutions of these models will be examined, the size of the cell and the cell membrane relationship will be examined, and details will be given with numerical examples. However, in order to consider this biological phenomenon from different perspectives and compare the results, the relevant event will be modeled using multiplicative analysis, one of the Non-Newtonian analyses. The new models will be solved using multiplicative analysis techniques, and the results will be compared with classical analysis. With this new model, it is planned to clarify the results obtained in the classical case, to reveal more clearly the relationship between the size of the cell and nutrient absorption and consumption in the cell membrane, and to obtain important results.

1. Introduction

A spherical cell absorbs nutrients at a rate proportional to its surface area S, but consumes nutrients at a rate proportional to its volume V (Figure 1.1). Some constants and their equivalents that will appear in the cell model to be established are as follows.

***Email addresses and ORCID numbers*: zeynepalty2@gmail.com, 0009-0007-5053-6240 (Z. Altay), emrah231983@gmail.com, 0000-0002-7822-9193 (E. Yılmaz), musenmeryem@gmail.com, 0009-0001-9426-6779 (M. Uşen), fadimea1453@gmail.com, 0009-0005-8137-6257 (F. Demirbağ),**
Cite as "Z. Altay, E. Yılmaz, M. Uşen, F. Demirbağ, *Radius Model for Some Cells in Human Body on Multiplicative Calculus*, J. Math. Sci. Model., 7(3) (2024), 112-120"

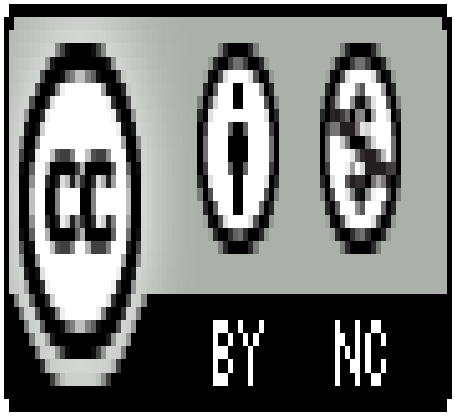

Figure 1.1: Arbitrary Spherical Cell

A: Net absorption rate of nutrients per unit time,
C: Net rate of consumption of nutrients per unit time,
V: Volume of the cell,
S: Surface area of the cell,
r: Radius of the cell,
In this study, the change of four cell models radii with respect to time was analyzed in classical and multiplicative analyses and each case was numerically examined and comparisons were made. To establish model, following assumptions are considered [1–10].
1. The cell is roughly spherical.
2. The cell absorbs oxygen and nutrients from its surface. The larger the surface area S, the faster the overall absorption rate. The rate of absorption of nutrients (or oxygen) is assumed to be proportional to the surface area of the cell.
3. The rate at which nutrients are consumed (i.e. depleted) in metabolism is proportional to the volume V of the cell. The larger the volume, the more nutrients are needed to keep the cell alive.
Now let's restate the assumptions mathematically. According to second assumption, the absorption rate A is proportional to S. This means:

$$A = k_1 S,$$

where k_1 is proportional constant. Since absorbance and surface area are positive quantities, only positive values of the proportionality constant are significant, so k_1 must be positive (This is consistent with multiplicative analysis). The value of this constant depends on its properties, such as the permeability of the cell membrane or how many pores it contains to allow the passage of nutrients. By using a general constant called a parameter to represent this proportionality constant, the model is kept general enough to apply to many different cell types. According to third assumption, the rate of food consumption, C is proportional to V:

$$C = k_2 V,$$

where k_2 is positive proportional constant. k_2 depends on cell metabolism, that is, how fast it consumes nutrients while performing its activities. According to first assumption, the cell is spherical, so

$$S = 4\pi r^2, \quad V = \frac{4}{3}\pi r^3,$$

where S is surface area and V is its volume. Putting these rationales together gives the following relationships between nutrient absorption A, consumption C, and cell radius r:

$$\begin{aligned} A(r) &= (4\pi k_1) r^2, \\ C(r) &= \left(\frac{4}{3}\pi k_2\right) r^3. \end{aligned}$$

These equations will contribute to seeing how nutrient balance depends on cell size. Here, functions A and C are second and third degree polynomial functions, respectively, depending on the radius of the cell. Nutrient balance depends on the radius of a cell. First, the answer to the question of whether nutrient absorption or nutrient consumption is more effective for small, medium or large cells will be sought [11]. The problem expressed in the following classical case is the problem on which we base our study and make comparisons.

Motivation question: For what cell size is the consumption rate exactly balanced by the absorption rate? What ratio (consumption or absorption) dominates for small or large cells?
If the consumption rate for the cell is in equilibrium with the absorption rate, it yields

$$A(r) = C(r).$$

Then,

$$(4\pi k_1) r^2 = \left(\frac{4}{3}\pi k_2\right) r^3.$$

$r = 0$ is trivial solution of this equation. This is not biologically meaningful anyway. Non-trivial solutions are required for this study. From the above relation, we get

$$r = \frac{3k_1}{k_2},$$

where $r \neq 0$. This means that the rates of absorption and consumption are equal for cells of this size. For small r values, $C(r)$ dominates. Thus, absorption dominates for smaller cells, while consumption dominates for larger cells. From here, cells larger than the critical size $r = \frac{3k_1}{k_2}$ cannot meet the nutrient demand and the cell dies because consumption cannot meet nutrient absorption [1–8].
Using the simple geometric argument above, it can be concluded that cell size has strong effects on its ability to absorb nutrients or oxygen fast enough to feed itself. If a cell absorbs nutrients faster than the food consumed $(A > C)$, some of the excess nutrients accumulate and this accumulation of nutrient mass can be converted into cell mass. This can cause growth (increase in cell mass).
Conversely, if the rate of consumption exceeds the rate of absorption of nutrients, $C > A$, the cell has a metabolic "fuel" shortage and must convert some of its own mass into energy reserves that can power its metabolism, resulting in a loss of cell mass. We can track such changes in cell mass using a simple "equilibrium equation" using differential equations in classical analysis. The equilibrium equation is the difference between the rate of change of cell mass (A) incoming nutrient (mass) ratio (C);

$$\frac{dm}{dt} = A - C, \tag{1.1}$$

Each term in this equation must have the same units of nutrient mass per unit time. A is a depletion rate that contributes positively to mass gain, while C is a depletion rate that negatively contributes to mass gain. This is already the basic logic in the creation of the model. If we consider the expressions

$$A = k_1 S, \quad C = k_2 V, \quad m = pV$$

in (1.1), we get

$$\frac{d(pV)}{dt} = k_1 S - k_2 V, \tag{1.2}$$

where S is surface area, V is volume and p is density of the cell. The above equation is quite general and does not depend on the cell shape. Let us now consider the special case of a cell being spherical. Eq. (1.1) will be converted into an equation showing the variation of the cell radius with time where

$$S = 4\pi r^2, \quad V = 4/3\pi r^3.$$

By (1.2) and after some adjustments and implementation of chain rule, we get

$$\frac{dr}{dt} = \frac{1}{p}\left(k_1 - \frac{k_2}{3}r\right). \tag{1.3}$$

With an explanation of how the cell mass changes, a result estimate of the rate of change of the cell radius is reached. This was done using classical analysis methods. The resulting equation is a differential equation that tells us about a growing cell. This model will be used as a tool to understand how it predicts the dynamics of cells with different initial sizes. The differential equation (1.3) is a linear differential equation. The general solution of this equation is given below as a preliminary conclusion for the study. Eq. (1.3) will be solved in the classical case by the method of variation of parameters. If this equation is adapted to the solution and some adjustments are made, we get

$$r(t) = \frac{3k_1}{k_2} + ke^{-\frac{k_2 t}{3p}}, \tag{1.4}$$

where k is an arbitrary constant. Using this solution, the variation of the radius of the cell with time can be obtained for different times [1]. Some considerations will be made on two problems involving stomach and blood cells.
Let's express some information about stomach cell, which we will examine on the first example.

Example 1.1 (Stomach Cell-Usual Case, [1–8])**.** *The stomach is a muscular, expandable digestive system organ. A healthy stomach cell radius value is approximately between* $10 - 30\mu m$ *and the cell density is* $p = 1.04gr/(cm)^3$ *. Based on this information, let's analyze the cell radius variation for classical model. Let's fix the cell radius at* $r(t) = 20\mu m$*. If we consider the initial condition* $r(0) = 20\mu m$ *in general solution (1.4), we get*

$$r(t) = \frac{3k_1}{k_2} + \left(20 - \frac{3k_1}{k_2}\right)e^{-\frac{k_2 t}{3(1,06)}},$$

and

$$\frac{k_1}{k_2} \cong 6.6.$$

This value is the equilibrium state. Now let's observe the change in the cell by changing this ratio. Since $r(0) = 20$ *for* $\frac{k_1}{k_2} \cong 6.6$*, it can be said that the balance situation continues. Now let's observe the state of the cell for different values of the ratio by changing the variable t for* $k_2 = 10$ *in Table 1.1.*

$\frac{k_1}{k_2}$	$r(0)$	$r(1)$	$r(2)$	$r(3)$	$r(4)$	...	$r(10)$
6,6	20	19.8081	19.8003	19.8000	19.800	...	19.800
6,5	20	19.5081	19.5003	19.5000	19.5000	...	19.5000
6,4	20	19.2081	19.2003	19.2000	19.2000	...	19.2000
6,3	20	18.9081	18.9003	18.9000	18.9000	...	18.9000
6,2	20	18.6081	18.6003	18.6000	18.6000	...	18.6000
6,1	20	18.3081	18.3003	18.3000	18.3000	...	18.3000
6,0	20	18.0081	18.0003	18.0000	18.0000	...	18.0000

Table 1.1: Change of stomach cell radius over time according to the change

In equilibrium, it can be easily seen that

$$r(5) = r(6) = r(7) = r(8) = r(9) = 19.800.$$

As can be seen in this example, for $\frac{k_1}{k_2} = 6.6$*, there is a 1% decrease, which is the most stable condition. For* $\frac{k_1}{k_2} = 6.3 - 6.4$*, there is a* $4 - 5.5\%$ *decrease, which is within normal limits. For* $\frac{k_1}{k_2} = 6.0 - 6.1$*, there is a* $8.5 - 10\%$ *decrease, which is the condition that should be monitored.*

Example 1.2 (Blood Cell-Usual Case, [1–8])**.** *Eristocytes, or red blood cells, are the main oxygen-carrying components of blood. Red blood cells are small* $(3.5\mu m)$*, round cells shaped in cross section as two concave discs. Let's examine the cell radius situation in general solution (1.4) according to these values. Dense of a blood cell is* $p = 1,10gr/cm^3$ *. The equilibrium state for this cell is*

$$\frac{k_1}{k_2} = 1.17,$$

for

$$r(t) = \frac{3k_1}{k_2} + \left(3.5 - \frac{3k_1}{k_2}\right)e^{-\frac{k_2 t}{3p}},$$

where $r(0) = 3.5$ *for* $k_2 = 10$*. Now let's observe the change in the blood cell by changing this ratio for* $p = 1,10gr/cm^3$ *by Table 1.2.*

$\frac{k_1}{k_2}$	$r(0)$	$r(1)$	$r(2)$	$r(3)$	$r(4)$	...	$r(10)$
1.17	3.5000	3.5096	3.5112	3.5116	3.5117	...	3.5117
1,16	3.5000	3.4796	3.4812	3.4816	3.4817	...	3.4817
1,15	3.5000	3.4496	3.4512	3.4516	3.4517	...	3.4517
1,14	3.5000	3.4196	3.4212	3.4216	3.4217	...	3.4217
1,13	3.5000	3.3896	3.3912	3.3916	3.3917	...	3.3917
1,12	3.5000	3.3596	3.3612	3.3616	3.3617	...	3.3617
1,11	3.5000	3.3296	3.3312	3.3316	3.3317	...	3.3317

Table 1.2: Change of blood cell radius over time according to the change

In equilibrium, it can be easily seen that

$$r(5) = r(6) = r(7) = r(8) = r(9) = 3.5117.$$

As can be seen in this example, for $\frac{k_1}{k_2} > 1.17$ *the cell expands and for* $\frac{k_1}{k_2} < 1.17$ *the cell shrinks. The changes are gradual and controlled and the final values are within physiological limits. The main changes occur in the first 3 hours. After the 4th hour, complete stability occurs.*

Example 1.3 (Brain Cell-Usual Case, [1–8])**.** *The brain cell is known as a neuron. The average radius of a healthy brain cell is* $r(t) = 10\mu m$ *and its density is* $p = 1.03gr/cm^3$ *. The equilibrium state for this cell is*

$$\frac{k_1}{k_2} = 3.3,$$

for

$$r(t) = \frac{3k_1}{k_2} + (10 - \frac{3k_1}{k_2})e^{-\frac{k_2 t}{3p}},$$

where $r(0) = 10$ *for* $k_2 = 10$*. Now let's observe the change in the blood cell by changing this ratio for* $p = 1,03gr/cm^3$ *by Table 1.3.*

$\frac{k_1}{k_2}$	$r(0)$	$r(1)$	$r(2)$	$r(3)$	$r(4)$	...	$r(10)$
3.3	10.0000	9.9039	9.9004	9.9001	9.9000	...	9.9000
3.2	10.0000	9.6039	9.6004	9.6001	9.6000	...	9.6000
3.1	10.0000	9.3039	9.3004	9.3001	9.3000	...	9.3000
3.0	10.0000	9.0039	9.004	9.0001	9.0000	...	9.0000
2.9	10.0000	8.7039	8.7004	8.7001	8.7000	...	8.7000
2.8	10.0000	8.4039	8.4004	8.4001	8.4000	...	8.4000
2.7	10.0000	8.1039	8.1004	8.1001	8.1000	...	8.1000

Table 1.3: Change of brain cell radius over time according to the change

In equilibrium, it can be easily seen that

$$r(5) = r(6) = r(7) = r(8) = r(9) = 9.9000.$$

As can be seen in this example, for $k_1/k_2 \geq 3.2$, there is less than 4% change in size and normal neuronal function is preserved. For $3.0 \leq k_1/k_2 < 3.1$, there is a $7-10\%$ change in size and functional changes may occur. For $k_1/k_2 \leq 2.9$, there is a 13% change in size and neuronal function is at risk.

Example 1.4 (Liver Cell-Usual Case, [1–8]). *Liver cells (hepatocytes) are the basic functional units of the liver. They are large cells with a polygonal shape, usually 25 micrometers in diameter. Their density is approximately $p = 1,09gr/cm^3$. These cells perform vital functions such as protein synthesis, detoxification of toxins, bile production, and glycogen storage. The equilibrium state for this cell is*

$$\frac{k_1}{k_2} = 8.3,$$

for

$$r(t) = \frac{3k_1}{k_2} + \left(25 - \frac{3k_1}{k_2}\right) e^{-\frac{k_2 t}{3p}}$$

where $r(0) = 25$ for $k_2 = 10$. Now let's observe the change in the blood cell by changing this ratio for $p = 1,09gr/cm^3$ by Table 1.4.

$\frac{k_1}{k_2}$	$r(0)$	$r(1)$	$r(2)$	$r(3)$	$r(4)$	...	$r(10)$
8.3	25.0000	24.3752	24.0282	23.8162	23.6799	...	23.4270
8.2	25.0000	24.0752	23.7282	23.5162	23.3799	...	23.1270
8.1	25.0000	23.7752	23.4282	23.2162	23.0799	...	22.8270
8.0	25.0000	23.4752	23.1282	22.9162	22.7799	...	22.5270
7.9	25.0000	23.1752	22.8282	22.6162	22.4799	...	22.2270
7.8	25.0000	22.8752	22.5282	22.3162	22.1799	...	21.9270
7.7	25.0000	22.5752	22.2282	21.0162	21.8799	...	21.6270

Table 1.4: Change of liver cell radius over time according to the change

In equilibrium, it can be easily seen that

$$r(5) = 23.5901, r(6) = 23.5294, r(7) = 23.4881, r(8) = 23.4599, r(9) = 23.4405.$$

As can be seen in this example, for $k_1/k_2 \geq 8.1$, there is less than 8% change in size and normal hepatocyte function is preserved. For $7.9 \leq k_1/k_2 \leq 8.0$, there is a 9-10% change in size and regular monitoring is required. For $k_1/k_2 \leq 7.8$, there is a risk because there is more than 12% change in size and close monitoring is required.

Remark 1.5. *There is no particular reason to examine only the stomach, blood, brain and liver cells here. The changes of four cells radii in both classical and multiplicative analysis will be examined.*
In the next section, we will examine the cell radius models on multiplicative analysis. For this reason, it would be useful to explain the multiplicative analysis in general terms in this section.
The classical analysis most commonly used today was founded by Gottfried Leibnitz and Isaac Newton in the second half of the 17th century. Since the basic operation in this analysis is addition, it is called additive (classical) analysis or Newtonian analysis. Many new types of analysis have emerged as a result of the ideas of establishing new analysis with different arithmetic operations based on classical analysis. An example of these analyzes is multiplicative analysis. This type of analysis is generally called non-Newtonian analysis in the literature. The first example of studies carried out with different arithmetic operations can be given as Volterra type analysis defined by Vito Volterra in 1887. Since this new approach is based on multiplication, it is called multiplicative analysis. The first study for Volterra type analysis was conducted by Volterra and Hostinsky in 1938 [9]. In the period from 1967 to 1970, Michael Grossman and Robert Katz gave definitions of a new type of derivative and integral, transferring the roles of subtraction and addition operations to division and multiplication operations, thus introducing a new calculus called multiplicative analysis [10, 11].
Multiplicative analysis is a field of study that can be easily used in solving many scientific problems and provides great advantages. As a result of the researches on the subject, it is seen that some problems encountered in applied sciences can be complicated to express with classical analysis. The multiplicative analysis facilitates the solution of these problems and offers a different perspective in the mathematical modeling of these problems. In this direction, multiplicative analysis emerged as an alternative to classical analysis. Many important studies have been carried out in different fields related to multiplicative analysis [12–16].

Definition 1.6. *Let $f : A \to \mathbb{R}^+$ be a positive function for all x on $A \subseteq \mathbb{R}$. The multiplicative derivative of f is defined by [17]*

$$f^*(x) = \lim_{h \to 0} \left(\frac{f(x+h)}{f(x)} \right)^{\frac{1}{h}}.$$

Theorem 1.7. *A positive function f is multiplicatively differentiable at x if and only if it is usual differentiable at that point [18]. There is a relationship between derivative in classical sense and derivative in multiplicative sense as [19],*

$$f^*(x) = e^{\frac{f'(x)}{f(x)}}.$$

Definition 1.8 ([19]). *$F:(a,b)\to\mathbb{R}$ is called multiplicative anti-derivative of $f:(a,b)\to\mathbb{R}$ where $F^*(x)=f(x)$ for each $x\in(a,b)$. Following presentation is used for this concept.*

$$\int f(x)^{dx}=F(x).$$

Remark 1.9 ([20]). *If f is positive and continuous on [a,b], it is integrable in multiplicative sense and*

$$\int_a^b f(t)^{dx}=e^{\int_a^b \ln(f(t))\,dt}.$$

Definition 1.10 ([20]). *An $n-th$ order multiplicative differential equation is defined by*

$$f(t,y,y^*,y^{(**)},\dots,y^{(*(n-1))},y^{(*n)}(t))=1,\quad (t,y)\in\mathbb{R}\times\mathbb{R}^+$$

for a positive function f.

2. Radius Analysis for Some Cells in Multiplicative Calculus

In this section, it is thought that original results will be obtained regarding the change of cell size due to different definitions of derivative, integral and differential equations in multiplicative analysis. These solutions will then be evaluated with mathematical and numerical examples. The differential equation discussed in the article proposal will be established in multiplicative analysis and will be solved using multiplicative analysis techniques. Multiplicative analysis has a very strong literature and different application areas [9–20].
In the classical case, the equation (1.4) discussed in the first section can be written as follows in multiplicative analysis;

$$r^*(t)r^{\frac{k_2}{3p}}=e^{\frac{k_1}{p}}. \tag{2.1}$$

This multiplicative equation will be solved using the method of indefinite exponents in multiplicative analysis. According to this method, the homogeneous solution of the equation is

$$r_h=e^{c_1e^{\frac{-k_2t}{3p}}},$$

where

$$r+\frac{k_2}{3p}=0\quad\to\quad r=-\frac{k_2}{3p}.$$

Let $r_p(t)=e^A$ be particular solution. If multiplicative derivative is taken for $r_p(t)$ to find the constant A and substituted in Eq. (2.1), we get

$$r^*r^{\frac{k_2}{3p}}=e^{\frac{k_2}{p}}\quad\to\quad A=\frac{3k_1}{k_2}.$$

Then, the general solution of (2.1) is

$$r(t)=e^{c_1e^{\frac{-k_2t}{3p}}}e^{\frac{3k_1}{k_2}},$$

where $r=r_hr_p$.
Now, let's examine the change in the radii of the stomach, blood, brain and liver cells using this solution in multiplicative analysis.

Example 2.1 (Stomach Cell-Multiplicative Case). *Let $r(0)=20\mu m$ and $p=1,04gr/cm^3$ for a stomach cell. We will analyse the change of radius for a stomach cell in multiplicative analysis by using the following general solution;*

$$r(t)=e^{c_1e^{\frac{-k_2t}{3p}}}e^{\frac{3k_1}{k_2}}.$$

If this solution is used, the equilibrium ratio for stomach cell is obtained as;

$$\frac{k_1}{k_2}=0.99,$$

for $r(0)=20$. Here, calculations will be made for particular selections of $k_1=99$ and $k_2=100$ in Table 2.1.

$\frac{k_1}{k_2}$	$r(0)$	$r(1)$	$r(2)$	$r(3)$	$r(4)$	...	$r(10)$
0.99	20.000	19.9967	19.9967	19.9967	19.9967	...	19.9967
0.89	20.000	19.1967	19.1867	19.1867	19.1867	...	19.1867
0.79	20.000	18.3967	18.3767	18.3767	18.3767	...	18.3767
0.69	20.000	17.5967	17.5667	17.5667	17.5667	...	17.5667
0.59	20.000	16.7967	16.7567	16.7567	16.7567	...	16.7567
0.49	20.000	15.9967	15.9467	15.9467	15.9467	...	15.9467
0.39	20.000	15.1967	15.1367	15.1367	15.1367	...	15.1367

Table 2.1: Change of stomach cell radius over time according to the change in multiplicative case

In equilibrium, it can be easily seen that

$$r(5) = r(6) = r(7) = r(8) = r(9) = 19.9967$$

According to the results obtained in the multiplicative model, There is a decrease in the first 2 hours, and a constant value is reached after the 2nd hour. There is a different balance status for each k_1/k_2 value. Health Status Assessment: $k_1/k_2 > 0.89$ is a safe status, $0.69 \leq k_1/k_2 \leq 0.89$ is a monitoring status, and $k_1/k_2 < 0.69$ is a risk status. The classical model is in normal physiological adaptation, while the multiplicative model may be an acute stress response. The classical model is in a safer range, while the multiplicative model shows riskier changes. These two models may represent the response of the stomach cell to different conditions (normal adaptation vs. severe stress).

Example 2.2 (Blood Cell-Multiplicative Case)**.** *Let $r(0) = 3.5\mu m$ and $p = 1.10 gr/cm^3$ for a blood cell. Again, we will examine cell radius change for blood cell using the solution (2.1) in the multiplicative case. If this solution is used, the equilibrium ratio for the cell is obtained as;*

$$\frac{k_1}{k_2} = 0.41,$$

for $r(0) = 3.5$. Here the calculations will be made for particular selections of $k_1 = 41$ and $k_2 = 100$. in Table 2.2.

$\frac{k_1}{k_2}$	$r(0)$	$r(1)$	$r(2)$	$r(3)$	$r(4)$	...	$r(10)$
0.41	3.5000	3.4984	3.4984	3.4984	3.4984	...	3.4984
0.36	3.5000	3.3484	3.3484	3.3484	3.3484	...	3.3484
0.31	3.5000	3.1984	3.1984	3.1984	3.1984	...	3.1984
0.26	3.5000	3.0484	3.0484	3.0484	3.0484	...	3.0484
0.21	3.5000	2.8984	2.8984	2.8984	2.8984	...	2.8984
0.16	3.5000	2.7484	2.7484	2.7484	2.7484	...	2.7484
0.11	3.5000	2.5984	2.5984	2.5984	2.5984	...	2.5984

Table 2.2: Change of blood cell radius over time according to the change in multiplicative case

In equilibrium, it can be easily seen that

$$r(5) = r(6) = r(7) = r(8) = r(9) = 3.4984.$$

Similarly, in this example, for $k_1/k_2 \geq 0.36$, there is less than 5% change in size and normal erythrocyte function is preserved. For $0.26 \leq k_1/k_2 < 0.36$, there is a 10-15% change in size and oxygen carrying capacity may be affected. For $k_1/k_2 < 0.26$, there is a change in size of more than 15%, in which case there is a risk of Hemolysis and cell function is seriously compromised.
The classical model represents normal adaptation, while the multiplicative model represents the acute stress response. The classical model appears more physiological, while the multiplicative model represents pathological conditions. These two models may represent the response of erythrocytes to different conditions (normal vs. extreme stress).

Example 2.3 (Brain Cell-Multiplicative Case)**.** *Let $r(0) = 10$ and $p = 1.03 gr/cm^3$ for a brain cell. Again, we will examine the cell radius change for the brain cell using solution (2.1) in the multiplicative case. If this solution is used, the equilibrium ratio brain the cell is obtained as;*

$$\frac{k_1}{k_2} = 0.76,$$

for $r(0) = 10$. Here the calculations will be made for particular selections of $k_1 = 76$ and $k_2 = 100$ in Table 2.3.

$\frac{k_1}{k_2}$	$r(0)$	$r(1)$	$r(2)$	$r(3)$	$r(4)$	...	$r(10)$
0.76	10.0000	9.9984	9.9984	9.9984	9.9984	...	9.9984
0.66	10.0000	9.4984	9.4984	9.4984	9.4984	...	9.4984
0.56	10.0000	8.9984	8.9984	8.9984	8.9984	...	8.9984
0.46	10.0000	8.4984	8.4984	8.4984	8.4984	...	8.4984
0.36	10.0000	7.9984	7.9984	7.9984	7.9984	...	7.9984
0.26	10.0000	7.4984	7.4984	7.4984	7.4984	...	7.4984
0.16	10.0000	6.9984	6.9984	6.9984	6.9984	...	6.9984

Table 2.3: Change of brain cell radius over time according to the change in multiplicative case

In equilibrium, it can be easily seen that

$$r(5) = r(6) = r(7) = r(8) = r(9) = 9.9984.$$

In this example, for $k_1/k_2 > 0.66$ there is minimal dimensional change and normal neuronal function is present. For $0.46 \leq k_1/k_2 \leq 0.66$ there is moderate change and neuroprotective treatment may be required. For $k_1/k_2 < 0.46$ there is significant dimensional change and intensive neuroprotective treatment may be required.
There are following differences between brain cells model in classical analysis and multiplicative analysis. Multiplicative model shows more dramatic changes, while classical model appears more physiological. Both models reach stable end states. The multiplicative model responds faster.

Example 2.4 (Liver Cell-Multiplicative Case)**.** *Let $r(0) = 25$ and $p = 1.09 gr/cm^3$ for a liver cell. Again, we will examine the cell radius change for the liver cell using solution (2.1) in the multiplicative case. If this solution is used, the equilibrium ratio for the cell is obtained as;*

$$\frac{k_1}{k_2} = 1.07,$$

for $r(0) = 25$. Here the calculations will be made for particular selections of $k_1 = 107$ and $k_2 = 100$ in Table 2.4.

$\frac{k_1}{k_2}$	$r(0)$	$r(1)$	$r(2)$	$r(3)$	$r(4)$	...	$r(10)$
1.07	25.0000	24.9984	24.9984	24.9984	24.9984	...	24.9984
0.97	25.0000	23.9984	23.9984	23.9984	23.9984	...	23.9984
0.87	25.0000	22.9984	22.9984	22.9984	22.9984	...	22.9984
0.77	25.0000	21.9984	21.9984	21.9984	21.9984	...	21.9984
0.67	25.0000	20.9984	20.9984	20.9984	20.9984	...	20.9984
0.57	25.0000	19.9984	19.9984	19.9984	19.9984	...	19.9984
0.47	25.0000	18.9984	18.9984	18.9984	18.9984	...	18.9984

Table 2.4: Change of liver cell radius over time according to the change in multiplicative case

In equilibrium, it can be easily seen that

$$r(5) = r(6) = r(7) = r(8) = r(9) = 24.9984.$$

In this example, for $k_1/k_2 = 1.07$, there is a 0.006% change, which is the ideal situation. For $k_1/k_2 = 0.97 - 0.87$, a 4-8% reduction is within normal limits. For $k_1/k_2 = 0.77 - 0.67$, a 12-16% reduction is the situation that should be monitored. For $k_1/k_2 = 0.57 - 0.47$, there is a 20-24% reduction, which is a risk situation. Hepatoprotective treatment is required.
There are following differences between liver cells model in classical analysis and multiplicative analysis. In the classical case, the rate of change is slow and continuous, while in multiplicative analysis it is fast and one-time. While in the classical case there is a stability in the form of an asymptotic approach, in the multiplicative case there is an instantaneous stability.

3. Conclusion

In this study, four types of cells (Stomach, Blood, Brain, Liver) were considered and the change in the radii of the cells was examined by establishing the classical model in multiplicative analysis. In the classical and multiplicative case, the change in the radius of the cell membrane as time passes has been examined. In the multiplicative case, changes occur faster than in the classical case and the cells are in a more difficult situation than in the classical case.

Article Information

Acknowledgements: The authors are grateful to The Scientific and Technological Research Council of Türkiye (TUBITAK) for their financial support within the scope of -2209 project.

Author's contributions: All authors contributed equally to the writing of this paper. All authors read and approved the final manuscript.

Conflict of interest disclosure: No potential conflict of interest was declared by the authors.

Supporting/Supporting organizations: This article was supported by TUBITAK with student project 2209.

Ethical approval and participant consent: It is declared that during the preparation process of this study, scientific and ethical principles were followed and all the studies benefited from are stated in the bibliography.

Plagiarism statement: This article was scanned by the plagiarism program.

References

[1] B. Alberts, A. Johnson, J. Lewis, M. Raff, K. Roberts and P. Walter, *Molecular Biology of the Cell*, Garland Science (4th Edition): New York, 2002.
[2] L. Edelstein-Keshet, *Differential Calculus for the Life Sciences*, Published by the author at the University of British Colombia, Canada, 2020.
[3] A. Maton, *Cells: Building Blocks of Life*, Prentice-Hall (3rd Edition): USA, 1997.
[4] H. Meinhardt, *Models for the ontogenetic development of higher organisms*, Reviews of Physiology, Biochem. Pharmacol., **80** (1978) 47–104.
[5] N.A. Campbell, J.B. Reece, L.A. Urry, M.L. Cain, S.A. Wasserman, P.V. Minorsky and R.B. Jackson, *Biology*, 9th Edition, Benjamin Cummings, San Francisco, 2011.
[6] L. Edelstein-Keshet, *Mathematical Models in Biology*, Society for Industrial and Applied Mathematics Philadelphia: USA, 2005.
[7] H. Lodish, M. Krieger, M.P. Scott, A. Bretscher, H. Ploegh, P. Matsudaira, A. Berk, C.A. Kaiser, *Moleküler Hücre Biyolojisi*, Palme Yayınevi, Baskı 6, 2020.
[8] A. Öber, G.T. İzzetoğlu, *Histoloji*, Nobel Akademik Yayıncılık, Baskı 7, 2024.
[9] V. Volterra, B. Hostinský, *Operations Infinitesimales Lineares*, Applications aux équations différentielles et fonctionnelles, Paris, Gauthier-Villars, 1938.
[10] M. Grossman, *The First Nonlinear System of Differential and Integral Calculus*, Massachusetts, 1979.
[11] M. Grossman, R. Katz, *Non-Newtonian Calculus*, Massachusetts: Lee Press, 1972.
[12] A.E. Bashirov, E.M. Kurpınar, A. Özyapıcı, *Multiplicative calculus and its applications*, J. Math. Anal. Appl., **337** (2008), 36–48.
[13] S. Goktas, E. Yilmaz, A.C. Yar, *Multiplicative derivative and its basic properties on time scales*, Math. Methods Appl. Sci., **45** (2022), 2097-2109.
[14] T. Gulsen, E. Yilmaz, S. Goktas, *Multiplicative Dirac system*, Kuwait J. Sci., **49(3)** (2022), 1-11.

[15] E. Yilmaz, *Multiplicative bessel equation and its spectral properties*, Ric. Mat., **73** (2024), 1289-1305.
[16] S. Goktas, H. Kemaloglu, E. Yilmaz, *Multiplicative conformable fractional Dirac system*, Turkish J. Math., **46** (2022), 973-990.
[17] Y. Gürefe, *Multiplikatif diferansiyel denklemler ve uygulamaları üzerine*, Ph.D Thesis, Ege University, 2013.
[18] Y. Gürefe, *Çarpımsal analiz ve Uygulamaları*, M. Sc Thesis, Ege University, 2009.
[19] D. Stanley, *A multiplicative calculus*, Primus, **9** (1999), 310–326.
[20] A. Özyapıcı, *Çarpımsal analiz ve uygulamaları*, Ph.D Thesis, Ege University, 2009.

Journal of Mathematical Sciences and Modelling, 7(3) (2024) 121-127
Research Article

Journal of Mathematical Sciences and Modelling

Journal Homepage: www.dergipark.gov.tr/jmsm
ISSN: 2636-8692
DOI: https://doi.org/10.33187/jmsm.1504151

Controllability Analysis of Fractional-Order Delay Differential Equations via Contraction Principle

Okan Duman

Department of Mathematics, Yildiz Technical University, Istanbul, Türkiye

Article Info

Keywords: *Controllability, Delay differential equations, Fractional order derivative*
2010 AMS: *26A33, 34A08, 34K37, 47H10*
Received: *24 June 2024*
Accepted: *27 November 2024*
Available online: *17 December 2024*

Abstract

This paper investigates the existence of solutions and the controllability for three distinct types of fractional-order delay differential equations, aiming to establish sufficient conditions for both existence and uniqueness while demonstrating controllability. Beginning with a fractional-order delayed system containing a nonzero control function, we apply the Banach fixed-point theorem to show that this system has a unique solution and satisfies the controllability property. Extending our analysis, we introduce an integral function with a delay term on the right-hand-side of the system, forming a more complex integro-fractional delay system. With a Lipschitz condition imposed on this newly introduced function, we establish the existence and uniqueness of solution, as well as the controllability of this system. In the final system, an integro-fractional hybrid model, an additional delayed function is embedded within the Caputo derivative operator, introducing distinct analytical challenges. Despite these complexities, we use the Banach fixed-point theorem and certain assumptions to demonstrate that the systems are controllable. Our approach is distinctive in incorporating delay functions on both sides of the related systems, which we support with theoretical results and illustrative examples. The paper outlines the fundamentals of fractional calculus, specifies the necessary assumptions, and uses fixed-point criteria to establish controllability with the existence of a solution, providing a clear framework for analyzing fractional-order control systems with delay functions.

1. Introduction

Control theory, a branch of applied mathematics, deals with the key theoretical and practical aspects of designing and analysing control systems. These systems can be viewed as dynamical systems in which the rules of behaviour are determined by parameters called control functions. As in structures such as dynamical systems on manifolds, Lie groups and semigroups [1, 2], the question of controllability is also essential for fractional systems [3–6]. Recently, fractional-order differential equations have been increasingly recognised for their applications in physics, engineering and finance, and for their ability to model real-world problems. Unlike classical integer-order differential equations, they offer a more general approach [7–10]. However, similar to classical differential equations, there is no universal method to solve them explicitly, making existence and uniqueness theorems an important topic of discussion [11–14].
The controllability of fractional differential equations has been the subject of extensive study by numerous authors. In [15], M. Benchohra examined the sufficient conditions of controllability property by using semi-group theory. N.I. Mahmudov et al. addressed the controllability of semilinear integro-differential systems in Hilbert spaces, while V. Vijayakumar et al. provided results for these type of systems using resolvent operators [16, 17]. Moreover, M.M. Raja et al. obtain some results with the help of sectorial operators and Bohnenblust–Karlin's fixed point theorem [18]. Subsequently, many authors also explored fractional systems with delays, incorporating delay terms to make the models more applicable to real-life problems. Recently, K.S. Nisar et al. employed degree theory to analyze the controllability of delayed impulsive fractional integro-differential equations through numerical computations [19], while another study by Nisar et al. utilized integrated resolvent operator theory with Lipschitz conditions to demonstrate the existence and uniqueness of solutions for this type equations with nonlocal conditions and finite delay functions [20]. To emphasize the importance of the theory, it is worthy of note that there are studies on various spaces and different types of fractional type differential equations. In [21], K. Kavitha et al. proposed existence results for

***Email address and ORCID number*: oduman@yildiz.edu.tr, 0000-0001-9848-0759**
Cite as "O. Duman, *Controllability analysis of fractional-order delay differential equations via contraction principle*, J. Math. Sci. Model., 7(3) (2024), 121–127"

Sobolev-type Hilfer fractional integro-differential systems with infinite delay, and in [22], K. Kavitha et al. investigated the controllability of Hilfer fractional neutral Volterra-Fredholm delay integro-differential systems by using Dhage's fixed point theorem. In obtaining results related to controllability and existence/uniqueness of solutions, the use of tools such as fixed point theories like Banach, Schauder and Krasnoselskii, and Gronwall type inequalities, fractional calculus analysis and even topological degree theory is frequently seen, which shows how important and broad the field the theory studied is. For further details, we refer the reader to the papers [3–6] with [14–25] and the references therein.

The primary aim of this paper is to establish the existence and uniqueness of solutions for some fractional-order delay differential equations and to demonstrate that these systems possess the controllability property using a clear and more understandable way. For this we first consider the following fractional-order delayed system with the continuous function f from $[0,T]\times\mathbb{R}^2$ to $\mathbb{R}$:

$$
\begin{aligned}
{}^{c}\mathscr{D}^{\kappa}\rho(\varsigma) &= f(\varsigma,\rho(\varsigma),\rho(g(\varsigma)))-Bu(\varsigma), \quad \varsigma\in[0,T] && (1.1)\\
\rho(\varsigma) &= \varpi(\varsigma), \quad \varsigma\in[-\tau,0]. && (1.2)
\end{aligned}
$$

where our initial condition $\varpi\in C([-\tau,0],\mathbb{R})$, delayed term $g\in C([0,T],[-\tau,T])$ satisfying $g(\varsigma)\leq\varsigma$, and control function $u(\cdot)$ is given in $L^2([0,T],U)$ with admissible control functions space U, B is a bounded linear operator and ${}^{c}\mathscr{D}^{\kappa}$ is the fractional derivative of order $0<\kappa<1$ w.r.t. Caputo. The case where the control function in the system (1.1)-(1.2) is zero is discussed in [14], where a Lipschitz condition is imposed on the right-hand side with respect to the second and third variables to ensure the existence of a solution. In this study, we extend this by treating the nonzero control function, introducing some hypotheses based only on the control function and some hypotheses related to it. We then show, just using the Banach fixed-point theorem, that the system (1.1)-(1.2) satisfies both the existence and uniqueness of solution as well as the controllability property. We then add an integral function with delay function to the right hand side of the system (1.1)-(1.2), and we get the following integro-fractional-order delayed system:

$$
\begin{aligned}
{}^{c}\mathscr{D}^{\kappa}\rho(\varsigma) &= f(\varsigma,\rho(\varsigma),\rho(g(\varsigma)))-Bu(\varsigma)+F\Big(\varsigma,\rho(\varsigma),\int_0^{\varsigma}\zeta(\varsigma,s,\rho(g(s)))\Big)ds, \quad \varsigma\in[0,T] && (1.3)\\
\rho(\varsigma) &= \varpi(\varsigma), \quad \varsigma\in[-\tau,0]. && (1.4)
\end{aligned}
$$

Since the system (1.3)-(1.4) is more complex than the initial system, we demonstrate the existence and uniqueness of the solution, as well as the controllability property, using the Banach fixed-point theorem and the Lipschitz condition related to the newly added function on the right-hand side, along with the hypotheses established in the first system. Next, we consider the system of and integro-fractional-order hybrid delayed system, defined as follows, which is obtained when another function involving delay function is added to the Caputo derivative operator in the system (1.3)-(1.4):

$$
\begin{aligned}
{}^{c}\mathscr{D}^{\kappa}\Big(\rho(\varsigma)+\xi(\varsigma,v(g(\varsigma)))\Big) &= f(\varsigma,\rho(\varsigma),\rho(g(\varsigma)))-Bu(\varsigma)+F\Big(\varsigma,\rho(\varsigma),\int_0^{\varsigma}\zeta(\varsigma,s,\rho(g(s)))\Big)ds, \quad \varsigma\in[0,T] && (1.5)\\
\rho(\varsigma) &= \varpi(\varsigma), \quad \varsigma\in[-\tau,0]. && (1.6)
\end{aligned}
$$

Here, in addition to the conditions of the previous system, we also impose the Lipschitz condition on the function within the Caputo derivative operator. This allows us to establish the existence and uniqueness of solutions for this system and to verify the controllability property by Banach fixed-point theorem. Unlike most studies focusing on these type of systems, we introduce delay functions in the functions on both the right and left sides for related systems. This addition of delay functions brings a new perspective to the problem, making our approach distinctive and challenging. The paper is organized as follows: Section 2 provides an introduction to the Caputo fractional-order derivative and discusses the concept of controllability. Here we outline the fundamental properties of the Caputo fractional-order derivative, the relevant inequalities and the main assumptions. In the Section 3, we explore the controllability of the systems and establish the existence and uniqueness of solutions for our problems. By converting the problems into well-defined fixed point statements, we prove our results relying mainly on Lipschitz conditions and the contraction mapping theorem. Finally, in Section 4 we illustrate our results with examples.

2. Preliminaries

This section introduces the notations, definitions and basic concepts employed in the all of the paper.

Definition 2.1 ([26,27]). *Let $\kappa>0$ be a number and $\Gamma(\cdot)$ be the Gamma function. Assume that ς is any real number in the interval $[0,T]$.*

(1) The Riemann–Liouville integral for the function ρ is defined as follows w.r.t. the order κ

$$
I^{\kappa}\rho(\varsigma)=\frac{1}{\Gamma(\kappa)}\int_0^{\varsigma}(\varsigma-s)^{\kappa-1}\rho(s)ds. \tag{2.1}
$$

(2) The Caputo derivative for the function ρ is defined as follows w.r.t. the order κ

$$
D^{\kappa}\rho(\varsigma)=\frac{1}{\Gamma(n-\kappa)}\int_0^{\varsigma}(\varsigma-s)^{n-\kappa-1}\rho^{(n)}(s)ds,
$$

where $n=[\kappa]+1$ and $[\kappa]$ denotes the integer part of κ.

Before presenting our main assumptions, we give the definition of the concept of controllability given in [28], adapted to the differential equation of interest.

Definition 2.2. *The fractional control system (1.1)-(1.2) is called to be controllable on the given interval if for every points $\rho_0,\rho_1\in\mathscr{C}$ there exists a control function $u\in L^2([0,T],U)$ such that the solution $\rho(\cdot)$ of (1.1)-(1.2) satisfies $\rho(0)=\rho_0$ and $\rho(\varsigma)=\rho_1$. The same definition applies to systems (1.3)-(1.4) and (1.5)-(1.6).*

Note that throughout this paper all operations on continuous function spaces are conducted using the standard uniform convergence norm. Otherwise, it will be specified.

Let us now state the hypotheses we will use in the proofs of our results:

(C1) Assume that there exists $L>0$. Let the following inequality hold for all $\rho_i,\overline{\rho}_i\in\mathbb{R}$ $(i=1,2)$ and $\varsigma\in[0,T]$

$$|f(\varsigma,\rho_1,\overline{\rho}_1)-f(\varsigma,\rho_2,\overline{\rho}_2)|\leq L(|\rho_1-\rho_2|+|\overline{\rho}_1-\overline{\rho}_2|).$$

(C2) Suppose that $\mathscr{X}$ be a linear operator from $L^2([0,T],U)$ to $\mathbb{R}$ defined as follows

$$\mathscr{X}u:=\frac{1}{\Gamma(\kappa)}\int_0^{\varsigma}(\varsigma-s)^{\kappa-1}Bu(s)ds.$$

Then, we see that it induces an inverse operator $\overline{\mathscr{X}}^{-1}$ which is bounded and defined on the coset space $L^2([0,T],U)/ker\mathscr{X}$, and there is a constant $K>0$ satisfying $\left|B\overline{\mathscr{X}}^{-1}\right|\leq K$.

Remark 2.3 ([29]). *We give the sketch for the construction of $\overline{\mathscr{X}}^{-1}$ as follows. Let us think a Banach space M and let J be a closed interval of $\mathbb{R}$. Now take into account of the coset sapce $Y=L^2[J,U]/\ker(\mathscr{X})$. Since $\ker(\mathscr{X})$ is closed, Y is a Banach space w.r.t. the following norm*

$$\|[u]\|_Y=\inf_{u\in[u]}\|u\|_{L^2[J,U]}=\inf_{\mathscr{X}\hat{u}=0}\|u+\hat{u}\|_{L^2[J,U]}$$

where $[u]$ are classes of equivalence for u. Define $\overline{\mathscr{X}}:Y\to M$ by $\overline{\mathscr{X}}[u]=\mathscr{X}u$ for all $u\in[u]$. Then we have that $\overline{\mathscr{X}}$ is one-to-one and

$$\|\overline{\mathscr{X}}[u]\|_M\leq\|\mathscr{X}\|\,.\,\|[u]\|_Y.$$

Moreover, $V:=R(\mathscr{X})$ (i.e. range of $\mathscr{X}$) is a Banach space with the following norm

$$\|v\|_V=\left\|\overline{\mathscr{X}}^{-1}v\right\|_Y.$$

To see this, note that this norm is equivalent to the graph norm on the domain of $\overline{\mathscr{X}}^{-1}$, i.e., we have that $D\left(\overline{\mathscr{X}}^{-1}\right)=R(\overline{\mathscr{X}})$. On the other hand $\overline{\mathscr{X}}$ is bounded, and since $D(\overline{\mathscr{X}})=Y$ is closed, $\overline{\mathscr{X}}^{-1}$ must be closed. Then we get that $R(\mathscr{X})=V$ is a Banach space with respect to the above norm. Also, we get the following relation

$$\|\mathscr{X}u\|_V=\left\|\overline{\mathscr{X}}^{-1}\mathscr{X}u\right\|_Y=\left\|\overline{\mathscr{X}}^{-1}\overline{\mathscr{X}}[u]\right\|=\|[u]\|=\inf_{u\in[u]}\|u\|\leq\|u\|.$$

Since the space $L^2[J,U]$ is reflexive and the set $\ker(\overline{\mathscr{X}})$ is closed (weakly sense), the infimum value mentioned above has been attained. Hence, for any $v\in V$, there exists a control $u\in L^2[J,U]$ such that $u=\overline{\mathscr{X}}^{-1}v$.

3. Controllability Results

In this section, we present the controllability results for the systems (1.1)-(1.2), (1.3)-(1.4) and (1.5)-(1.6). For the sake of simplicity, the space $C([-\tau,T],\mathbb{R})$ will be referred to as $\mathscr{C}$ for short in this and the following sections.

Theorem 3.1. *If the assumptions (C1)-(C2) are satisfied, then the control system (1.1)-(1.2) is controllable provided that*

$$\Lambda_1:=L\Big(\frac{T^{\kappa}}{\Gamma(\kappa+1)}+K\frac{T^{2\kappa}}{\Gamma(\kappa+1)^2}\Big)<\frac{1}{2}.$$

Proof. First we reconsider the our problem (1.1)-(1.2) as a fixed point problem. Then we make a detailed analysis of the following operator

$$\mathscr{F}:\mathscr{C}\to\mathscr{C}$$

defined by

$$\mathscr{F}\rho(\varsigma)=\begin{cases}\varpi(\varsigma), & \varsigma\in[-\tau,0]\\ \varpi(0)+\int_0^{\varsigma}\frac{(\varsigma-s)^{\kappa-1}}{\Gamma(\kappa)}f(s,\rho(s),\rho(g(s))ds-\int_0^{\varsigma}\frac{(\varsigma-s)^{\kappa-1}}{\Gamma(\kappa)}Bu(s)ds, & \varsigma\in[0,T].\end{cases}$$

Now, using a suitable control function u, our goal is to identify a unique fixed point of $\mathscr{F}$. If any $\rho(\varsigma)$ and $\overline{\rho}(\varsigma)$ satisfy $\mathscr{F}\rho(\varsigma)=\mathscr{F}\overline{\rho}(\varsigma)$ for $\varsigma\in[-\tau,0]$, then this equality is extended to $\varsigma\in[0,T]$. In addition, let us choose the control function u as follows:

$$u(\varsigma)=\overline{\mathscr{X}}^{-1}\Big(\rho_0-\rho_1+\int_0^{\varsigma}\frac{(\varsigma-s)^{\kappa-1}}{\Gamma(\kappa)}f(s,\rho(s),\rho(g(s))ds\Big)\quad\text{for all}\quad\rho_0,\rho_1\in\mathbb{R}.$$

Now, using this control, let us determine the fixed point of the operator $\mathscr{F}$.

$$\begin{aligned}
&\left|\mathscr{F}\rho(\varsigma)-\mathscr{F}\overline{\rho}(\varsigma)\right| \\
&\quad\leq \frac{1}{\Gamma(\kappa)}\int_0^{\varsigma}(\varsigma-s)^{\kappa-1}\left|f(s,\rho(s),\rho(g(s)))-f(s,\overline{\rho}(s),\overline{\rho}(g(s)))\right|ds \\
&\quad+ \frac{1}{\Gamma(\kappa)}\int_0^{\varsigma}(\varsigma-s)^{\kappa-1}\left(Bu(s)-B\overline{u}(s)\right)ds \\
&\quad\leq \frac{L}{\Gamma(\kappa)}\int_0^{\varsigma}(\varsigma-s)^{\kappa-1}\left(|\rho(s)-\overline{\rho}(s)|+|\rho(g(s))-\overline{\rho}(g(s))|\right)ds \\
&\quad+ \frac{1}{\Gamma(\kappa)}\int_0^{\varsigma}(\varsigma-s)^{\kappa-1}\left[B\overline{\mathscr{X}}^{-1}\left(\left(\int_0^{\varsigma}\frac{(\varsigma-s)^{\kappa-1}}{\Gamma(\kappa)}(f(s,\rho(s),\rho(g(s))-f(s,\overline{\rho}(s),\overline{\rho}(g(s)))ds)\right)\right)\right] \\
&\quad\leq 2L\frac{T^{\kappa}}{\Gamma(\kappa+1)}\left|\rho-\overline{\rho}\right|+\frac{1}{\Gamma(\kappa)}\int_0^{\varsigma}(\varsigma-s)^{\kappa-1}\left|B\overline{\mathscr{X}}^{-1}\right|\int_0^{\varsigma}\frac{(\varsigma-s)^{\kappa-1}}{\Gamma(\kappa)}\left|(f(s,\rho(s),\rho(g(s))-f(s,\overline{\rho}(s),\overline{\rho}(g(s)))\right|ds \\
&\quad\leq 2L\frac{T^{\kappa}}{\Gamma(\kappa+1)}\left|\rho-\overline{\rho}\right|+2KL\frac{T^{2\kappa}}{\Gamma(\kappa+1)^2}\left|\rho-\overline{\rho}\right| \\
&\quad\leq \left[2L\left(\frac{T^{\kappa}}{\Gamma(\kappa+1)}+K\frac{T^{2\kappa}}{\Gamma(\kappa+1)^2}\right)\right]\left|\rho-\overline{\rho}\right|.
\end{aligned}$$

Since $\Lambda_1<\frac{1}{2}$, then there exists a fixed point $\rho(\cdot)$ of the operator $\mathscr{F}$ w.r.t. the control function u by the Banach Contraction Principle. Thus this fixed point is the solution of the systems (1.1)-(1.2). Also,these control systems is controllable since (i) $(\mathscr{F}\rho)(\varsigma)=\varpi(\varsigma)=\rho(\varsigma)$ on $[-\tau,0]$ and (ii) $(\mathscr{F}\rho)(\varsigma)=\rho(\varsigma)$ with $(\mathscr{F}\rho)(T)=\rho(T)=\rho_1$ on $[0,\tau]$. Thus, it is concluded that the our systems is controllable on the whole interval $[-\tau,T]$. □

Theorem 3.2. *Let the assumptions (C1)-(C2) be satisfied. Suppose that*

(C3) The function $\zeta:\Delta\times\mathbb{R}\to\mathbb{R}$ is continuous and there is a constant $H>0$ such that

$$|\zeta(\varsigma,s,\rho)-\zeta(\varsigma,s,\overline{\rho})|\leq H\left|\rho-\overline{\rho}\right|.$$

(C4) The function $F:[0,T]\times\mathbb{R}\times\mathbb{R}\to\mathbb{R}$ is continuous and there is a constant $P>0$ such that

$$|F(s,\rho_1,\overline{\rho}_1)-F(s,\rho_2,\overline{\rho}_2)|\leq P\left(|\rho_1-\rho_2|+|\overline{\rho}_1-\overline{\rho}_2|\right).$$

for all $\rho_i,\overline{\rho}_i\in\mathbb{R}$ $(i=1,2)$ and $\varsigma,s\in[0,T]$. Also we denote here that $\Delta:=\{(\varsigma,s):0\leq s\leq\varsigma\leq T\}$ and $\mathscr{H}\rho(\varsigma)=\int_0^{\varsigma}\zeta(\varsigma,s,\rho(s))ds$ for brevity.

Then the control system (1.3)-(1.4) is controllable provided that

$$\Lambda_2:=\Lambda_1+P(1+H)\frac{T^{\kappa}}{\Gamma(\kappa+1)}<1.$$

Proof. By analogy, we need to make the problem (1.3)-(1.4) into a fixed point problem. In the next step we shall analyse the operator

$$\Psi:\mathscr{C}\to\mathscr{C}$$

defined by

$$\Psi\rho(\varsigma)=\begin{cases}\varpi(\varsigma), & \varsigma\in[-\tau,0]\\ \varpi(0)+\int_0^{\varsigma}\frac{(\varsigma-s)^{\kappa-1}}{\Gamma(\kappa)}f(s,\rho(s),\rho(g(s))ds-\int_0^{\varsigma}\frac{(\varsigma-s)^{\kappa-1}}{\Gamma(\kappa)}Bu(s)ds+\int_0^{\varsigma}\frac{(\varsigma-s)^{\kappa-1}}{\Gamma(\kappa)}F\left(s,\rho(s),\mathscr{H}\rho(g(s))\right)ds, & \varsigma\in[0,T]\end{cases}$$

Similar to what was done above, we find the fixed point of the operator Ψ via a suitable control function u. If any $\rho(\varsigma),\overline{\rho}(\varsigma)$ satisfying $\Psi\rho(\varsigma)=\Psi\overline{\rho}(\varsigma)$ for $\varsigma\in[-\tau,0]$, then we take it in the interval $[0,T]$. Now let us determine the control function as follow:

$$u(\varsigma)=\overline{\mathscr{X}}^{-1}\left(\rho_0-\rho_1+\int_0^{\varsigma}\frac{(\varsigma-s)^{\kappa-1}}{\Gamma(\kappa)}f(s,\rho(s),\rho(g(s))ds\right)-\int_0^{\varsigma}\frac{(\varsigma-s)^{\kappa-1}}{\Gamma(\kappa)}F\left(s,\rho(s),\mathscr{H}\rho(g(s))\right)ds \quad \text{for all} \quad \rho_0,\rho_1\in\mathbb{R}.$$

Next we show that the operator Ψ has a fixed point with the following steps:

$$\begin{aligned}
\left|\Psi\rho(\varsigma)-\Psi\overline{\rho}(\varsigma)\right| &\leq \frac{1}{\Gamma(\kappa)}\int_0^{\varsigma}(\varsigma-s)^{\kappa-1}\left|f(s,\rho(s),\rho(g(s)))-f(s,\overline{\rho}(s),\overline{\rho}(g(s)))\right|ds \\
&+ \frac{1}{\Gamma(\kappa)}\int_0^{\varsigma}(\varsigma-s)^{\kappa-1}\left(Bu(s)-B\overline{u}(s)\right)ds \\
&+ \frac{1}{\Gamma(\kappa)}\int_0^{\varsigma}(\varsigma-s)^{\kappa-1}\left[F\left(s,\rho(s),\mathscr{H}\rho(g(s))\right)-F\left(s,\overline{\rho}(s),\mathscr{H}\overline{\rho}(g(s))\right)\right]ds \\
&\leq \Lambda_1+\frac{1}{\Gamma(\kappa)}\int_0^{\varsigma}(\varsigma-s)^{\kappa-1}\left|F\left(s,\rho(s),\mathscr{H}\rho(g(s))\right)-F\left(s,\overline{\rho}(s),\mathscr{H}\overline{\rho}(g(s))\right)\right|ds \\
&\leq \Lambda_1+P|\rho-\overline{\rho}|\frac{1}{\Gamma(\kappa)}\int_0^{\varsigma}(\varsigma-s)^{\kappa-1}ds+PH|\rho-\overline{\rho}|\frac{1}{\Gamma(\kappa)}\int_0^{\varsigma}(\varsigma-s)^{\kappa-1}ds \\
&\leq \underbrace{\left[\Lambda_1+P(1+H)\frac{T^{\kappa}}{\Gamma(\kappa+1)}\right]}_{\Lambda_2}|\rho-\overline{\rho}|.
\end{aligned}$$

Since $\Lambda_2 < 1$, then there exists a fixed point $\rho(\cdot)$ of the operator Ψ w.r.t. the control function u by the Banach Contraction Principle. Therefore, this fixed point serves as the solution to the systems (1.3)-(1.4). Also,these control systems is controllable since (i) $(\Psi\rho)(\varsigma) = \varpi(\varsigma) = \rho(\varsigma)$ on $[-\tau, 0]$ and (ii) $(\Psi\rho)(\varsigma) = \rho(\varsigma)$ with $(\Psi\rho)(T) = \rho(T) = \rho_1$ on $[0, \tau]$. Hence, we conclude that the systems is controllable on the interval $[-\tau, T]$. Thus the proof is complete. □

Theorem 3.3. *Let the assumptions (C1)-(C4) be satisfied. Suppose that the function $\xi : [0,T] \times \mathbb{R} \to \mathbb{R}$ is continuous and there is a constant $\delta > 0$ such that*

$$|\xi(\varsigma, \rho(\varsigma)) - \xi(\varsigma, \overline{\rho}(\varsigma))| \leq \delta \, |\rho - \overline{\rho}| .$$

Then the control system (1.5)-(1.6) is controllable provided that

$$\Lambda_3 := (\delta + M)\left(\frac{KT^{\kappa}}{\Gamma(\kappa+1)} + 1\right) < 1$$

where the constant $M = \frac{T^{\kappa}}{\Gamma(\kappa+1)}(2L + P(1+HT))$.

Proof. Analogously,let us turn the problem (1.5)-(1.6) into a fixed point problem.

$$\Theta : \mathscr{C} \to \mathscr{C}$$

defined by

$$\Theta\rho(\varsigma) = \begin{cases} \varpi(\varsigma), \quad \varsigma \in [-\tau, 0] \\ \varpi(0) + \xi(0, \rho_0) - \xi(\varsigma, \rho(g(\varsigma))) + \int_0^{\varsigma} \frac{(\varsigma - s)^{\kappa-1}}{\Gamma(\kappa)} f(s, \rho(s), \rho(g(s)))ds \\ - \int_0^{\varsigma} \frac{(\varsigma - s)^{\kappa-1}}{\Gamma(\kappa)} Bu(s)ds + \int_0^{\varsigma} \frac{(\varsigma - s)^{\kappa-1}}{\Gamma(\kappa)} F\Big(s, \rho(s), \mathscr{H}\rho(g(s))\Big)ds, \ \varsigma \in [0, T] \end{cases}$$

Analogously, let us begin with the steps above. If any $\rho(\varsigma), \overline{\rho}(\varsigma)$ satisfying $\Theta\rho(\varsigma) = \Theta\overline{\rho}(\varsigma)$ for $\varsigma \in [-\tau, 0]$, then we take $\varsigma \in [0, T]$. Now let us determine the control function as follow:

$$\begin{aligned} u(\varsigma) &= \overline{\mathscr{X}}^{-1}\Big(\rho_0 - \rho_1 + \xi(0, \rho_0) - \xi(\varsigma, \rho(g(\varsigma))) + \int_0^{\varsigma} \frac{(\varsigma - s)^{\kappa-1}}{\Gamma(\kappa)} f(s, \rho(s), \rho(g(s)))ds\Big) \\ &- \int_0^{\varsigma} \frac{(\varsigma - s)^{\kappa-1}}{\Gamma(\kappa)} F\Big(s, \rho(s), \mathscr{H}\rho(g(s))\Big)ds \quad \text{for all} \quad \rho_0, \rho_1 \in \mathbb{R}. \end{aligned}$$

Next we show that the operator Θ has a fixed point:

$$\begin{aligned} \big|\Theta\rho(\varsigma) - \Theta\overline{\rho}(\varsigma)\big| &\leq \big|\xi(\varsigma, \rho(g(\varsigma))) - \xi(\varsigma, \overline{\rho}(g(\varsigma)))\big| \\ &\leq \frac{1}{\Gamma(\kappa)} \int_0^{\varsigma} (\varsigma - s)^{\kappa-1} \big|f(s, \rho(s), \rho(g(s))) - f(s, \overline{\rho}(s), \overline{\rho}(g(s)))\big|ds \\ &+ \frac{1}{\Gamma(\kappa)} \int_0^{\varsigma} (\varsigma - s)^{\kappa-1} \big(Bu(s) - B\overline{u}(s)\big)ds \\ &+ \frac{1}{\Gamma(\kappa)} \int_0^{\varsigma} (\varsigma - s)^{\kappa-1} \Big[F\Big(s, \rho(s), \mathscr{H}\rho(g(s))\Big) - F\Big(s, \overline{\rho}(s), \mathscr{H}\overline{\rho}(g(s))\Big)\Big]ds \\ &\leq \delta\big|\rho - \overline{\rho}\big| + 2L\frac{T^{\kappa}}{\Gamma(\kappa+1)}\big|\rho - \overline{\rho}\big| \\ &+ \frac{KT^{\kappa}}{\Gamma(\kappa+1)}\Big[\delta + \frac{T^{\kappa}}{\Gamma(\kappa+1)}\big(2L + P(1+HT)\big)\Big]\big|\rho - \overline{\rho}\big| \\ &+ \frac{T^{\kappa}}{\Gamma(\kappa+1)}P(1+HT)\big|\rho - \overline{\rho}\big| = (\delta + M)\left(\frac{KT^{\kappa}}{\Gamma(\kappa+1)} + 1\right) \end{aligned}$$

Since $\Lambda_3 < 1$, then there exists a fixed point $\rho(\cdot)$ of the operator Θ w.r.t. the control function u by the Banach Contraction Principle. Consequently, this fixed point gives the solution to the systems (1.5)-(1.6). Also, these control systems is controllable since (i) $(\Theta\rho)(\varsigma) = \varpi(\varsigma) = \rho(\varsigma)$ on $[-\tau, 0]$ and (ii) $(\Theta\rho)(\varsigma) = \rho(\varsigma)$ with $(\Theta\rho)(T) = \rho(T) = \rho_1$ on $[0, \tau]$. Hence, we conclude that the systems is controllable on the entire interval $[-\tau, T]$. Thus the proof is complete.

□

4. Examples

Example 4.1. *Let us examine the fractional-order differential equation below:*

$$\begin{cases} {}^{c}D^{\frac{1}{2}}\rho(\varsigma) = \frac{|\rho(\varsigma)|}{8+8|\rho(\varsigma)|} + \frac{\cos\rho(\varsigma^2)}{8} - u(\varsigma) & \varsigma \in [0,1] \\ \rho(\varsigma) = \varsigma & \varsigma \in [-1, 0]. \end{cases} \tag{4.1}$$

Let $f(\varsigma, \rho, \overline{\rho}) = \frac{|\rho|}{8+8|\rho|} + \frac{\cos\overline{\rho}}{8}$ and $g(\varsigma) = \varsigma^2$. It is obtained that

$$\big|f(\varsigma, \rho_1, \overline{\rho}_1) - f(\varsigma, \rho_2, \overline{\rho}_2,)\big| \leq \frac{1}{8}\Big(\big|\rho_1 - \rho_2\big| + \big|\overline{\rho}_1 - \overline{\rho}_2\big|\Big)$$

for all $\rho_i, \overline{\rho}_i \in \mathbb{R}$ where $i = 1,2$ with $\varsigma \in [0,1]$ and u is a control function. Now, assume that the operator $\mathscr{X} : L^2([0,T],U) \to \mathbb{R}$ defined by

$$\mathscr{X}u := \frac{1}{\Gamma(\frac{1}{2})}\int_0^{\varsigma}(\varsigma - s)^{-\frac{1}{2}}Bu(s)ds.$$

induces a bounded inverse operator $\overline{\mathscr{X}}^{-1}$ on the coset $L^2([0,T],U)/ker\mathscr{X}$. Choose $K < 2$ in such a way $\Lambda_1 < \frac{1}{2}$. Indeed,

$$\Lambda_1 = \frac{1}{8}\left(\frac{1}{\Gamma(\frac{1}{2}+1)} + K\frac{1}{\Gamma(\frac{1}{2}+1)^2}\right) < \frac{1}{2} \iff \Lambda_1 = \left(\frac{1}{\Gamma(\frac{1}{2}+1)} + K\frac{1}{\Gamma(\frac{1}{2}+1)^2}\right) < 4 \iff K < 2{,}2552$$

where $\Gamma(\frac{1}{2}+1) \approx 0{,}8862$. Since the all required conditions of Theorem 3.1 are satisfied, then we obtain that the problem (4.1) is controllable.

Example 4.2. *Now, let us think the following integro-fractional order differential equation:*

$$\begin{cases} {}^{c}D^{\frac{1}{2}}\rho(\varsigma) = \frac{\sin\rho(\varsigma)}{10} + \frac{\rho(\varsigma-1)}{10} - u(\varsigma) + \frac{e^{-\varsigma}\left|\rho(\varsigma)\right|}{(2+e^{-\varsigma})(1+\left|\rho(\varsigma)\right|)} \\ \qquad\qquad + \frac{1}{3}\int_0^{\varsigma} e^{\frac{-1}{3}}\rho(g(s))ds & \varsigma \in [0,1] \\ \rho(\varsigma) = e^{\varsigma} & \varsigma \in [-1,0]. \end{cases} \tag{4.2}$$

Let $f(\varsigma,\rho,\overline{\rho}) = \frac{1}{10}\left(\sin\rho + \overline{\rho}\right)$, $g(\varsigma) = \varsigma - 1$ and $F\left(\varsigma,\rho,\mathscr{H}\rho\right) = \frac{e^{-\varsigma}\left|\rho(\varsigma)\right|}{(2+e^{-\varsigma})(1+\left|\rho(\varsigma)\right|)} + \mathscr{H}\rho$ where $\mathscr{H}\rho(\varsigma) = \frac{1}{3}\int_0^{\varsigma} e^{\frac{-1}{3}}\rho(s)ds$. It is hold that

$$\begin{aligned} |f(\varsigma,\rho_1,\overline{\rho}) - f(\varsigma,\rho_2,\overline{\rho})| &\leq \frac{1}{10}\left(|\rho_1 - \rho_2| + |\overline{\rho}_1 - \overline{\rho}_2|\right) \\ \left|\mathscr{H}\rho - \mathscr{H}\overline{\rho}\right| &\leq \frac{1}{3}|\rho - \overline{\rho}| \\ \left|F(\varsigma,\rho,\mathscr{H}\rho) - F(\varsigma,\overline{\rho},\mathscr{H}\overline{\rho})\right| &\leq \frac{1}{3}(|\rho - \overline{\rho}| + \left|\mathscr{H}\rho - \mathscr{H}\overline{\rho}\right|). \end{aligned}$$

for all $\rho_i, \overline{\rho} \in \mathbb{R}$ where $i = 1,2$ with $\varsigma \in [0,1]$ and u is a control function. Therefore, $H = \frac{1}{3}$, $P = \frac{1}{3}$. Using similar calculations above we have that $\Lambda_1 = 0{,}240161$ and find that $\Lambda_2 = 0{,}741663 < 1$. Since the remaining conditions of Theorem 3.2 are satisfied, then we obtain that the problem (4.2) is controllable.

Conclusion

In this paper we have established the existence and uniqueness of solutions for several fractional-order delay differential equations, while demonstrating their controllability properties. We began by analysing a fractional-order delay control system with a nonzero control function, and successfully applied the Banach fixed point theorem to show that the solution exists and is unique. Meanwhile, in Theorem 3.1, we have shown that the system is controllable using the function detailed in Remark 2.3. We then introduced an additional function involving integral part on the right-handside with delay function, which led to a more complex integro-fractional-order delayed system. Here we imposed a Lipschitz condition on the new function to verify the existence and uniqueness of solutions and the controllability property in Theorem 3.2. In addition, we extended our work to an integro-fractional-order hybrid delayed system by incorporating another delayed function into the Caputo derivative operator. This presented different challenges, particularly in formulating appropriate conditions for our analyses in Theorem 3.3. Despite these difficulties, our new approach, which included the introduction of delay functions on both the right and left sides of the equations, provides a uncomplicated perspective on control systems in fractional calculus and enhances the understanding of their dynamics. The use of Banach fixed point theory as the basis for the proofs of these theorems emphasizes the simplicity and clarity of our method and makes it applicable to different types of control systems.

Article Information

Acknowledgements: The author would like to express his sincere thanks to the editor and the reviewers for their helpful comments and suggestions.

Author's contributions: The article has a single author. The author has read and approved the final manuscript.

Conflict of Interest Disclosure: No potential conflict of interest was declared by the author.

Supporting/Supporting organizations: No grants were received from any public, private or non-profit organizations for this research.

Ethical approval and participant consent: It is declared that during the preparation process of this study, scientific and ethical principles were followed and all the studies benefited from are stated in the bibliography.

Plagiarism statement: This article was scanned by the plagiarism program.

References

[1] A. Da Silva, *Controllability of linear systems on solvable Lie groups*, SIAM J. Control Optim., **54** (2016), 372–390.
[2] E. Kizil, *Control Homotopy of Trajectories*, J. Dyn. Control Syst., **77** (2021), 683–692.
[3] A. Ali, S. Khalid, G. Rahmat, G. Ali, K. S. Nisar, B. Alshahrani, *Controllability and Ulam–Hyers stability of fractional order linear systems with variable coefficients*, Alex. Eng. J., **61**(8) (2022), 6071-6076.
[4] A. Shukla, R. Patel, *Controllability results for fractional semilinear delay control systems*, J. Appl. Math. Comput., **65** (2021), 861–875.
[5] B. Radhakrishnan, K. Balachandran, P. Anukokila, *Controllability results for fractional integrodifferential systems in Banach spaces*, Int. J. Comput. Sci. Math., **5**(2) (2014), 184-97.
[6] PS. Kumar, K. Balachandran, N. Annapoorani, *Controllability of nonlinear fractional Langevin delay systems*, Nonlinear Anal. Model. Control, **23**(3) (2018), 321-340.
[7] H.G. Sun, Y. Zhang, D. Baleanu, W. Chen, Y.Q. Chen, *A new collection of real world applications of fractional calculus in science and engineering*, Commun. Nonlinear Sci. Numer. Simul., **64** (2018), 213-231.
[8] G.Z. Voyiadjis, W. Sumelka, *Brain modelling in the framework of anisotropic hyperelasticity with time fractional damage evolution governed by the Caputo-Almeida fractional derivative*, J. Mech. Behav. Biomed., **89** (2019), 209-216.
[9] R. Hilfer, *Applications of Fractional Calculus in Physics*, World Scientific, Singapore, 2000.
[10] V.E. Tarasov, *Fractional Dynamics: Applications of Fractional Calculus to Dynamics of Particles, Fields and Media*, Springer, Heidelberg, 2010.
[11] T.A. Burton, *A fixed-point theorem of Krasnoselskii*, Appl. Math. Lett., **11**(1) (1998), 85-88.
[12] T.A. Burton, *A note on existence and uniqueness for integral equations with sum of two operators: progressive contractions*, Fixed Point Theory, **20**(1) (2019), 107-113.
[13] T.A. Burton, I.K. Purnaras, *Global existence and uniqueness of solutions of integral equations with delay: progressive contractions*, Electron. J. Qual. Theory Differ. Equ., **49** (2017), 1-6.
[14] F. Develi, O. Duman, *Existence and stability analysis of solution for fractional delay differential equations*, Filomat, **37** (2023), 1869–1878.
[15] M. Benchohra, D. Seba, *Impulsive fractional differential equations in Banach spaces*, Electron. J. Differ. Equ., **8** (2009), 1–14.
[16] N.I. Mahmudov, R. Murugesu, C. Ravichandran, V. Vijayakumar, *Approximate controllability results for fractional semilinear integro-differential inclusions in Hilbert spaces*, Results Math., **71** (2017), 45-61.
[17] V. Vijayakumar, K.S. Nisar, D. Chalishajar, A. Shukla, M. Malik, A. Alsaadi, S.F. Aldosary, *A note on approximate controllability of fractional semilinear integrodifferential control systems via resolvent operators*, Fractal and Fractional, **6**(2) (2022), 1-14.
[18] M.M. Raja, V. Vijayakumar, A. Shukla, K.S. Nisar, H.M. Baskonus, *On the approximate controllability results for fractional integrodifferential systems of order 1¡ r¡ 2 with sectorial operators*, J. Comput. Appl. Math.J. Comput. Appl. Math., **415** (2022), 114492.
[19] K.S. Nisar, K. Muthuselvan, *A new effective technique of nonlocal controllability criteria for state delay with impulsive fractional integro-differential equation*, Results Appl. Math, **21** (2024), 100437.
[20] K.S. Nisar, K. Munusamy, C. Ravichandran, *Results on existence of solutions in nonlocal partial functional integrodifferential equations with finite delay in nondense domain*, Alex. Eng. J., **73** (2023), 377-384.
[21] K. Kavitha, K.S. Nisar, A. Shukla, V. Vijayakumar, S. Rezapour, *A discussion concerning the existence results for the Sobolev-type Hilfer fractional delay integro-differential systems*, Adv. Differ. Equ., 2021, 1-18.
[22] K. Kavitha, V. Vijayakumar, K.S. Nisar, *On the approximate controllability of non-densely defined Sobolev-type nonlocal Hilfer fractional neutral Volterra-Fredholm delay integro-differential system*, Alex. Eng. J., **69** (2023), 57-65.
[23] A. Shukla, V. Vijayakumar, K.S. Nisar, *A new exploration on the existence and approximate controllability for fractional semilinear impulsive control systems of order* $r \in (1,2)$, Chaos, Solitons and Fractals, **154** (2022), 111615.
[24] K. Muthuvel, K. Kaliraj, K.S. Nisar, V. Vijayakumar, *Relative controllability for* Ψ*-Caputo fractional delay control system*, Results Control Optim., **16** (2024), 100475.
[25] G. Jothilakshmi, B. Sundaravadivoo, K.S. Nisar, S. Alsaeed, *Impulsive fractional integro-delay differential equation-controllability through delayed Mittag-Leffler function perturbation*, Int. J. Dyn. Contr., **12**(11) (2024), 4178-4187.
[26] I. Podlubny, *Fractional Differential Equation*, Academic Press, San Diego, 1999.
[27] A. A. Kilbas, H. M. Srivastava, J. J. Trujillo, *Theory and Applications of Fractional Differential Equations*, Elsevier Science, Amsterdam, 2006.
[28] D.Y. Khusainov, G.V. Shuklin, *Relative controllability in systems with pure delay*, Int. J. Appl. Mech., **41** (2005), 210-221.
[29] M.D. Quinn, N. Carmichael, *An approach to nonlinear control problem using fixed point methods, degree theory and pseudo-inverses*, Numer. Funct. Anal. Optim., **7** (1984), 197–219.

Journal of Mathematical Sciences and Modelling, 7(3) (2024) 128-145
Research Article

Journal of Mathematical Sciences and Modelling

Journal Homepage: www.dergipark.gov.tr/jmsm
ISSN: 2636-8692
DOI: https://doi.org/10.33187/jmsm.1587499

Medical Waste Management Based on an Interval-Valued Fermatean Fuzzy Decision-Making Method

Murat Kirişci

Department of Biostatistics and medical Informatics, Cerrahpaşa Medicine Faculty, Istanbul University-Cerrahpaşa, Istanbul, Türkiye

Article Info

Keywords: *Decision-making, Entropy, Interval-valued Fermatean fuzzy set, MARCOS, Medical waste, PIPRECIA*
2010 AMS: *03E72, 94A17, 94D05*
Received: *18 November 2024*
Accepted: *10 November 2024*
Available online: *18 December 2024*

Abstract

Due to its infectious and hazardous nature, medical waste poses risks to people and the environment. For patients to receive medical attention and recover in a safe environment, waste must be disposed of correctly. Improper medical waste disposal poses a severe risk to society, which can accelerate the development of various pandemics and epidemics. In this case, medical waste disposal should be handled appropriately. This study presents an integrated multi-criteria decision-making method consisting of entropy, the Pivot Pairwise Relative Criteria Importance Assessment, and Measurement of Alternatives and Ranking according to Compromise Solution methods based on an interval-valued Fermatean fuzzy set. This method can guarantee high safety and security for health practitioners and society through effective modeling and ranking of risks associated with medical waste disposal. Five alternatives and eight criteria were determined. According to the results, incineration is the most suitable disposal process for medical waste. The performance was then assessed and validated using a sensitivity analysis. A sensitivity analysis has been conducted across the range of values for the α parameter. It was examined whether the rankings of the alternatives changed when the α values in the integrated weight determination model for sensitivity analysis were altered. When the different α values were reviewed with the selected α value in the application example, it was seen that incineration was the first alternative. In addition, the study's findings and their consequences for lawmakers, businesspeople, technologists, and practitioners are examined. In the future, these stakeholders can concentrate on these deficiencies and provide long-term remedies.

1. Introduction

Concerns over the health of people and animals are legitimate, given the world's population growth and the rise in pandemic diseases. One of these issues is the appropriate disposal of the enormous volumes of medical waste (MW) produced by hospitals, labs, and other healthcare facilities. Managing the MW generated by their operations is among the most significant issues facing healthcare facilities worldwide [1]. Inappropriately disposing of hazardous goods, such as used needles and personal protective equipment, is risky because MW is communicable. Several pandemic infections can spread more quickly when MW is not managed correctly, which is a severe worry for the general public. The problem of how to dispose of MW in this situation needs careful consideration [2].

MW impacts the environment, the general public, employees, and patients. Selecting a technique for disposing of MW is among the most crucial decisions healthcare institutions must make. This situation is a complicated problem with multiple competing requirements and options. Nevertheless, decision specialists could feel uncertain about themselves when assessing these possibilities. Further, one of the biggest challenges that healthcare organizations confront globally is managing the MW that their activities generate. The improper disposal of hazardous waste poses a significant risk to society and can hasten the spread of several pandemic illnesses. The problem of deciding how to get rid of MW needs to be given serious thought right away. Because a MW method selection problem has several criteria and options, it can be classified as a multi-criteria decision-making(MCDM) problem. However, specialists assessing these issues are limited to linguistically assessing the qualitative criteria. Fuzzy logic addresses the ambiguity in these verbal formulations, while MCDM approaches

Email address and ORCID number: mkirisci@hotmail.com, 0000-0003-4938-5207
Cite as "M. Kirişci, *Medical waste management based on an Interval-Valued Fermatean Fuzzy decision-making method*, J. Math. Sci. Model., 7(3) (2024), 128-145"

allow for converting these evaluations into a numerical format. This research offers novel fuzzy MCDM approaches for evaluating MW disposal options. This method includes the interval-valued Fermatean Fuzzy Set(IVFFS)-defined entropy, PIPCERIA(the PIvot Pairwise RElative Criteria Importance Assessment), and MARCOS(the Measurement of Alternatives and Ranking based on COmpromise Solution) methods. In the MCDM process, attribute weights play a vital role. In this study, IVFFS-entropy and IVFFS-PIPCERIA methods will be used to calculate objective and subjective weights, and IVFFS-MARCOS methods will be used to rank the alternatives.

1.1. Motivation

Pythagorean Fuzzy sets(PFS) introduced by Yager [3] are more efficient in modeling problems with incomplete information than intuitionistic fuzzy sets(IFS), which is due to the flexibility given in the case of PFSs that the sum of squares of membership and non-membership degrees of any element in the PFSs must be less than or equal to 1. The efficiency obtained using PFSs was further improved by utilizing FFSs introduced by Senapati and Yager [4]. In a practical scenario, many real-life problems involve incomplete and vague information. These problems can be modeled better using FFSs than PFSs. However, it may only be possible to give precise Fermatean fuzzy values for some problems with incomplete information in real-life problems.

The IVFF environment-based DM model can reveal obscure information more flexibly and in detail due to its broad scope of application. Therefore, the DM model within the IVFF context demands more attention. The main advantage of IVFFS is that it can be used to model the problem with incomplete and vague information much better than IVPFSs. For example, let us assume that a decision expert (DE) defines the membership value (support) of an alternative as $[0.58, 0.66]$ and DE defines the non-membership value of an alternative as $[0.69, 0.78]$. Here, the sum of squares of an upper bound of the membership value (0.66^3) and an upper bound of the non-membership value (0.78^3) is greater than 1, the given value is neither IVIFS nor IVPFS. However, they can be considered IVFFS since $0.66^3 + 0.78^3 \leq 1$. Hence, the IVFFSs are more capable of modeling problems with incomplete and imprecise information than the IVIFSs and IVPFSs. The main advantage of IVFFS is that it can be used to model the problem with incomplete and vague information much better than IVPFSs. Studies in the literature show that the IVFFS structure is a more flexible and superior way of modeling the vagueness and imprecision of complex MCDM problems. Experts can use the proposed methodology to assign a two-point interval from a predetermined linguistic scale. The interval values are then converted into IVFFNs, which describe the confirmed and undetermined sections of the assessment in lower and upper approximations. The defined structure of IVFFS offers vast opportunities for uncertainty assessment in MW management. It is very easy to determine with the help of IVFFNs what the main criteria are to choose the most suitable MW method with uncertain information. Again, finding the essential criteria in MW disposal evaluation, selecting the most appropriate method for a sustainable world, and ranking the methods can be quickly done with IVFFNs.

1.2. Literature

In human cognitive and DM activities, quantifying the degrees of membership ($\mathscr{M}$) and non-membership degree($\mathscr{N}$) in a single numeric value is only partially justifiable or technically sound. The usage of interval numbers might be involved when there is a need to provide information as intervals instead of single-valued numbers. Instead, it is convenient for the decision-expert(DE) to employ intervals to express his/her preference for $\mathscr{M}$ and $\mathscr{N}$. In some real DM problems, it may be difficult for DEs to precisely quantify their opinions with a crisp number due to insufficient information. Still, they can be represented by an interval number within $[0, 1]$. Therefore, it is essential to present the idea of IVFFSs, which permit the $\mathscr{M}$ and $\mathscr{N}$ to a given set to have an interval value.

The $\mathscr{M}$'s ambiguity and vagueness were illustrated using [5] 's concept of an FS. Atanassov's intuitionistic FS (IFS) [6] links an element's $\mathscr{N}$ to an item, providing a more comprehensive explanation of assessment data. Kirisci [7] has defined the concept of Fibonacci statistical convergence on intuitionistic fuzzy normed space. Yager [3], [8] developed the Pythagorean FS(PFS) idea to broaden the range of $\mathscr{M}$ and $\mathscr{N}$ so that $\mathscr{M}^2 + \mathscr{N}^2 \leq 1$ in response to the IFS vulnerability previously described. Because of this, PFS offers professionals more evaluation opportunities to express their opinions on various objectives. The complexity of the DM framework increases the difficulties specialists have in producing reliable evaluation data. IFS and PFS have been developed to overcome the ambiguity and vagueness brought on by the intricate subjectivity of human cognition. By adding the cubic sum of $\mathscr{M}$ and $\mathscr{N}$, the FFS was the first to broaden the reach of information assertions. As a result, FFS handles ambiguous choice problems more effectively and practically than IFS and PFS. Senapati and Yager [9] initiated the FFS. Senapati and Yager [4], [10] were the first to give the basic features of FFS.

Ejegwa and Onyeke [11] proposed a three-way approach by adding the degree of hesitation to the correlation coefficients related to IFS. Ejegwa et al. [12] modified the distance operators between IFSs belonging to Szmidt and Kacprzyk. Theorems related to the modified distance operators are proven. To overcome the shortcomings of the distance and similarity measurements given in PFSs, Ejegwa et al. [13] gave new measurements with more reliable performance. In the article by Ejegwa et al. [14], a three-way approach to calculating the correlation coefficients between PFSs is proposed using the concepts of variance and covariance. Ejegwa et al. [15] established an FF-composite relation based on a max-average rule to enhance the viability of FFSs in machine learning via a soft computing approach. An innovative Spearman's type FF correlation coefficient method is built to enhance trustworthy insecurity assessment by Ejegwa et al. [16]. Garg et al. [17] have established general aggregation operators, based on Yager's t-norm and t-conorm, to cumulate the FF data in decision-making environments. In [18], a hybrid MCDM based on IVFF was proposed for risk analysis related to autonomous vehicle driving systems. Kirisci [19] defined new correlation coefficients based on the Fermatean hesitant fuzzy elements and interval-valued Fermatean hesitant fuzzy elements. The least common multiple expansion was used in the newly defined correlation coefficients. In [20], a three-way method for computing the correlation coefficients between FFSs has been given using the notions of variance and covariance. New distance and cosine similarity measures amongst FFSs have been defined [21]. A method was established to construct similarity measures between FFSs based on the cosine similarity and Euclidean distance measures. In [22], a new correlation coefficient and weighted correlation coefficient formularization to evaluate the affair between two FFSs have been proposed. In [23], an extended version of the ELECTRE-I model called the FF ELECTRE-I method for multi-criteria group decision-making with FF human assessments has been presented. Kirisci [24] defined the Fermatean hesitant fuzzy set and gave aggregation operations based on the Fermatean hesitant fuzzy set. The interval-valued

Fermatean fuzzy linguistic Kernel Principal Component Analysis model has been given in [25]. The definition of FF soft sets and some properties were introduced [26]. Furthermore, the Fermatean fuzzy soft entropy and the formulas for standard distance measures, such as Hamming and Euclidean distance, were defined [26]. Riaz et al [27] Fermatean developed fuzzy prioritized weighted average and geometric operators. A new model for group decision-making methods in which experts' preferences can be expressed as incomplete FF-preference relations has been presented [28]. A multi-criteria decision-making strategy to evaluate the risk probabilities of autonomous vehicle driving systems by combining the AHP technique with interval-valued FFSs has been proposed in [29]. First, the interval-valued IFS was described in [30]. It represented the $\mathscr{M}$ and $\mathscr{N}$ by the closed subinterval of the interval $[0,1]$. The interval-valued PFS (IVPFS), whose $\mathscr{M}$ and $\mathscr{N}$ are represented by an interval number, was further proposed by [31]. Several operations and relations of IVPFS are also examined. Jeevaraj defined the IVFFS [32].

PIPRECIA is a subjective weighting model, and MARCOS is a ranking model. Objective and subjective criterion weighting models are the two models found in the literature. The contrast intensity of each criterion and conflicts between criteria are used in this approach to describe the objective relevance of the criteria. A relatively new weight-determining tool that avoids the drawbacks of the SWARA tool while retaining its advantages is the PIPRECIA ([33]). The PIPRECIA model's main advantage is that it allows criteria to be evaluated without being sorted by significance rating. Stevic et al. [34] provided an extension of PIPRECIA under FSs and used it to identify the SWOT matrix's components. Demir et al. [35] used the fuzzy SWARA for prioritizing and ranking the criteria in the wind farm installation and used fuzzy MARCOS to determine the most suitable location for the wind farm. Stevic et al. [36] invented the MARCOS, a tool for DM. Combining the ideal and anti-ideal solutions is the foundation for its development. Additionally, the alternatives' utility is measured, and their rank is then determined by computing various utility functions depending on the value of the alternative utilities. Demir et al. [37] reviewed the studies conducted on MARCOS between 2020 and 2024. Mishra et al. [38] gave an integrated MCDM with PF-fairly operator-based entropy, PIPRECIA, and MARCOS methods to solve the sustainable circular supplier selection problem. Farit et al. [39] prepared a hybrid q-step orthopair fuzzy-based methodology including CRITIC and EDAS and proposed this method as a sustainable approach for smart waste management of road freight vehicles. In [40], new cosine and distance measures were defined with cubic m-polar fuzzy sets, and an application was carried out for a sustainable solid waste treatment and recycling approach.

1.3. Necessity

MW produced by healthcare facilities has the potential to endanger patients, staff, the environment, and the general public. One of the most essential choices that healthcare organizations have to make is how to dispose of MW, and there are several conflicting factors and options to consider. On the other hand, when assessing these options, decision experts could be somewhat unsure. Municipal authorities in developing countries need help in selecting appropriate MW disposal strategies. This process can be framed as an MCDM problem involving tangible and intangible criteria.

The following research topics are intended to be addressed by the hybrid framework established by this study:

i. Which factors must be considered when choosing waste disposal techniques in the healthcare sector?

ii. How can the existing methodologies derive the significance weights of the established evaluation criteria?

iii. How effective is it to rank healthcare waste disposal options using the IVFF-MARCOS method while objectively determining the criteria weights using the IVFF-entropy and IVFF-PIPCERIA approaches?

iv. Which approach is best for eliminating medical waste in general?

v. How do the suggested approaches fare in scenarios involving the distribution of decision expert weights and other criteria?

vi. Compared to other well-known MCDM techniques, how consistent are the results?

1.4. Originality

MW impacts the environment, the general public, employees, and patients. Selecting a technique for disposing of MW is among the most crucial decisions healthcare institutions must make. This is a complicated problem with multiple competing requirements and options. Nevertheless, decision specialists could feel uncertain about themselves when assessing these possibilities. This research offers novel fuzzy MCDM approaches for evaluating MW disposal options. This method includes the IVFFS-defined entropy, PIPCERIA, and MARCOS methods. One of the biggest challenges that healthcare organizations confront globally is managing the MW that their activities generate. The improper disposal of hazardous waste poses a significant risk to society and can hasten the spread of several pandemic illnesses. The problem of deciding how to get rid of MW needs to be given serious thought right away. Because a MW method selection problem has several criteria and options, it can be classified as an MCDM problem. However, specialists assessing these issues are limited to linguistically assessing the qualitative criteria. Fuzzy logic addresses the ambiguity in these verbal formulations, while MCDM approaches allow for converting these evaluations into a numerical format.

1.5. Research gap

This study uses MCDM techniques based on IVFFLs to rank MW disposal techniques, simulate the associated uncertainty, and optimize their advantages. One urgent issue that the recommended methodology addresses is the planning of MW disposal.

The methodology developed for this work goals to fill in the following research gaps that we identify:

(i) Which criteria will be used to assess the effectiveness of the methods to be used in the MW disposal planning?

(ii) Is utilizing IVFFLs the most effective way to eliminate MW?

(iii) In comparison to other well-known MCDM approaches, how consistent are the results?

(iv) What are the primary and secondary requirements required to evaluate the risk of disposing of MW?

(v) Considering the variables considered, which criterion depends on which?

(vi) Which criteria can be critical in the risk assessment by proving their criticality inside the constructed system?

(vii) What are the best practices for eliminating MW?

(viii) What findings can be made based on the relevant analysis and application that have been completed?

1.6. Contribution

The methodological component of the work states that a strategy based on IVFFLs has been developed to rank the possibilities for disposing of MW. An MCDM issue has been examined in a risk assessment of MW disposal. Furthermore, comparative analyses are performed to confirm the accuracy of the recommended decisions and procedures. The application part also makes it clear that the danger issue surrounding the disposal of MW was solely given technical considerations based on assessments of earlier research publications. It is more challenging for safety specialists to take preventive measures later since they must allow the social setting. Therefore, potential issues could arise.

The main contributions:

1. Using the MCDM framework model, which integrates IVFF-entropy, -PIPCERIA, and -MARCOS methodologies, ensures high safety and security for healthcare practitioners and society by effectively modeling and ranking the hazards associated with MW disposal. Using the proposed methodology, the DEs can identify a range of two scale points from the preset language scale. Once the interval data have been translated into IVFFNs, the confirmed and indeterminate components of the evaluation are further described in lower and higher approximation, respectively.

2. Each alternative's criterion separately assesses the risks associated with MW disposal plans.

3. A comparative study is offered to determine how well the suggested model ranks MW disposal methods.

4. In-depth ramifications are provided based on the findings.

2. Preliminaries

Definition 2.1 ([9]). *Let $\ddot{E}$ be the universal set. The FFS is defined as the set $A = \{(x, \mu_A(x), \upsilon_A(x)) : x \in \ddot{E}\}$, where with $0 \leq \mu_A^3 + \upsilon_A^3 \leq 1$ and $\mu_A, \upsilon_A \in [0,1]$. The hesitation degree has been shown with $\theta_A = (1 - \mu_A^3 + \upsilon_A^3)^{1/3}$.*

Definition 2.2 ([32]). *Let $\ddot{\mathscr{I}}[0,1]$ show the set of all closed subintervals of the unit interval. The IVFFS is defined as $A = \{(x, \mu_A(x), \upsilon_A(x)) : x \in \ddot{E}\}$, where $\mu_A(x), \upsilon_A(x) \in \ddot{\mathscr{I}}[0,1]$ with $0 < \sup_x(\mu_A(x))^3 + \sup_x(\upsilon_A(x))^3 \leq 1$.*

The set $A = \left\{(x, [\mu_A^-(x), \mu_A^+(x)], [\upsilon_A^-(x), \upsilon_A^+(x)]) : x \in \ddot{E}\right\}$, is also defined as IVFFS. Here, $0 \leq (\mu_A^+(x))^3 + (\upsilon_A^+(x))^3 \leq 1$ and $\theta_A = [\theta_A^-, \theta_A^+] = [(1 - (\mu_A^-)^3 + (\upsilon_A^-)^3)^{1/3}, (1 - (\mu_A^+)^3 + (\upsilon_A^+)^3)^{1/3}]$.

Definition 2.3 ([32]). *For IVFFSs* $A = ([\mu_A^-(x), \mu_A^+(x)], [\upsilon_A^-(x), \upsilon_A^+(x)])$,
$A_1 = ([\mu_{A1}^-(x), \mu_{A1}^+(x)], [\upsilon_{A1}^-(x), \upsilon_{A1}^+(x)])$, $A_2 = ([\mu_{A2}^-(x), \mu_{A2}^+(x)], [\upsilon_{A2}^-(x), \upsilon_{A2}^+(x)])$,

- $A_1 \cup A_2 = \left([\max(\mu_{A1}^-, \mu_{A2}^-), \max(\mu_{A1}^+, \mu_{A2}^+)], [\min(\upsilon_{A1}^-, \upsilon_{A2}^-), \min(\upsilon_{A1}^+, \upsilon_{A2}^+)]\right)$
- $A_1 \cap A_2 = \left([\min(\mu_{A1}^-, \mu_{A2}^-), \min(\mu_{A1}^+, \mu_{A2}^+)], [\max(\upsilon_{A1}^-, \upsilon_{A2}^-), \max(\upsilon_{A1}^+, \upsilon_{A2}^+)]\right)$
- $A^c = ([\upsilon_A^-, \upsilon_A^+], [\mu_A^-, \mu_A^+])$
- $A_1 \oplus A_2 = \left(\left[\sqrt[3]{(\mu_{A1}^-(x))^3 + (\mu_{A2}^-(x))^3 - (\mu_{A1}^-(x))^3.(\mu_{A2}^-(x))^3}, \right.\right.$
  $\left.\left. \sqrt[3]{(\mu_{A1}^+(x))^3 + (\mu_{A2}^+(x))^3 - (\mu_{A1}^+(x))^3.(\mu_{A2}^+(x))^3} \right], \left[\upsilon_{A1}^- \upsilon_{A2}^-, \upsilon_{A1}^+ \upsilon_{A2}^+\right] \right)$
- $A_1 \otimes A_2 = \left(\left[\mu_{A1}^- \mu_{A2}^-, \mu_{A1}^+ \mu_{A2}^+\right], \left[\sqrt[3]{(\upsilon_{A1}^-(x))^3 + (\upsilon_{A2}^-(x))^3 - (\upsilon_{A1}^-(x))^3.((\upsilon_{A2}^-)(x))^3}, \right.\right.$
  $\left.\left. \sqrt[3]{(\upsilon_{A1}^+(x))^3 + (\upsilon_{A2}^+(x))^3 - (\upsilon_{A1}^+(x))^3.(\upsilon_{A2}^+(x))^3} \right] \right)$

- $\lambda A = \left(\left[\sqrt[3]{1-\left(1-(\mu_A^-)^3\right)^\lambda}, \sqrt[3]{1-\left(1-(\mu_A^+)^3\right)^\lambda} \right], \left[(\upsilon_A^-)^\lambda, (\upsilon_A^+)^\lambda \right] \right)$
- $A^\lambda = \left(\left[(\mu_A^-)^\lambda, (\mu_A^+)^\lambda \right], \left[\sqrt[3]{1-\left(1-(\upsilon_A^-)^3\right)^\lambda}, \sqrt[3]{1-\left(1-(\upsilon_A^+)^3\right)^\lambda} \right] \right)$

Definition 2.4 ([41]). *For the IVFFS* $A = ([\mu_A^-(x), \mu_A^+(x)], [\upsilon_A^-(x), \upsilon_A^+(x)])$,

$$\begin{aligned} SC(A) &= \frac{1}{2}\left([(\mu_A^-(x))^3 + (\mu_A^+(x))^3] - [(\upsilon_A^-(x))^3 + (\upsilon_A^+(x))^3] \right) \\ AC(A) &= \frac{1}{2}\left([(\mu_A^-(x))^3 + (\mu_A^+(x))^3] + [(\upsilon_A^-(x))^3 + (\upsilon_A^+(x))^3] \right) \\ \overline{SC}(A) &= \frac{1}{2}\left(SC(A) + 1 \right) \end{aligned}$$

are called score, accuracy, and normalized score functions, respectively, where $SC(A) \in [-1,1]$, $AC(A) \in [0,1]$, *and* $\overline{SC}(A) \in [0,1]$.

3. Fairly Aggregation Operators for IVFFSs

The fair aggregation operators for FFNs have been defined by [42]. The fair aggregation operators on interval-valued PFSs are presented by [43]. Based on these two studies, fair aggregation operators based on IVFFSs will be defined, and their basic properties will be examined.

For IVFFSs $A_1 = ([(\mu_{A1}^-), (\mu_{A1}^+)], [(\upsilon_{A1}^-), (\upsilon_{A1}^+)])$, $A_2 = ([(\mu_{A2}^-), (\mu_{A2}^+)], [(\upsilon_{A2}^-), (\upsilon_{A2}^+)])$, the fairly operations are defined on FFNs [42], which as

$$\begin{aligned} A_1 \times A_2 = \Bigg\{ & \left[\sqrt[3]{\left(\frac{(\mu_{A1}^-)^3 (\mu_{A2}^-)^3}{(\mu_{A1}^-)^3 (\mu_{A2}^-)^3 + (\upsilon_{A1}^-)^3 (\upsilon_{A2}^-)^3} \right) \times \left(1 - \left(1-(\mu_{A1}^-)^3 - (\upsilon_{A1}^-)^3\right)\left(1-(\mu_{A2}^-)^3 - (\upsilon_{A2}^-)^3\right)\right)}, \right. \\ & \left. \sqrt[3]{\left(\frac{(\mu_{A1}^+)^3 (\mu_{A2}^+)^3}{(\mu_{A1}^+)^3 (\mu_{A2}^+)^3 + (\upsilon_{A1}^+)^3 (\upsilon_{A2}^+)^3} \right) \times \left(1 - \left(1-(\mu_{A1}^+)^3 - (\upsilon_{A1}^+)^3\right)\left(1-(\mu_{A2}^+)^3 - (\upsilon_{A2}^+)^3\right)\right)} \right], \\ & \left[\sqrt[3]{\left(\frac{(\upsilon_{A1}^-)^3 (\upsilon_{A2}^-)^3}{(\mu_{A1}^-)^3 (\mu_{A2}^-)^3 + (\upsilon_{A1}^-)^3 (\upsilon_{A2}^-)^3} \right) \times \left(1 - \left(1-(\mu_{A1}^-)^3 - (\upsilon_{A1}^-)^3\right)\left(1-(\mu_{A2}^-)^3 - (\upsilon_{A2}^-)^3\right)\right)}, \right. \\ & \left. \sqrt[3]{\left(\frac{(\upsilon_{A1}^+)^3 (\upsilon_{A2}^+)^3}{(\mu_{A1}^+)^3 (\mu_{A2}^+)^3 + (\upsilon_{A1}^+)^3 (\upsilon_{A2}^+)^3} \right) \times \left(1 - \left(1-(\mu_{A1}^+)^3 - (\upsilon_{A1}^+)^3\right)\left(1-(\mu_{A2}^+)^3 - (\upsilon_{A2}^+)^3\right)\right)} \right] \Bigg\} \end{aligned}$$

$$\begin{aligned} \lambda * A_i = \Bigg\{ & \left[\sqrt[3]{\left(\frac{(\mu_{Ai}^-)^{3\lambda}}{(\mu_{Ai}^-)^{3\lambda} + (\upsilon_{Ai}^-)^{3\lambda}} \right) \times \left(1 - \left(1-(\mu_{Ai}^-)^3 - (\upsilon_{Ai}^-)^3\right)^\lambda\right)}, \right. \\ & \left. \sqrt[3]{\left(\frac{(\mu_{Ai}^+)^{3\lambda}}{(\mu_{Ai}^+)^{3\lambda} + (\upsilon_{Ai}^+)^{3\lambda}} \right) \times \left(1 - \left(1-(\mu_{Ai}^+)^3 - (\upsilon_{Ai}^+)^3\right)^\lambda\right)} \right], \\ & \left[\sqrt[3]{\left(\frac{(\upsilon_{Ai}^-)^{3\lambda}}{(\upsilon_{Ai}^-)^{3\lambda} + (\upsilon_{Ai}^-)^{3\lambda}} \right) \times \left(1 - \left(1-(\mu_{Ai}^-)^3 - (\upsilon_{Ai}^-)^3\right)^\lambda\right)}, \right. \\ & \left. \sqrt[3]{\left(\frac{(\upsilon_{Ai}^+)^{3\lambda}}{(\upsilon_{Ai}^+)^{3\lambda} + (\upsilon_{Ai}^+)^{3\lambda}} \right) \times \left(1 - \left(1-(\mu_{Ai}^+)^3 - (\upsilon_{Ai}^+)^3\right)^\lambda\right)} \right] \Bigg\}, \quad \lambda > 0 \end{aligned}$$

Proposition 3.1. *Take two IVFFSs* $A_1 = ([(\mu_{A1}^-), (\mu_{A1}^+)], [(\upsilon_{A1}^-), (\upsilon_{A1}^+)])$, $A_2 = ([(\mu_{A2}^-), (\mu_{A2}^+)], [(\upsilon_{A2}^-), (\upsilon_{A2}^+)])$. *For* $\lambda > 0$, *if* $\mu_{A_1} = \upsilon_{A_1}$ *and* $\mu_{A_2} = \upsilon_{A_2}$ *,then*

i. $\mu_{A_1 \otimes A_2} = \upsilon_{A_1 \otimes A_2}$,
ii. $\mu_{\lambda * A_1} = \upsilon_{\lambda * A_1}$.

Proof. (i.) If $\mu_{A_1} = \upsilon_{A_1}$ and $\mu_{A_2} = \upsilon_{A_2}$,then $\frac{\mu_{A_1 \otimes A_2}}{\upsilon_{A_1 \otimes A_2}} = 1$ and $\mu_{A_1 \otimes A_2} = \upsilon_{A_1 \otimes A_2}$.
(ii.) Using the (i.), $\mu_{\lambda * A_1} = \upsilon_{\lambda * A_1}$ is obtained. □

Proposition 3.2. *For any two IVFFSs* $A_1 = ([(\mu_{A1}^-), (\mu_{A1}^+)], [(\upsilon_{A1}^-), (\upsilon_{A1}^+)])$, $A_2 = ([(\mu_{A2}^-), (\mu_{A2}^+)], [(\upsilon_{A2}^-), (\upsilon_{A2}^+)])$ *and* $\lambda, \lambda_1, \lambda_2 > 0$,

i. $A_1 \otimes A_2 = A_2 \otimes A_1$,
ii. $\lambda(A_1 \otimes A_2) = (\lambda * A_1) \otimes (\lambda * A_1)$,
iii. $(\lambda_1 + \lambda_2) * A_i = (\lambda_1 * A_i) \otimes (\lambda_2 * A_i)$.

Definition 3.3. *Consider a set of IVFFNs* $A_i = ([(\mu_{Ai}^-),(\mu_{Ai}^+)],[(\upsilon_{Ai}^-),(\upsilon_{Ai}^+)])$ *and let* ω_i *be a weight of* A_i*. Then, the IVFF fairly weighted aggregation operator is given by*

$$IVFFWF(A_1,A_2,\cdots,A_n) = (\omega_1 * A_1) \otimes (\omega_2 * A_2) \otimes \cdots (\omega_n * A_n).$$

Theorem 3.4. *The aggregation with the IVFFWF operator is an IVFFN and presented by*

$$\begin{aligned} IVFFWF(A_1,A_2,\cdots,A_n) \quad = \quad & \left\{ \left[\sqrt[3]{\frac{\prod_{i=1}^n (\mu_i^-)^{3\omega_i}}{\prod_{i=1}^n (\mu_i^-)^{3\omega_i} + \prod_{i=1}^n (\upsilon_i^-)^{3\omega_i}} \times \left(1 - \prod_{i=1}^n \left(1-(\mu_i^-)^3 - (\mu_i^-)^3\right)^{\omega_i} \right)}, \right. \right. \\ & \left. \sqrt[3]{\frac{\prod_{i=1}^n (\mu_i^+)^{3\omega_i}}{\prod_{i=1}^n (\mu_i^+)^{3\omega_i} + \prod_{i=1}^n (\upsilon_i^+)^{3\omega_i}} \times \left(1 - \prod_{i=1}^n \left(1-(\mu_i^+)^3 - (\mu_i^+)^3\right)^{\omega_i} \right)} \right], \\ & \left[\sqrt[3]{\frac{\prod_{i=1}^n (\upsilon_i^-)^{3\omega_i}}{\prod_{i=1}^n (\mu_i^-)^{3\omega_i} + \prod_{i=1}^n (\upsilon_i^-)^{3\omega_i}} \times \left(1 - \prod_{i=1}^n \left(1-(\mu_i^-)^3 - (\mu_i^-)^3\right)^{\omega_i} \right)}, \right. \\ & \left. \left. \sqrt[3]{\frac{\prod_{i=1}^n (\upsilon_i^+)^{3\omega_i}}{\prod_{i=1}^n (\mu_i^+)^{3\omega_i} + \prod_{i=1}^n (\upsilon_i^+)^{3\omega_i}} \times \left(1 - \prod_{i=1}^n \left(1-(\mu_i^+)^3 - (\mu_i^+)^3\right)^{\omega_i} \right)} \right] \right\}. \end{aligned} \tag{3.1}$$

Proof. To prove this theorem, the Mathematical Induction Principle will be used.

For $n = 2$, Equation 3.1 becomes $IVFFWF(A_1,A_2) = (\omega_1 * A_1) \otimes (\omega_2 * A_2)$. Then,

$$\begin{aligned} IVFFWF(A_1,A_2) \quad = \quad & \left\{ \left[\sqrt[3]{\frac{\prod_{i=1}^2 (\mu_i^-)^{3\omega_i}}{\prod_{i=1}^2 (\mu_i^-)^{3\omega_i} + \prod_{i=1}^2 (\upsilon_i^-)^{3\omega_i}} \times \left(1 - \prod_{i=1}^2 \left(1-(\mu_i^-)^3 - (\mu_i^-)^3\right)^{\omega_i} \right)}, \right. \right. \\ & \left. \sqrt[3]{\frac{\prod_{i=1}^2 (\mu_i^+)^{3\omega_i}}{\prod_{i=1}^2 (\mu_i^+)^{3\omega_i} + \prod_{i=1}^2 (\upsilon_i^+)^{3\omega_i}} \times \left(1 - \prod_{i=1}^2 \left(1-(\mu_i^+)^3 - (\mu_i^+)^3\right)^{\omega_i} \right)} \right], \\ & \left[\sqrt[3]{\frac{\prod_{i=1}^2 (\upsilon_i^-)^{3\omega_i}}{\prod_{i=1}^2 (\mu_i^-)^{3\omega_i} + \prod_{i=1}^2 (\upsilon_i^-)^{3\omega_i}} \times \left(1 - \prod_{i=1}^2 \left(1-(\mu_i^-)^3 - (\mu_i^-)^3\right)^{\omega_i} \right)}, \right. \\ & \left. \left. \sqrt[3]{\frac{\prod_{i=1}^2 (\upsilon_i^+)^{3\omega_i}}{\prod_{i=1}^2 (\mu_i^+)^{3\omega_i} + \prod_{i=1}^2 (\upsilon_i^+)^{3\omega_i}} \times \left(1 - \prod_{i=1}^2 \left(1-(\mu_i^+)^3 - (\mu_i^+)^3\right)^{\omega_i} \right)} \right] \right\}. \end{aligned}$$

That is Equation 3.1 holds for $n = 2$. Now, let Equation 3.1 hold for $n = k$. Then, it will be shown that Equation 3.1 is valid for $n = k+1$:

$$\begin{aligned} IVFFWF(A_1,A_2,\cdots,A_n,A_{n+1}) \quad = \quad & \left\{ \left[\sqrt[3]{\frac{\prod_{i=1}^n (\mu_i^-)^{3\omega_i}}{\prod_{i=1}^n (\mu_i^-)^{3\omega_i} + \prod_{i=1}^n (\upsilon_i^-)^{3\omega_i}} \times \left(1 - \prod_{i=1}^n \left(1-(\mu_i^-)^3 - (\mu_i^-)^3\right)^{\omega_i} \right)}, \right. \right. \\ & \left. \sqrt[3]{\frac{\prod_{i=1}^n (\mu_i^+)^{3\omega_i}}{\prod_{i=1}^n (\mu_i^+)^{3\omega_i} + \prod_{i=1}^n (\upsilon_i^+)^{3\omega_i}} \times \left(1 - \prod_{i=1}^n \left(1-(\mu_i^+)^3 - (\mu_i^+)^3\right)^{\omega_i} \right)} \right], \\ & \left[\sqrt[3]{\frac{\prod_{i=1}^n (\upsilon_i^-)^{3\omega_i}}{\prod_{i=1}^n (\mu_i^-)^{3\omega_i} + \prod_{i=1}^n (\upsilon_i^-)^{3\omega_i}} \times \left(1 - \prod_{i=1}^n \left(1-(\mu_i^-)^3 - (\mu_i^-)^3\right)^{\omega_i} \right)}, \right. \\ & \left. \left. \sqrt[3]{\frac{\prod_{i=1}^n (\upsilon_i^+)^{3\omega_i}}{\prod_{i=1}^n (\mu_i^+)^{3\omega_i} + \prod_{i=1}^n (\upsilon_i^+)^{3\omega_i}} \times \left(1 - \prod_{i=1}^n \left(1-(\mu_i^+)^3 - (\mu_i^+)^3\right)^{\omega_i} \right)} \right] \right\} \\ & \otimes \sqrt[3]{\frac{(\mu_{k+1}^-)^{3\omega_{k+1}}}{(\mu_{k+1}^-)^{3\omega_{k+1}} + (\upsilon_{k+1}^-)^{3\omega_{k+1}}} \times \left(1 - \left(1-(\mu_{k+1}^-)^3 - (\mu_{k+1}^-)^3\right)^{\omega_{k+1}} \right)}, \\ & \left[\sqrt[3]{\frac{(\mu_{k+1}^+)^{3\omega_{k+1}}}{(\mu_{k+1}^+)^{3\omega_{k+1}} + (\upsilon_{k+1}^+)^{3\omega_{k+1}}} \times \left(1 - \left(1-(\mu_{k+1}^+)^3 - (\mu_{k+1}^+)^3\right)^{\omega_{k+1}} \right)}, \right. \\ & \left. \sqrt[3]{\frac{(\upsilon_{k+1}^-)^{3\omega_{k+1}}}{(\mu_{k+1}^-)^{3\omega_{k+1}} + (\upsilon_{k+1}^-)^{3\omega_{k+1}}} \times \left(1 - \left(1-(\mu_{k+1}^-)^3 - (\mu_{k+1}^-)^3\right)^{\omega_{k+1}} \right)}, \right. \\ & \left. \left. \sqrt[3]{\frac{(\upsilon_{k+1}^+)^{3\omega_{k+1}}}{(\mu_{k+1}^+)^{3\omega_{k+1}} + (\upsilon_{k+1}^+)^{3\omega_{k+1}}} \times \left(1 - \left(1-(\mu_{k+1}^+)^3 - (\mu_{k+1}^+)^3\right)^{\omega_{k+1}} \right)} \right] \right\}. \end{aligned}$$

Using Definition 3.3, it is seen that Equation 3.1 is valid for $n = k+1$. That is, Equation 3.1 is true for all n. □

Definition 3.5. *Consider a set of IVFFNs* $A_i = ([(\mu_{Ai}^-),(\mu_{Ai}^+)],[(\upsilon_{Ai}^-),(\upsilon_{Ai}^+)])$ *and let* ω_i *be a weight of* A_i. *Let* $(\sigma(1),\sigma(2),\cdots,\sigma_(n))$ *be signify permutation of* $(1,2,\cdots,n)$ *with* $A_{\sigma(i-1)} \geq A_{\sigma(i)}$. *Then, the IVFF fairly ordered weighted aggregation operator is given by*

$$IVFFOWF(A_1,A_2,\cdots,A_n) = (\omega_1 * F_{\sigma(1)}) \otimes (\omega_2 * F_{\sigma(2)}) \otimes \cdots (\omega_n * A_{\sigma(n)}).$$

Theorem 3.6. *The aggregation with the IVFFOWFF operator is an IVFFN and presented by*

$$\begin{aligned} IVFFOWF(A_1,A_2,\cdots,A_n) \quad = \quad & \left\{ \left[\sqrt[3]{\frac{\prod_{i=1}^n (\mu_{\sigma(i)}^-)^{3\omega_i}}{\prod_{i=1}^n (\mu_{\sigma(i)}^-)^{3\omega_i} + \prod_{i=1}^n (\upsilon_{\sigma(i)}^-)^{3\omega_i}}} \times \left(1 - \prod_{i=1}^n \left(1 - (\mu_{\sigma(i)}^-)^3 - (\mu_{\sigma(i)}^-)^3 \right)^{\omega_i} \right), \right. \right. \\ & \left. \sqrt[3]{\frac{\prod_{i=1}^n (\mu_{\sigma(i)}^+)^{3\omega_i}}{\prod_{i=1}^n (\mu_{\sigma(i)}^+)^{3\omega_i} + \prod_{i=1}^n (\upsilon_{\sigma(i)}^+)^{3\omega_i}}} \times \left(1 - \prod_{i=1}^n \left(1 - (\mu_{\sigma(i)}^+)^3 - (\mu_{\sigma(i)}^+)^3 \right)^{\omega_i} \right) \right], \\ & \left[\sqrt[3]{\frac{\prod_{i=1}^n (\upsilon_{\sigma(i)}^-)^{3\omega_i}}{\prod_{i=1}^n (\mu_{\sigma(i)}^-)^{3\omega_i} + \prod_{i=1}^n (\upsilon_{\sigma(i)}^-)^{3\omega_i}}} \times \left(1 - \prod_{i=1}^n \left(1 - (\mu_{\sigma(i)}^-)^3 - (\mu_{\sigma(i)}^-)^3 \right)^{\omega_i} \right), \right. \\ & \left. \left. \sqrt[3]{\frac{\prod_{i=1}^n (\upsilon_{\sigma(i)}^+)^{3\omega_i}}{\prod_{i=1}^n (\mu_{\sigma(i)}^+)^{3\omega_i} + \prod_{i=1}^n (\upsilon_{\sigma(i)}^+)^{3\omega_i}}} \times \left(1 - \prod_{i=1}^n \left(1 - (\mu_{\sigma(i)}^+)^3 - (\mu_{\sigma(i)}^+)^3 \right)^{\omega_i} \right) \right] \right\}. \end{aligned}$$

Proof. It can be proven in a similar way to Theorem 3.4. □

Using Theorems 3.4 and 3.6, the following properties can be given:

Idempotency: If all IVFFNs $A_i = ([(\mu_{Ai}^-),(\mu_{Ai}^+)],[(\upsilon_{Ai}^-),(\upsilon_{Ai}^+)])$ are identical, i.e., $A_i = A$, then $IVFFWF(A_1,A_2,\cdots,A_n) = A$ and $IVFFWF(A_1,A_2,\cdots,A_n) = A$.

Boundedness: For a set of IVFFNs $A_i = ([(\mu_{Ai}^-),(\mu_{Ai}^+)],[(\upsilon_{Ai}^-),(\upsilon_{Ai}^+)])$, let $A^- = ([\min_i(\mu_{Ai}^-),\min_i(\mu_{Ai}^+)],[\max_i(\upsilon_{Ai}^-),\max_i(\upsilon_{Ai}^+)])$ and $A^+ = ([\max_i(\mu_{Ai}^-),\max_i(\mu_{Ai}^+)],[\min_i(\upsilon_{Ai}^-),\min_i(\upsilon_{Ai}^+)])$. Then

$$A^- \leq IVFFWF(A_1,A_2,\cdots,A_n) \leq A^+,$$
$$A^- \leq IVFFOWF(A_1,A_2,\cdots,A_n) \leq A^+.$$

Monotonicity: Consider $A_i = ([(\mu_{Ai}^-),(\mu_{Ai}^+)],[(\upsilon_{Ai}^-),(\upsilon_{Ai}^+)])$ and $A_i* = ([(\mu_{Ai}^-)*,(\mu_{Ai}^+)*],[(\upsilon_{Ai}^-)*,(\upsilon_{Ai}^+)]*)$ be collections of IVFFNs. If $(\mu_{Ai}^-)* \leq (\mu_{Ai}^-)$, $(\mu_{Ai}^+)* \leq (\mu_{Ai}^+)$, $(\upsilon_{Ai}^-)* \geq (\upsilon_{Ai}^-)$ and $(\upsilon_{Ai}^+)* \geq (\upsilon_{Ai}^+)$, then

$$IVFFWF(A_1*,A_2*,\cdots,A_n*) \leq IVFFWF(A_1,A_2,\cdots,A_n),$$
$$IVFFOWF(A_1*,A_2*,\cdots,A_n*) \leq IVFFOWF(A_1,A_2,\cdots,A_n).$$

4. IVFF-entropy Measure

Peng and Li [44] have given IVPFS-similarity measures, -distance measures, and -entropy. Kirisci [26] has presented a definition of the FF soft entropy and also acquired the formulae for standard distance measures such as Hamming and Euclidean distance. Based on Kirisci [26] entropy measure for FFSS we develop new entropy measure for IVFFS.

Definition 4.1. *Let A and B be two IVFFSs. A real-valued function* $E : IVFFS(\ddot{E}) \to [0,1]$ *is called an entropy for IVFFSs with the following properties:*

Ent1. $0 \leq E(A) \leq 1$,
Ent2. $E(A) = 0$ *if and only if A is a crisp set,*
Ent3. $E(A) = 1$ *if and only if* $(\mu_{Ai}^-)(x_i) = (\upsilon_{Ai}^-)(x_i)$, $(\mu_{Ai}^+)(x_i) = (\upsilon_{Ai}^+)(x_i)$ *for each* $x_i \in \ddot{E}$,
Ent4. $E(A) = E(A^c)$,
Ent5. $E(A) \leq E(B)$ *if and only if*

- *If* $(\mu_{Ai}^-)(x_i) \leq (\upsilon_{Ai}^-)(x_i)$, $(\mu_{Ai}^+)(x_i) \leq (\upsilon_{Ai}^+)(x_i)$, *then* $A \subseteq B$,
- *If* $(\mu_{Ai}^-)(x_i) \geq (\upsilon_{Ai}^-)(x_i)$, $(\mu_{Ai}^+)(x_i) \geq (\upsilon_{Ai}^+)(x_i)$, *then* $A \supseteq B$.

Theorem 4.2. *The entropy measure is given as*

$$E_t(A) \quad = \quad 1 - \sqrt[t]{\frac{1}{2n} \sum_{i=1}^n \left(\left| ((\mu_{Ai}^-)(x_i))^3 - ((\upsilon_{Ai}^-)(x_i))^3 \right|^t + \left| ((\mu_{Ai}^+)(x_i))^3 - ((\upsilon_{Ai}^+)(x_i))^3 \right|^t \right)}. \tag{4.1}$$

Proof. It must be shown that $E_t(A)$ satisfies the conditions in Definition 4.1. It is straightforward to show axioms $[Ent1.] - [Ent4.]$. To save space, let's prove only axiom $[Ent5.]$.
1. If $(\mu_{Ai}^-)(x_i) \leq (\upsilon_{Ai}^-)(x_i)$, $(\mu_{Ai}^+)(x_i) \leq (\upsilon_{Ai}^+)(x_i)$, then $A \subseteq B$: We have,

$$(\mu_{Ai}^-)(x_i) \leq \mu_{Bi}^-(x_i) \leq \upsilon_{Bi}^-(x_i) \leq (\upsilon_{Ai}^-)(x_i),$$
$$(\mu_{Ai}^+)(x_i) \leq \mu_{Bi}^+(x_i) \leq \upsilon_{Bi}^+(x_i) \leq (\upsilon_{Ai}^+)(x_i).$$

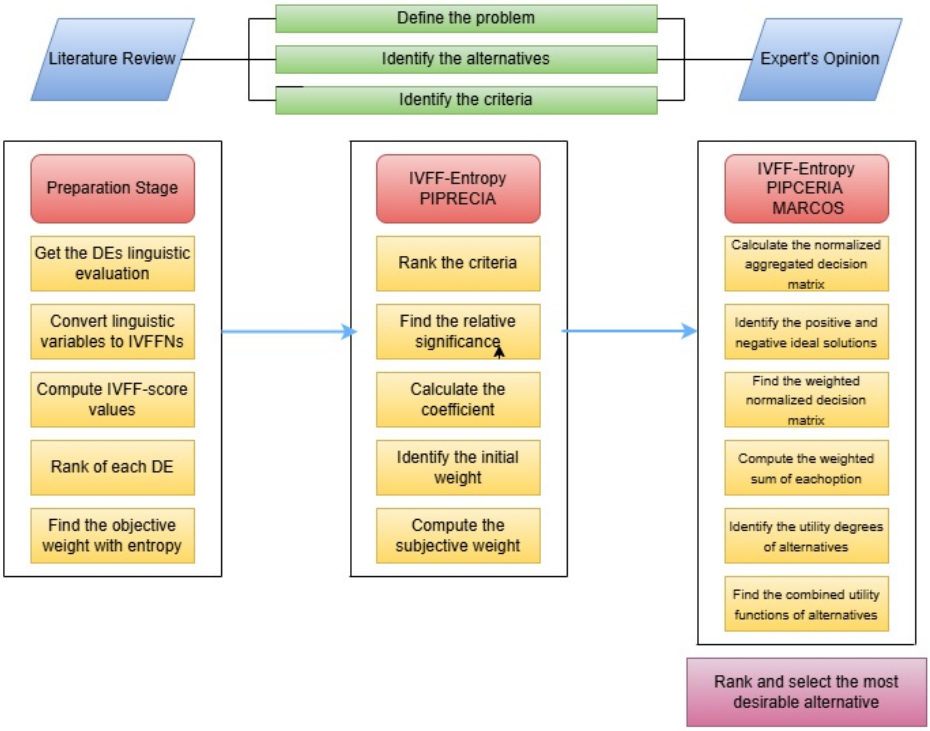

Figure 5.1: Flowchart of method

Therefore,

$$\left|((\mu_{Ai}^{-})(x_i))^3 - ((\upsilon_{Ai}^{-})(x_i))^3\right| \geq \left|(\mu_{Bi}^{-}(x_i))^3 - (\upsilon_{Bi}^{-}(x_i))^3\right|,$$
$$\left|((\mu_{Ai}^{+})(x_i))^3 - ((\upsilon_{Ai}^{+})(x_i))^3\right| \geq \left|(\mu_{Bi}^{+}(x_i))^3 - (\upsilon_{Bi}^{+}(x_i))^3\right|.$$

Thus,

$$1 - \sqrt[t]{\frac{1}{2n}\sum_{i=1}^{n}\left(\left|((\mu_{Ai}^{-})(x_i))^3 - ((\upsilon_{Ai}^{-})(x_i))^3\right|^t + \left|((\mu_{Ai}^{+})(x_i))^3 - ((\upsilon_{Ai}^{+})(x_i))^3\right|^t\right)}$$
$$\leq 1 - \sqrt[t]{\frac{1}{2n}\sum_{i=1}^{n}\left(\left|(\mu_{Bi}^{-}(x_i))^3 - (\upsilon_{Bi}^{-}(x_i))^3\right|^t + \left|(\mu_{Bi}^{+}(x_i))^3 - (\upsilon_{Bi}^{+}(x_i))^3\right|^t\right)}.$$

So, $E_t(A) \leq E_t(B)$.

2. If $(\mu_{Ai}^{-})(x_i) \geq (\upsilon_{Ai}^{-})(x_i)$, $(\mu_{Ai}^{+})(x_i) \geq (\upsilon_{Ai}^{+})(x_i)$, then $A \supseteq B$: Similarly, It can be shown that $E_t(A) \leq E_t(B)$ is the same for this condition. □

5. Proposed Method

When there are several alternative outcomes of a particular event, but their likelihood is unknown, this is known as uncertainty. As a result, the DM must comprehend uncertainty. It takes time and effort to comprehend the likelihood that events will occur in reality. Consequently, there is uncertainty at every stage of the DM process. A solid basis for logical reasoning with vague and imperfect data is provided by fuzzy logic theory. Thanks to fuzzy logic theory, computers can understand human language and apply human knowledge. At this point, it starts employing symbols instead of numerical expressions. Fuzzy sets (FS) are symbolic expressions of this type. FSs are known to include choice variables, such as probability states. FSs are generated when each alternative is assigned an objective membership degree ($\mathscr{M}$) instead of the corresponding probability values.

This study proposes an integrated approach to treating the MCDM problems under IVFFSs by integrating the IVFF-entropy, -PIPRECIA, and -MARCOS tools. The core principles of IVFFSs and the corresponding MCDM techniques have been described independently utilizing pseudo representations (Figure 5.1).

Using the newly created IVFF-entropy and suggested IVPF fairly WFA operator, we provide a hybrid integrated IVFF-entropy-PIPRECIA-MARCOS model. Here, the criteria weights are estimated using the entropy-PIPRECIA model, which is discussed in the context of IVFFS. At the same time, the integrated IVFF-MARCOS model is used to determine the options' rank.

Consider the DEs set $U=\{U_1,U_2,\cdots,U_t\}$ to choice the appropriate option among a set of options $S=\{S_1,S_2,\cdots,S_m\}$ over th criterion set $D=\{D_1,D_2,\cdots,D_n\}$. Suppose that the $M=(\mu_{ij})_{m\times n}$ be a linguistic decision matrix (DEMA) for DEs. Therefore, convert it into an FF-DEMA using linguistic scales.

In order to find the weight of DEs, the significance ratings of DEs are primarily defined by linguistic values and then expressed in the form of FFNs. Let $F_s=([\mu_{F_{sL}},\mu_{F_{sU}}],[\upsilon_{F_{sL}},\upsilon_{F_{sU}}])$ be a IVFFN of sth DE. Hence, the expression for finding the weight is given by

$$\vartheta_s=\frac{1}{2}\left(\frac{\frac{1}{2}\left((\mu_{Fs}^{-})^3+(\mu_{Fs}^{+})^3-(\upsilon_{Fs}^{-})^3-(\upsilon_{Fs}^{+})^3\right)+1}{\sum_{s=1}^{t}\left[\frac{1}{2}\left((\mu_{Fs}^{-})^3+(\mu_{Fs}^{+})^3-(\upsilon_{Fs}^{-})^3-(\upsilon_{Fs}^{+})^3\right)+1\right]}+\frac{s-\overline{SC}(s)+1}{\sum_{s=1}^{t}\left(s-\overline{SC}(s)+1\right)}\right) \tag{5.1}$$

where $\vartheta_s\geq 0$ and $\sum_{s=1}^{t}\vartheta_s=1$.

The steps of our proposed method shown in Figure 5.1 are given below:

Entropy assesses the aspirational information by the substance of confirmed information. The entropy could estimate the vague information. The information entropy can adjust the course of DM because existent contrasts among plentiful details can measure it and clarify the internal information for DEs. A novel entropy approach for calculating the objective weights is presented in Theorem 4.2.

Determine objective weight of each criterion with IVFF-entropy:

For an information entropy $E_j=\frac{1}{m}\sum_{i=1}^{m}E_{ij}\ j=1,2,\cdots,n$ of criteria, then the objective weights

$$\omega_j^{O}=\frac{1-E_j}{\sum_{j=1}^{n}(1-E_j)}. \tag{5.2}$$

where E_{ij} signifies the entropy and given in Equation 4.1.

We use the IVFF-PIPRECIA model for subjective weights. In this approach, first, the appropriate assessment criteria are considered, and their expected significance using the FF-score function rating is found.

Step 1: Starting with the second criterion, DMs evaluate the criteria in order to obtain the relative importance of the criteria, given as

$$s_j=\begin{cases}1+[\overline{SC}(U_j)-\overline{SC}(U_{j-1})] & , \quad if \quad U_j>U_{j-1},\\ 1 & , \quad if \quad U_j=U_{j-1},\\ 1-[\overline{SC}(U_{j-1})-\overline{SC}(U_j)] & , \quad if \quad U_j<U_{j-1},\end{cases} \tag{5.3}$$

where U_j and U_{j-1} symbolize the significance rating of the criterion jth and $(j-1)$th criterion, respectively.

Step 2: Based on relative significance, compute the coefficient by

$$K_j=\begin{cases}1 & , \quad if \quad j=1,\\ 2-s_j & , \quad if \quad j>1.\end{cases} \tag{5.4}$$

Step 3: Determine the initial weight by

$$Q_j=\begin{cases}1 & , \quad if \quad j=1,\\ \frac{Q_{j-1}}{K_j} & , \quad if \quad j>1.\end{cases}$$

Step 4: Obtain the subjective weight of jth criterion by

$$\omega_j^{s}=\frac{Q_j}{\sum_{j=1}^{n}Q_j}, \quad \forall j.$$

Step 5: An integrated weight-determining model is presented as

$$\omega_j=\alpha\omega_j^{O}+(1-\alpha)\omega_j^{s} \tag{5.5}$$

to get the benefits of objective and subjective weighting models, where $j=1,2,\cdots,n$ and $\alpha\in[0,1]$ represents the strategic coefficient to assess the changes of criterion weights.

The FF-MARCOS method is given, which describes the association between options and the ideal and negative-ideal alternatives on IVFF-information.

Step 6: Normalized the aggregated FF-DEMA by

$$N_{ij}=\begin{cases}([\mu_{ijF}^{-},\mu_{ijF}^{+}],[\upsilon_{ijF}^{-},\upsilon_{ijF}^{+}]) & , \quad \textit{for benefit-type criteria},\\ ([\upsilon_{ijF}^{-},\upsilon_{ijF}^{+}],[\mu_{ijF}^{-},\mu_{ijF}^{+}]) & , \quad \textit{for cost-type criteria}.\end{cases}$$

Step 7: Computing positive ideal solutions and negative ideal solutions by

$$N_j^+ = \max_i N_{ij} \quad and \quad N_j^- = \min_i N_{ij}.$$

Step 8: Find the weighted normalized IVFF-DEMA using the Equation 3.1.

Step 9: Obtain the weighted sum of each option using score function by

$$S_i = \sum_{j=1}^{n} \overline{(}SC)(N_{ij}), \tag{5.6}$$

where $\overline{(}SC)(N_{ij})$ signifies the score values of each element of the weighted normalized IVFF-DEMA.

Step 10: Computing the utility degree with the following equations:

$$U_i^- = \frac{S_i}{S_{PIS}} \quad and \quad U_i^+ = \frac{S_i}{S_{NIS}},$$

where S_{PIS} and S_{NIS} signify the sum of score degrees of weighted values N_j^+ and N_j^-.

Step 11: For $f(U_i^+) = \frac{U_i^-}{U_i^- + U_i^+}$ and $f(U_i^-) = \frac{U_i^+}{U_i^- + U_i^+}$, the final values of utility functions by

$$f(U_i) = \frac{U_i^+ + U_i^-}{1 + \frac{1-f(U_i^+)}{f(U_i^+)} + \frac{1-f(U_i^-)}{f(U_i^-)}}. \tag{5.7}$$

Step 12: Rank the options according to the Equation 5.7. The appropriate choice is the maximum values obtained from Equation 5.7.

6. Results

6.1. Problem design

In the healthcare industry, waste management is essential. Waste handlers, the public, and medical professionals risk getting sick, suffering negative consequences, getting hurt, or contaminating the environment when MW is not properly managed. To reduce the adverse health effects of destructive behaviors, like exposure to infectious germs and toxic substances, managing MW requires greater attention and commitment. For progress to be universal, long-lasting, and sustainable, government assistance and effort are needed [45]. Because MW infects other animals with infectious diseases, it affects the ecology. Hospital employees risk infection from these MWs, which could harm their health. Along with other essential components and workable solutions, planning for MW management is an important issue that needs to be addressed. Figure 5.1 depicts the MW disposal selection problem in an MCDM architecture.

Incineration is a common disposal technique in underdeveloped countries due to its ease of use, safety, and practicality [46]. More important than 800 degrees Celsius is the temperature at the incinerator's exit. Most organic materials can be burned at this high temperature, eliminating pathogens and converting them to inorganic dust. After incineration, solid waste can be cut by $85-90\%$ [47]. Burning MWs other than radioactive and explosive wastes is an option. Several facilities offer waste processing, incineration, and flue gas purification as additional services for hospital trash combustion. Pyrolysis vaporization, plasma, and rotary kiln incinerators are examples of standard incineration technologies [48].

Chemical disinfection has several uses, and it has been used for a long time. Hospital trash is frequently crushed using mechanical and chemical methods. Chemical disinfectants are frequently mixed with crushed hospital trash and left to sit correctly. Pathogenic bacteria are either killed or put to sleep by disinfection. Organic substances decompose. Because of their low effective concentration, rapid action, homogeneity, and broad sterilizing spectrum, chemical disinfectants effectively eliminate bacteria and germs [49]. Because they are colorless, tasteless, safe, odorless, and readily soluble in water, chemicals like calcium hypochlorite, sodium hypochlorite, and chlorine dioxide are frequently used. Additionally, they have little toxicity, are resistant to both physical and chemical agents, and, once disinfected, pose no concern. When hospital waste volumes are minimal, chemical disinfection methods can be considered.

Encapsulation renders trash immobile by encasing trash in a solid matrix [50]. The nuclear industry's preferred approach to handling low- and intermediate-level radioactive waste has long been encapsulation in cement or its composites. Before disposing of waste in landfills or geological locations, medical sciences enclose it in polyethylene or iron barrels partially filled with inert fillers such as plastic foam, bituminous sand, lime, cement mortar, or clay. This stops sharp things (including scalpels, hypodermic needles, and breakable culture dishes), chemicals, pharmaceutical residues, and incinerator waste from contacting people or the environment.

When burned waste is disposed of, it releases phthalates and other heavy metals like lead, cadmium, and tin into the environment in addition to the dioxin produced during incineration. MW is separated from ordinary municipal solid waste before burning. In addition to being environmentally harmful, burning MW is more costly than disposing of it in a landfill. An alternative to incineration is landfill disposal. However, it is illegal to dispose of biohazardous waste. Particularly in developing nations, MW is routinely dumped in landfills. In a landfill cell, this mechanism isolates MW. To prevent ingress or escape, lime should be placed in MW, and the surrounding area walled off. There are

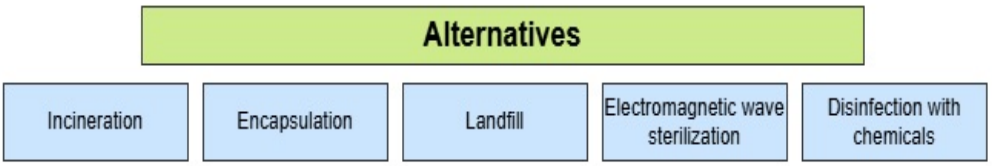

Figure 6.1: Alternatives

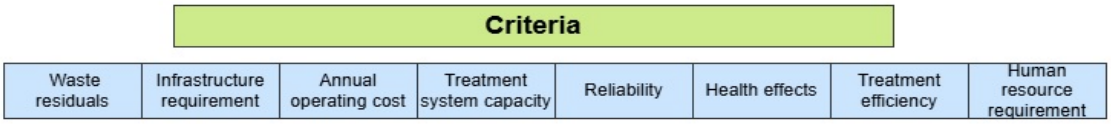

Figure 6.2: Criteria

several things to remember when getting rid of sharp waste. Building a dedicated landfill for MW is advised to properly dispose of hazardous MW and separate it from other forms of waste due to growing public and environmental awareness. During the COVID-19 pandemic, there were severe problems with how to get rid of dangerous medical supplies that affected people left behind.

Microwave technology is a low-temperature, steam-based thermal technique that disinfects with steam and wet heat. Neither water nor steam is used in dry heat treatments. Some use infrared heaters, forced convection, or heated air circulation to heat their waste. Therefore, reverse polymerization occurs in microwave technology at temperatures between 177 and 540 degrees Celsius. High-energy microwaves break down organic molecules. Internal energy is increased when molecules' bonds vibrate or rub against one another due to electromagnetic waves, which have a wavelength of one millimeter to one meter and a frequency of 300–3000 MHz. In a N2 atmosphere, oxygen cannot burn, unlike high-temperature disinfection. Disinfection lowers energy and temperature, preventing heat loss and environmental contamination because it leaves behind a harmless residue.

Alternatives to the application are Figure 6.1: S_1 Incineration, S_2 Encapsulation, S_3 Landfill, S_4 Electromagnetic wave sterilization, S_5 Disinfection with chemicals.

Criteria and their explanations are Figure 6.2: D_1 Waste residuals, D_2 Infrastructure requirement, D_3 Annual operating cost, D_4 Treatment system capacity, D_5 Reliability, D_6 Health effects, D_7 Treatment efficiency, D_8 Human resource requirement. Of these criteria, D_2 and D_3 are cost, and the other criteria are benefits.

6.2. Computation

Table 6.1 shows linguistic terms and their corresponding IVFFNs.

Linguistic Terms	μ_L	μ_U	υ_L	υ_U
Certainly High Importance(CH)	0.95	1	0	0
Very High Importance(VH)	0.8	0.9	0.1	0.2
High Importance(H)	0.7	0.8	0.2	0.3
Slightly More Importance(SM)	0.6	0.65	0.35	0.4
Equally Importance(E)	0.5	0.5	0.5	0.5
Slightly Less Importance(SL)	0.35	0.4	0.6	0.65
Low Importance(L)	0.2	0.3	0.7	0.8
Very Low Importance(VL)	0.1	0.2	0.8	0.9
Certainly Low Importance(CL)	0	0	0.95	1

Table 6.1: Scale Values according to IVFF

Step 1: Consider the alternative set S_i $(1,2,3,4,5)$, the criteria set D_j $(j = 1,2,\cdots,8)$, and the DEs set $U = \{U_1,U_2,U_3\}$.

Step 2: The linguistic variables of the DEs' weights are given as $U_1 = CH, U_2 = VH, U_3 = H$. The IVFFNs related to the linguistic variables are represented in Table 6.1. This information calculates the DEs' weights using Equation 5.1, and $\omega = \{0.38,0.32,0.30\}$ is obtained.

Step 3: Create the aggregated IVFF-DEMA with Definition 3.3 (Tables 6.2, 6.3).

The IVFF-entropy and IVFF-PIPRECIA model will be used to find the criteria weights. The criteria' objective weights are computed using Equation 5.2. Then, we have $\omega_1^O = 0.093$, $\omega_2^O = 0.123$, $\omega_3^O = 0.147$, $\omega_4^O = 0.105$, $\omega_5^O = 0.1$, $\omega_6^O = 0.187$, $\omega_7^O = 0.105$, $\omega_8^O = 0.14$.

	S_1	§2	S_3	S_4	S_5
D_1	(H, H, E)	(SM, E, H)	(E, SL, VL)	(H, SM, E)	(SL, E, SM)
D_2	(H, SL, SM)	(E, VH, H)	(SL, SM, H)	(H, E, SM)	(L, L, E)
D_3	(SL, E, SM)	(SL, E, H)	(H, VH, H)	(VH, H, VH)	(H, SL, SM)
D_4	(SL, E, H)	(SL, SM, VH)	(VH, E, H)	(SL, SL, VH)	(SL, E, H)
D_5	(SM, E, E)	(SM, SL, E)	(SL, SM, H)	(SL, H, H)	(E, SL, VL)
D_6	(CH, H, SM)	(SL, SM, L)	(VL, SM, L)	(VH, H, E)	(SM, E, H)
D_7	(H, SM, E)	(SL, SM, L)	(L, VL, L)	(E, SM, E)	(H, SL, SM)
D_8	(SL, E, H)	(H, VH, VH)	(E, H, VH)	(SL, E, H)	(E, SM, E)

Table 6.2: IVFFNs of linguistic values given by DEs

	S_1	S_2	S_3	S_4	S_5
D_1	[(0.67, 0.73), (0.3, 0.4)]	[(0.63, 0.68), (0.35, 0.42)]	[(0.3, 0.4), (0.7, 0.76)]	[(0.63, 0.68), (0.35, 0.42)]	[(0.5, 0.57), (0.59, 0.67)]
D_2	[(0.61, 0.67), (0.4, 0.5)]	[(0.72, 0.8), (0.23, 0.35)]	[(0.61, 0.67), (0.4, 0.5)]	[(0.63, 0.68), (0.35, 0.42)]	[(0.29, 0.38), (0.67, 0.74)]
D_3	[(0.5, 0.54), (0.5, 0.54)]	[(0.58, 0.62), (0.45, 0.5)]	[(0.74, 0.84), (0.16, 0.27)]	[(0.77, 0.88), (0.1, 0.23)]	[(0.61, 0.67), (0.4, 0.5)]
D_4	[(0.58, 0.62), (0.45, 0.5)]	[(0.61, 0.67), (0.4, 0.5)]	[(0.72, 0.68), (0.24, 0.35)]	[(0.63, 0.68), (0.35, 0.42)]	[(0.58, 0.62), (0.45, 0.5)]
D_5	[(0.54, 0.56), (0.45, 0.48)]	[(0.5, 0.547), (0.5, 0.54)]	[(0.61, 0.67), (0.4, 0.5)]	[(0.66, 0.73), (0.34, 0.45)]	[(0.3, 0.37), (0.64, 0.71)]
D_6	[(0.84, 1.0), (0.0, 0.0)]	[(0.61, 0.67), (0.4, 0.5)]	[(0.61, 0.28), (0.4, 0.71)]	[(0.71, 0.67), (0.27, 0.38)]	[(0.63, 0.68), (0.35, 0.42)]
D_7	[(0.65, 0.71), (0.32, 0.43)]	[(0.61, 0.67), (0.4, 0.5)]	[(0.16, 0.26), (0.74, 0.84)]	[(0.54, 0.56), (0.45, 0.47)]	[(0.61, 0.67), (0.4, 0.5)]
D_8	[(0.61, 0.67), (0.4, 0.5)]	[(0.77, 0.88), (0.1, 0.23)]	[(0.72, 0.8), (0.23, 0.35)]	[(0.58, 0.62), (0.45, 0.5)]	[(0.54, 0.56), (0.45, 0.47)]

Table 6.3: Aggregated DEMA

The subjective weight of the criteria will be obtained using the IVFF-PIPRECIA model. Equations (5.3)–(5.5) were used for the subjective weights, and the results were shown in Tables 6.4, 6.5.

	U_1	U_2	U_3	aggregated values	crisp values
D_1	E	H	E	[(0.61, 0.64), (0.39, 0.46)]	0.583
D_2	SM	SM	H	[(0.64, 0.71), (0.3, 0.37)]	0.636
D_3	SL	E	SL	[(0.4, 0.44), (0.58, 0.61)]	0.432
D_4	SM	SM	E	[(0.58, 0.61), (0.4, 0.44)]	0.568
D_5	L	SL	E	[(0.35, 0.42), (0.63, 0.68)]	0.388
D_6	H	VH	VH	[(0.77, 0.88), (0.13, 0.23)]	0.752
D_7	E	SM	VH	[(0.7, 0.76), (0.29 0.39)]	0.674
D_8	H	SM	SL	[(0.6, 0.67), (0.4, 0.48)]	0.586

Table 6.4: Significance ratings of criteria

	Crisp degrees	s_j	κ_j	Q_j	ω_j^S
D_1	0.583	-	1.000	1.000	0.12
D_2	0.636	1.053	0.947	1.056	0.12
D_3	0.432	0.796	1.204	0.877	0.1
D_4	0.568	1.136	0.864	1.015	0.116
D_5	0.388	0.820	1.180	0.860	0.1
D_6	0.752	1.364	0.636	1.352	0.16
D_7	0.674	0.922	1.078	1.254	0.15
D_8	0.586	0.912	1.088	1.153	0.134

Table 6.5: The weight of different criteria using IVFF-PIPRECIA

Further, the combined weight of each criterion based on IVFF-entropy and IVFF-PIPRECIA model is evaluated for $\alpha = 0.5$, then $\omega_j = \{0.093, 0.1215, 0.1235, 0.1105, 0.1, 0.1735, 0.1275, 0.137\}$. Since the criteria D_2 and D_3 difficulties are non-beneficial, and the rest are of beneficial criteria, the aggregated IVFF-DEMA is transformed into a normalized aggregated IVFF-DEMA Table 6.6. Positive and negative ideal solutions are as follows:

$$N_j^+ = \Big([(0.67,0.73),(0.3,0.4)],[(0.72,0.8),(0.23,0.35)],[(0.77,0.88),(0.1,0.23)],[(0.72,0.68),(0.24,0.35)],$$
$$[(0.66,0.73),(0.34,0.45)],[(0.84,1.0),(0.0,0.0)],[(0.65,0.71),(0.32,0.43)],[(0.77,0.88),(0.1,0.23)]\Big)$$

$$N_j^- = \Big([(0.3,0.4),(0.7,0.76)],[(0.61,0.67),(0.4,0.5)],[(0.5,0.54),(0.5,0.54)],[(0.58,0.62),(0.45,0.5)],$$
$$[(0.5,0.547),(0.5,0.54)],[(0.61,0.28),(0.4,0.71)],[(0.16,0.26),(0.74,0.84)],[(0.58,0.62),(0.45,0.5)]\Big)$$

The weighted normalized aggregated DEMA is created(Table 6.7) with Definition 3.3, Theorem 3.4 and Table 6.6. Using N_j^+, N_j^- and Table 6.7, the IVFF-score degree of each option, N_j^+, and N_j^- are determined and shown in Table 6.8. Using the Equation 5.6 and utility function values(Table 6.9), the prioritization of options is $S_1 > S_4 > S_5 > S_3 > S_2$, and S_1 is the best choice.

	S_1	§2	S_3	S_4	S_5
D_1	[(0.67, 0.73), (0.3, 0.4)]	[(0.63, 0.68), (0.35, 0.42)]	[(0.3, 0.4), (0.7, 0.76)]	[(0.63, 0.68), (0.35, 0.42)]	[(0.5, 0.57), (0.59, 0.67)]
D_2	[(0.4, 0.5), (0.61, 0.67)]	[(0.23, 0.35), (0.72, 0.8)]	[(0.4, 0.5), (0.61, 0.67)]	[(0.35, 0.42), (0.63, 0.68)]	[(0.67, 0.74), (0.29, 0.38)]
D_3	[(0.5, 0.54), (0.5, 0.54)]	[(0.45, 0.5), (0.58, 0.62)]	[(0.16, 0.27), (0.74, 0.84)]	[(0.1, 0.23), (0.77, 0.88)]	[(0.4, 0.5), (0.61, 0.67)]
D_4	[(0.58, 0.62), (0.45, 0.5)]	[(0.61, 0.67), (0.4, 0.5)]	[(0.72, 0.68), (0.24, 0.35)]	[(0.63, 0.68), (0.35, 0.42)]	[(0.58, 0.62), (0.45, 0.5)]
D_5	[(0.54, 0.56), (0.45, 0.48)]	[(0.5, 0.547), (0.5, 0.54)]	[(0.61, 0.67), (0.4, 0.5)]	[(0.66, 0.73), (0.34, 0.45)]	[(0.3, 0.37), (0.64, 0.71)]
D_6	[(0.84, 1.0), (0.0, 0.0)]	[(0.61, 0.67), (0.4, 0.5)]	[(0.61, 0.28), (0.4, 0.71)]	[(0.71, 0.67), (0.27, 0.38)]	[(0.63, 0.68), (0.35, 0.42)]
D_7	[(0.65, 0.71), (0.32, 0.43)]	[(0.61, 0.67), (0.4, 0.5)]	[(0.16, 0.26), (0.74, 0.84)]	[(0.54, 0.56), (0.45, 0.47)]	[(0.61, 0.67), (0.4, 0.5)]
D_8	[(0.61, 0.67), (0.4, 0.5)]	[(0.77, 0.88), (0.1, 0.23)]	[(0.72, 0.8), (0.23, 0.35)]	[(0.58, 0.62), (0.45, 0.5)]	[(0.54, 0.56), (0.45, 0.47)]

Table 6.6: Normalized DEMA

	S_1	§2	S_3	S_4	S_5
D_1	[(0.16, 0.23), (0.77, 0.81)]	[(0.19, 0.25), (0.75, 0.80)]	[(0.66, 0.72), (0.25, 0.27)]	[(0.19, 0.25), (0.75, 0.80)]	[(0.31, 0.40), (0.88, 0.96)]
D_2	[(0.20, 0.25), (0.80, 0.87)]	[(0.23, 0.29), (0.65, 0.74)]	[(0.20, 0.25), (0.80, 0.87)]	[(0.19, 0.25), (0.75, 0.80)]	[(0.16, 0.23), (0.77, 0.81)]
D_3	[(0.31, 0.39), (0.73, 0.84)]	[(0.91, 0.93), (0.81, 0.87)]	[(0.24, 0.36), (0.66, 0.70)]	[(0.29, 0.42), (0.57, 0.65)]	[(0.20, 0.25), (0.80, 0.87)]
D_4	[(0.79, 0.86), (0.77, 0.73)]	[(0.20, 0.25), (0.80, 0.87)]	[(0.23, 0.29), (0.65, 0.74)]	[(0.19, 0.23), (0.75, 0.80)]	[(0.79, 0.86), (0.77, 0.73)]
D_5	[(0.89, 0.92), (0.77, 0.72)]	[(0.31, 0.88), (0.73, 0.84)]	[(0.20, 0.25), (0.80, 0.87)]	[(0.18, 0.23), (0.76, 0.80)]	[(0.66, 0.72), (0.25, 0.27)]
D_6	[(0.36, 0.43), (0.0, 0.0)]	[(0.20, 0.35), (0.80, 0.87)]	[(0.20, 0.69), (0.80, 0.95)]	[(0.22, 0.25), (0.84, 0.81)]	[(0.19, 0.25), (0.75, 0.80)]
D_7	[(0.18, 0.22), (0.77, 0.80)]	[(0.20, 0.25), (0.80, 0.87)]	[(0.98, 0.91), (0.27, 0.32)]	[(0.39, 0.40), (0.81, 0.87)]	[(0.20, 0.25), (0.80, 0.87)]
D_8	[(0.20, 0.25), (0.80, 0.87)]	[(0.29, 0.42), (0.57, 0.65)]	[(0.23, 0.29), (0.65, 0.74)]	[(0.79, 0.86), (0.77, 0.73)]	[(0.89, 0.92), (0.77, 0.72)]

Table 6.7: Weighted Normalized Aggregated DEMA

	S_1	S_2	S_3	S_4	S_5	N_j^+	N_j^-
D_1	0.26	0.27	0.66	0.27	0.13	0.65	0.33
D_2	0.21	0.34	0.21	0.27	0.26	0.71	0.58
D_3	0.28	0.6	0.36	0.22	0.22	0.78	0.50
D_4	0.57	0.24	0.34	0.27	0.43	0.66	0.55
D_5	0.66	0.43	0.24	0.26	0.66	0.64	0.5
D_6	0.53	0.22	0.24	0.27	0.27	0.9	0.46
D_7	0.26	0.21	0.91	0.17	0.22	0.63	0.26
D_8	0.21	0.22	0.34	0.57	0.34	0.78	0.55

Table 6.8: Score Values

	U_i^-	U_i^+	$f(U_i)$	Ranking
S_1	0.738	1.104	0.581	1
S_2	0.460	0.687	0.217	5
S_3	0.487	704	0.388	4
S_4	0.523	0.782	0.412	2
S_5	0.513	0.767	0.404	3

Table 6.9: Utility Degrees and Utility Functions

Hence, the priority order of MW technique alternatives is found as $S_1 > S_4 > S_5 > S_3 > S_2$ and S_1 is the most desirable alternative. As a result, the final ranking of the options is obtained. Based on the ranking, Incineration is the best MW approach. It is followed by electromagnetic wave sterilization, chemical disinfection, and landfilling. Encapsulation gets the last position.

7. Discussion

The issue of health care has gained much attention in the modern world. It must be taken out and disposed of appropriately. There are numerous options for getting rid of waste. Here, a scenario-based multi-objective mathematical model was presented to design a viable MW chain. There are two benefits to this study. First, by employing a quantitative approach that considers ambiguities and uncertainties, this study can ascertain the causal linkages between these components. Second, we determine which seven are the most important by measuring the causal linkages between each element. These important components most significantly impact the entire factor system. Enhancing these important determinants significantly raises the MW management system's sustainability.

Consequently, it was decided that incineration was the most crucial factor. Handling MW properly safeguards patients, healthcare providers, and staff. It is essential for public health, safety, and the environment. For effective waste management, MW must be handled, stored, transported, processed, and disposed of properly. One crucial component of environmental sustainability is the handling of MW disposal. Healthcare waste is becoming increasingly abundant daily; hence, proper disposal is required. MW can be disposed of in various ways, with

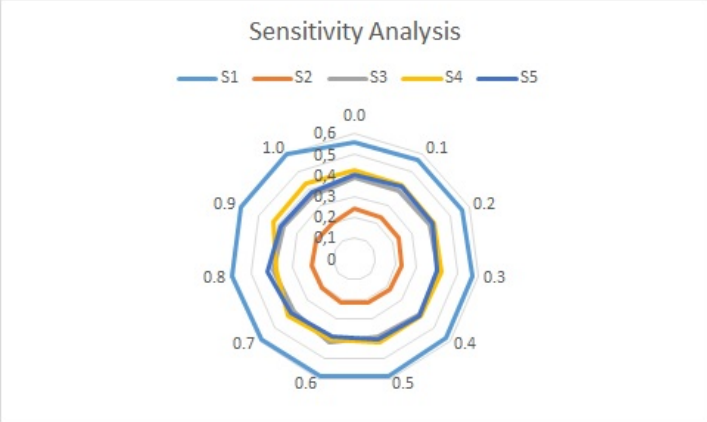

Figure 7.1: Sensitivity Analysis

incineration being one of the methods.

The results show that incinerator technology ranks higher than Electromagnetic Wave Sterilization, which indicates the current scenario. Incineration is one of the best options for disposing of medical waste since it requires less land, has a higher treatment capacity, costs less to transport garbage, and improves waste-to-energy operations [2]. This rating also aligns with the findings of [51] and [2], which indicate that electromagnetic wave sterilization disposal techniques—ranked second and third, respectively—are very successful because they produce non-hazardous residues and emit fewer pollutants than other approaches.

The presented hybrid IVFF model is proficient in producing stable and, simultaneously, flexible prioritization in variation in parameters. The results obtained showed that the developed approach could effectively address the concerns of healthcare professionals regarding the choice of the MW method in IVFFSs.

7.1. Sensitivity:

A sensitivity analysis has been conducted across the range of values for the α parameter. We systematically investigate how the parameters affect health practitioners' and society's high safety and security through effective modeling and ranking of risks associated with medical waste disposal. A range of α values were considered in the sensitivity study. This evaluation is discussed to convey how well the recently developed framework functions. DEs can assess how sensitive the introduced model is to changes by adjusting the α parameter. The best alternative, S_1, is the same for every parameter value, as indicated by the sensitivity analysis results in Table 7.1 and Figure 7.1. Therefore, MW treatment problem analysis depends on and is sensitive to α values. Thus, the proposed model has sufficient stability over various parameter values. Figure 7.1 shows that an alternate S_1 holds the first rank, and an alternate S_2 holds the last for every α. For $\alpha = 0.3, 0.6, 0.8$; S_3, S_4 and S_5 have different rankings. However, it is also seen that the results obtained for $\alpha = 0.0, 0.1, 0.2, 0.4, 0.7, 0.9, 1.0$ are the same as for $\alpha = 0.5$. The view Figure 7.1 demonstrates how changing the parameter degrees will improve the suggested framework's durability.

	$\alpha = 0.0$	$\alpha = 0.1$	$\alpha = 0.2$	$\alpha = 0.3$	$\alpha = 0.4$	$\alpha = 0.5$	$\alpha = 0.6$	$\alpha = 0.7$	$\alpha = 0.8$	$\alpha = 0.9$	$\alpha = 1.0$
S_1	0.560	0.562	0.568	0.570	0.575	0.581	0.583	0.585	0.590	0.594	0.596
S_2	0.243	0.239	0.235	0.227	0.225	0.217	0,215	0.210	0.207	0.204	0.202
S_3	0.388	0.390	0.396	0.404	0.405	0.388	0.415	0.383	0.390	0.424	0.428
S_4	0.426	0.421	0.420	0.416	0.414	0.412	0.399	0.419	0.380	0.385	0.381
S_5	0.403	0.410	0.408	0.401	0.412	0.404	0.385	0.397	0.421	0.371	0.366

Table 7.1: Sensitivity Analysis

7.2. Comparative analysis

MCDM is the process of choosing and assessing options from a small or large pool according to pertinent factors. An extensive range of alternatives are evaluated using various criteria as part of MCDM. The goal of applying MCDM techniques to these kinds of challenges is to assist DMs in identifying the best and most desirable solution. Thus, researchers have introduced numerous MCDM techniques. In this section, we tried two MCDM approaches in the FFS environment. The suggested methods' validity and accuracy have been validated by contrasting them with established techniques.

A comparative analysis with IVFF-WASPAS [41], IVFF-SWARA [52], Pythagorean fuzzy entropy-SWARA-WASPAS [53], and spherical fuzzy CRITIC-WASPAS [2] will be conducted to confirm the robustness of the suggested technique.

- In [41], (IVFF-WASPAS) IVFFS was defined, and its basic features were examined. A new MCDM method with the WASPAS has been proposed by giving aggregation operators based on IVFFS.

- In [52], (IVFF-SWARA) a new technique is proposed to solve MCDM problems with SWARA and ARAS techniques based on IVFFSs.
- In [53], (Pythagorean fuzzy entropy-SWARA-WASPAS) a new MCDM technique is presented by combining entropy, SWARA, and WASPAS techniques under PFSs.
- In [2], (CRITIC-WASPAS) a new spherical fuzzy-type MCDM method using CRITIC and WASPAS approaches has been used to evaluate HW disposal alternatives.

The comparison approaches' computations were done with the same decision matrices and sub-criteria weights. The comparisons have led to Table 7.2 results. Table 7.2 illustrates the differences between the compared approaches. Incineration was the first alternative in all applicable methodologies (S_1). The outputs of the approach proposed in this study are similar to those of the IVFF-WASPAS method, IVFF-SWARA method, Pythagorean fuzzy entropy-SWARA-WASPAS, and spherical fuzzy CRITIC-WASPAS, with a few minor variations. The proposed ways help tackle MCGDM concerns more practically and wisely since they use IVFFs instead of traditional methodology to evaluate criteria and alternatives.

There may be variations in the results obtained when using different MCDM methods to solve a given problem. It makes perfect sense to have various outcomes because different procedures have different methodological consequences and goals (Table 7.2). It is evident from the findings that there have also been modest adjustments, which is quite understandable given the unique characteristics of each decision-making process. FFS can deliver precise and adaptable outcomes because of their structure and distinct membership levels. Consequently, the analysis verifies that the suggested approach's outcomes are accurate.

Method	S_1	S_2	S_3	S_4	S_5
IVFF-WASPAS [41]	1	1	5	3	6
IVFF-SWARA [52]	1	1	4	5	9
Pythagorean fuzzy entropy-SWARA-WASPAS [53]	1	1	5	3	7
Spherical fuzzy CRITIC-WASPAS [2]	1	1	3	6	8

Table 7.2: Ranking comparison

7.3. Superiority of suggested method

The FFS is the result of combining the FS, IFS, and PFS. PFS is determined by total squares equal to or less than one and member and nonmember satisfaction levels. Seldom does the DE provide a particular feature to the $\mathscr{M}$ and $\mathscr{N}$ so that the sum of the squares is more than 1. The PFS is, therefore, unable to appropriately handle this occurrence. One of the most comprehensive techniques for circumventing this constraint is FFS, which can manage inconsistent and partially unknown data, both common in real-world scenarios.

The current and sensitivity analyses suggest that the offered strategy's results overlap with the accessible approaches. The main advantage of the proposed approach over easily accessible DM solutions is that it contains additional information and addresses data uncertainty by taking $\mathscr{M}$ and $\mathscr{N}$ of criteria into consideration features. Information regarding the item can be studied more accurately and objectively. It is also a valuable tool in the DM process when dealing with inaccurate and imprecise data. As a result, the rationale for assigning a score value to one parameter does not affect the other values, resulting in the predicted information loss.

On the contrary, our proposed technique does not result in significant information loss. The desired methodology has an advantage over present methods in that it detects the level of discrimination and similarity between data, preventing judgments made for incorrect reasons. Merging incorrect and ambiguous information can aid with the DM process.

8. Implications

Medical waste is becoming a significant environmental concern due to the negative consequences of its unplanned disposal. Healthcare and medical facilities must be aware of the harmful consequences of medical waste and take necessary action to address it. This study provides a strategy to assist health workers in determining which waste disposal alternatives to maintain, given the critical need to dispose of medical waste and the treatment processes that are now available. The study has the following implications for healthcare management: The methods for analyzing MW disposal choices provide a rapid and reliable way to analyze potential alternatives. This could be very useful for practitioners and administrators in the healthcare industry. Healthcare facilities can handle the problem of selecting a waste disposal strategy by utilizing the helpful and straightforward methods offered. Within this framework, the proposed approaches offer a reliable and expedient way to preliminary evaluate medical waste disposal options. Since it prioritizes practical waste disposal options based on the essential components and resources accessible to that hospital unit, this helps healthcare administrators and practitioners.

This study advances our theoretical and practical knowledge of medical waste disposal planning. Medical waste is a significant source of environmental and health issues. Adopting medical devices, particularly by individuals and healthcare workers, has also increased medical waste. Globally, managing medical waste presents formidable obstacles, irrespective of a robust infrastructure. As a result, the study's findings offer a theoretical viewpoint on the issue of medical waste and its handling. This study's risk analysis links the key obstacles and intricacy of sustainable medical waste disposal planning. Academics can gain from the research's findings in two ways: (1) It offers guidance on managing medical waste disposal planning wisely. (2) The findings have the potential to inspire several ideas and investments while also helping to resolve the difficulties associated with disposing of medical waste. The current study evaluates produced medical waste based on multiple parameters, which aids in the rating and classifying disposal methods. In other words, this study will help identify the best and worst disposal methods, ensuring that medical waste—which poses a risk—is disposed of in the most suitable way possible. Governments

must plan for the proper approach to dispose of medical waste in order to protect public health and minimize costs. Theoretical implications include

- suggestions on how to evolve the IVFFLS strategy,
- insights into using other methodologies for treating medical waste disposal,
- a detailed understanding of the research methods used.

An MCDM strategy was determined by considering aggregation operators and score-accuracy functions based on IVFFLS, so it offered a substantial contribution to the literature and shed light on medical waste disposal planning in a new context. Another practical application that combines the advantages of fuzzy and interval-valued techniques is the application of the IVFFLS approach. When evaluations are presented in linguistic values, fuzzy logic is used instead of typical numerical ratings to improve comprehension and interpretation. This kind of integration has been discussed in several studies in the literature on waste management, and several recommendations have been made for overcoming challenges and minimizing restrictions. This study's methodology offers a framework to generate outcomes that function in concert by taking more practical and accurate measures than earlier methods. The suggested framework helps businesses and regulators identify the significant obstacles that could arise while implementing an effective medical waste disposal planning system. The article primarily adds to the body of knowledge regarding identifying and analyzing obstacles to the implementation of the medical waste disposal system to address sustainability issues.

The following describes the theoretical and methodological consequences of the study: With the right mathematical software, the suggested approaches' adaptable structures allow them to be expanded to address any new DM challenge. All preference variables in the criterion are recorded based on the alternative assessment matrix. On the other hand, the score-accuracy functions of the proposed methods enable option ranking. This technique is dynamic and adaptable and may be applied to various DM situations since the user selects the parameter value based on the type of problem.

It is necessary to take into account the administrative consequences of incinerator technology. Investing much money in equipment and infrastructure is necessary to implement incineration as a medical waste disposal option. As a result, it is critical to thoroughly evaluate the operational aspects of incineration, including the cost of equipment and maintenance and the availability of adequate facilities. While pretending to be an incinerator for medical waste may come with a hefty initial cost, it can also yield long-term financial gains. The regulatory agency responsible for waste management and the environment must approve the implementation of incineration. In order to prevent fines or legal problems, the relevant permits must be obtained. Stakeholder participation, including local communities and government institutions, is necessary for implementing incineration. It is imperative to furnish these stakeholders with pertinent details regarding incineration's advantages and possible hazards, along with any safety and environmental preservation measures. Employees and other stakeholders will need to receive training and instruction in order to implement incineration. This covers the safe use of incinerator machinery as well as instruction on the advantages and restrictions of the technology. The incineration process can be continuously improved to make it more effective and efficient, but these advancements must be closely monitored. Therefore, it is critical to frequently assess and appraise the incineration process and pinpoint areas for improvement.

The study's conclusions have several significant ramifications for practitioners, academics, and policymakers in addition to its theoretical contribution. The research findings can support the conceptual premise that may aid sustainability and environmental managers in comprehending the significance of an efficient medical waste disposal system in emerging economies. This can help ensure sustainability and human well-being, identify the main obstacles to adoption, shape strategic decisions for successful medical waste disposal implementation, and maximize the financial value of efficient medical waste disposal practices in tangible and intangible forms. This study highlights the significance of efficient medical waste disposal in achieving operational excellence and sustainable development. The study's conclusions imply that, in order to maintain sustainability, medical waste disposal procedures must be implemented by the government and regulatory bodies. Therefore, the government and regulatory bodies must oversee sufficient resources to properly administer the system and actively participate in implementing medical waste disposal programs.

To evaluate from the perspective of Public Health, hospitals are responsible for the waste they produce. They must ensure that handling, treating, and disposing of that waste will not harm public health or the environment.

9. Conclusion

Preserving health, healing patients, and preserving lives are all achieved through healthcare operations. However, they also produce waste, 20% of which poses a danger of injury, infection, or exposure to chemicals or radiation. Waste management from health services is a complicated process. Even though hazardous medical waste poses risks, how to manage it is generally well-known and covered in manuals and other literature. Improper waste management can endanger patients, their families, medical waste workers, and the surrounding community. Furthermore, improper handling or disposal of such trash may contaminate or pollute the environment. This study uses the novel MCDM method for medical waste disposal planning to suggest solutions for the health system, human health, and environmental protection. To prioritize MW disposal methods, model the related uncertainty, and maximize their benefits, this work employs MCDM techniques based on IVFFLs. The planning of MW disposal is one pressing issue addressed by the suggested methodology. For this, a new decision-making methodology has been created. Therefore, the IVFF-entropy, IVFF-PIPCERIA combined IVFF-MARCOS procedures have been created. A unique fuzzy decision-making technique utilizing the entropy, PIPCERIA, and MARCOS approaches within the IVFF environment was given to evaluate the study framework. In assessing and determining the weights, it is crucial to use the DEs' role to calculate each difficulty's weight. As a result, each DE was asked to rank the significance of the MW treatment problem.
There are still several concerns with this study. First, there is a distinction between uncertainty and danger. Rather than favoring ambiguity, the main focus of this study is the effects of risk selection. Given that predicting the potential for an MW disposal service and its technology might be complicated, risk aversion is a crucial kind of uncertainty aversion. This study operationalized risk preference using prospect

theory. However, a more thorough assessment is required to detect potential problems with MW disposal. As a result, it could not identify the benefit and loss domains associated with MW disposal. Future studies should focus on merging specific MW disposal risk indicators with broad risk preference criteria.

Beyond the benefits of the proposed IVFF-based technique, its application in specific DM circumstances is restricted by its inability to evaluate the available options thoroughly. Building IVFFSs is easier when there are a lot of criteria and alternatives. To address these limitations, we would like to deepen our research in the following areas in our future work:

- Remanufacturing issues are less broadly applicable than the proposed solution. We aim to extend its application reach to include more intricate real-world disease management (DM) scenarios, including commercial, construction management, and medical.
- Extending the scope of outranking-based interval rough set theory methods—such as VIKOR, ELECTRE, DEMATEL, ANP, FMEA, BWM, and others—is another long-term objective.
- We aim to determine how various MCDM methods can be applied to the IVFF values.

Article Information

Acknowledgements: The author would like to express his sincere thanks to the editor and the anonymous reviewers for their helpful comments and suggestions.

Author's contributions: The article has a single author. The author has read and approved the final manuscript.

Conflict of interest disclosure: No potential conflict of interest was declared by the author.

Supporting/Supporting organizations: No grants were received from any public, private or non-profit organizations for this research.

Ethical approval and participant consent: It is declared that during the preparation process of this study, scientific and ethical principles were followed and all the studies benefited from are stated in the bibliography.

Plagiarism statement: This article was scanned by the plagiarism program.

References

[1] H. Yu, X. Sun, W.D. Solvang, X. Zhao, *Reverse logistics network design for effective management of medical waste in epidemic outbreaks: Insights from the coronavirus disease 2019 (covid-19) outbreak in Wuhan (china)*, Int. J. Environ. Res. Public Health, **17** (2020), 1770.
[2] A. Menekse, H.C. Akdag, *Medical waste disposal planning for healthcare units using spherical fuzzy CRITIC-WASPAS*, Appl Soft Comput., **144** (2023), 110480.
[3] R.R. Yager, *Pythagorean fuzzy subsets*, Proc. Joint IFSA World Congress and NAFIPS Annual Meeting, Edmonton, Canada, 2013.
[4] T. Senapati, R.R. Yager, *Fermatean fuzzy weighted averaging/geometric operators and its application in multi-criteria decision-making methods*, Engineering Applications of Artificial Intelligence, **85** (2019), 112–121.
[5] L.A. Zadeh, *Fuzzy sets*, Inf Comp **8** (1965), 338–353.
[6] K. Atanassov, *Intuitionistic fuzzy sets*, Fuzzy Sets and Systems, **20** (1986), 87–96.
[7] M. Kirişci, *Fibonacci statistical convergence on intuitionistic fuzzy normed spaces*, Journal of Intelligent & Fuzzy Systems, **36** (2019), 5597–5604.
[8] R.R. Yager, *Pythagorean membership grades in multicriteria decision-making*, IEEE Transactions on Fuzzy Systems **22**(4) (2014), 958–965.
[9] T. Senapati, R.R. Yager, *Fermatean fuzzy sets*, J. Ambient Intell. Hum. Comput., **11** (2020), 663–674.
[10] T. Senapati, R.R. Yager, *Some new operations over Fermatean fuzzy numbers and application of Fermatean fuzzy WPM in multiple criteria decision making*, Informatica **30**(2) (2019), 391–412.
[11] P. A. Ejegwa, I. Onyeke, *Medical diagnostic analysis on some selected patients based on modified Thao et al.'s correlation coefficient of intuitionistic fuzzy sets via an algorithmic approach*, Journal of Fuzzy Extension and Applications, **1**(2) (2020), 122—132, doi:10.22105/jfea.2020.250108.1014
[12] P. A. Ejegwa, I. Onyeke, B.T. Terhemen, M.P. Onoja, A. Ogiji, C.U. Opeh, *Modified Szmidt and Kacprzyk's Intuitionistic Fuzzy Distances and their Applications in Decision-making*, Journal of the Nigerian Society of Physical Sciences, **4**(2) (2022), 174–182, doi:10.46481/jnsps.2022.530
[13] P. A. Ejegwa, Y. Zhang, H. Li, Y. Feng, *Novel measuring techniques with applications in pattern classification and diagnostic process under Pythagorean fuzzy environment*, International Conference on New Trends in Computational Intelligence (NTCI 2023), **30** (2023), 28–35, doi:10.1109/NTCI60157.2023.10403717
[14] P. A. Ejegwa, S. Wen, Y. Feng, Y. W. Zhang, J. Liu, *A three-way Pythagorean fuzzy correlation coefficient approach and its applications in deciding some real-life problems*, Appl Intell, **53** (2023), 226–237, doi:10.1007/s10489-022-03415-5
[15] P. A. Ejegwa, D. Zuakwagh, *Fermatean fuzzy modified composite relation and its application in pattern recognition*, Journal of Fuzzy Extension and Applications, **3**(2) (2022), 140–151, doi: 10.22105/jfea.2022.335251.1210
[16] P. A. Ejegwa, N. Kausar, N. Aydin, Y. Feng, O. A. Olanrewaju, *A new Fermatean fuzzy Spearman-like correlation coefficient and its application in evaluating insecurity problem via multi-criteria decision-making approach*, Heliyon, **10**(22) (2024), e40403.
[17] H. Garg, G. Shahzadi, M. Akram, *Decision-making analysis based on Fermatean Fuzzy Yager aggregation operators with application in COVID-19 testing facility*, Math. Probl. Eng., (2020), Article ID 7279027, doi:10.1155/2020/7279027
[18] M. Kirişci, *Interval-valued fermatean fuzzy based risk assessment for self-driving vehicles*, Applied Soft Computing, **152** (2024), 111265.
[19] M. Kirişci, *Data analysis for panoramic X-ray selection: Fermatean fuzzy type correlation coefficients approach*, Engineering Applications of Artificial Intelligence **126** (2023), 106824.
[20] M. Kirişci, *Fermatean fuzzy type a three-way correlation coefficients*. In: Gayoso Martínez, V., Yilmaz, F., Queiruga-Dios, A., Rasteiro, D.M., Martín-Vaquero, J., Mierluş-Mazilu, I. (eds) Mathematical Methods for Engineering Applications, ICMASE 2023. Springer Proceedings in Mathematics & Statistics, **499** (2024), 325–338, doi: $10.1007/978-3-031-49218-1_24$.
[21] M. Kirişci, *New cosine similarity and distance measures for Fermatean fuzzy sets and TOPSIS approach*, Knowledge and Information Systems, **65**(2) (2023), 855–868.
[22] M. Kirişci, *Correlation Coefficients of Fermatean Fuzzy Sets with Their Application*, J. Math. Sci. Model. **5**(2) (2022), 16–23. doi: 10.33187/jmsm.1039613
[23] M. Kirişci, I. Demir, N. Simsek, *Fermatean fuzzy ELECTRE multi-criteria group decision-making and most suitable biomedical material selection*, Artificial Intelligence in Medicine, **127** (2022), 102278, doi:10.1016/j.artmed.2022.102278.
[24] M. Kirişci, *Data analysis for lung cancer: Fermatean Hesitant fuzzy sets approach*, Applied Mathematics, Modeling and Computer Simulation, **30** (2022), 701–710, doi:10.3233/ATDE221087
[25] M. Kirişci, N. Simsek, *A novel kernel principal component analysis with application disaster preparedness of hospital: interval-valued Fermatean fuzzy set approach*, The Journal of Supercomputing, **79** (2023), 19848–19878.

[26] M. Kirişci, *Measures of distance and entropy based on the Fermatean fuzzy-type soft sets approach*, Univ. J. Math. Appl., **7** (2024), 12–29.
[27] M. Riaz, H. M. A. Farid, H. M. Shakeel, D. Arif, *Cost effective indoor HVAC energy efficiency monitoring based on intelligent decision support system under Fermatean fuzzy framework*, Scientia Iranica, **30**(6) (2023), 2143–2161.
[28] N. Şimşek, M. Kirişci, *Incomplete Fermatean Fuzzy Preference Relations and Group Decision Making*, Topol. Algebra Appl., **11**(1) (2023), 20220125.
[29] N. Şimşek, M. Kirişci, *A new risk assessment method for autonomous vehicle driving systems: Fermatean fuzzy AHP Approach*, Istanbul Commerce University Journal of Science, **22**(44) (2023), 292–309.
[30] K. Atanassov, G. Gargov, *Interval valued intuitionistic fuzzy sets*, Fuzzy Sets and Systems, **31**(3) (1989), 343–349.
[31] X. Peng, Y. Yang, *Fundamental properties of interval-valued Pythagorean fuzzy aggregation operators*, Int. J. Intell. Syst., **31** (2016), 444–487.
[32] S. Jeevaraj, *Ordering of interval-valued Fermatean fuzzy sets and their applications*, Expert Systems with Applications, **185** (2021), 115613.
[33] D. Stanujkic, E.K. Zavadskas, D. Karabasevic, F. Smarandache, Z. Turskis, *The use of the PIvot Pairwise RElative Criteria Importance Assessment method for determining the weights of criteria*, Romanian Journal of Economic Forecasting, **20** (2017), 116–133.
[34] Z. Stevic, Z. Stjepanovic, Z. Bozickovic, D.K. Das, D. Stanujkic, *Assessment of conditions for implementing information technology in a warehouse system: A novel fuzzy PIPRECIA method*, Symmetry, **10** (2018), 1–28.
[35] G. Demir, M. Riaz, M. Deveci, *Wind farm site selection using geographic information system and fuzzy decision making model*, Expert System and Applications, **255** (2024), 124772.
[36] Z. Stevic, D. Pamucar, A. Puska, P. Chatterjee, *Sustainable supplier selection in healthcare industries using a new MCDM method: Measurement Alternatives and Ranking according to COmpromise Solution (MARCOS)*, Computers and Industrial Engineering, **140** (2020), 1–33.
[37] G. Demir, P. Chatterjee, S. Kadry, A. Abdelhadi, D. Pamucar, *Measurement of Alternatives and Ranking according to Compromise Solution (MARCOS) Method: A Comprehensive Bibliometric Analysis*, Decision-Making Applications in Management and Engineering, **7** (2024), 313–336.
[38] A.R. Mishra, P. Rani, D. Pamucar, A. Saha, *An integrated Pythagorean fuzzy fairly operator-based MARCOS method for solving the sustainable circular supplier selection problem*, Ann. Oper. Res., **342** (2024), 523–564.
[39] H. M. A. Farid, S. Dabic-Miletic, M. Riaz, V. Simic, D. Pamucar, *Prioritization of sustainable approaches for smart waste management of automotive fuel cells of road freight vehicles using the q-rung orthopair fuzzy CRITIC-EDAS method*, Information Sci., **661** (2024), 120162
[40] R. Kausar, M. Riaz, V. Simic, K. Akmal, M. U. Farooq, *Enhancing solid waste management sustainability with cubic m-polar fuzzy cosine similarity*, Soft Comput., (2023), 1-21, doi:10.1007/s00500-023-08801-w
[41] P. Rani, A.R. Mishra, *Interval-valued Fermatean fuzzy sets with multi-criteria weighted aggregated sum product assessment-based decision analysis framework*, Neural Computing and Applications, **34** (2022), 8051–8067.
[42] M. H. Mateen, I. Al-Dayel, T. Alsuraiheed, *Fermatean fuzzy fairly aggregation operators with multi-criteria decision-making*, Axioms, **12** (2023), 865.
[43] A.R. Mishra, P. Rani, A.F. Alrasheedi, R. Dwivedi, *Evaluating the blockchain-based healthcare supply chain using interval-valued Pythagorean fuzzy entropy-based decision support system*, Engineering Applications of Artificial Intelligence, **126** (2023), 107112.
[44] X. Peng, W. Li, *Algorithms for Interval-Valued Pythagorean Fuzzy Sets in Emergency Decision Making Based on Multiparametric Similarity Measures and WDBA*, IEEE Access, **7** (2019), 7419–7441.
[45] Medical waste, WHO, https://www.who.int/news-room/fact-sheets/detail/health-care-waste (Access: November 2024).
[46] M. Ghodrat, M. Rashidi, B. Samali, *Life cycle assessments of incineration treatment for sharp medical waste*, Energy Technology 2017 Conference Paper, (2017), 131–143.
[47] C. C. Lee, G. L. Huffman, *Medical waste management/incineration*, J. Hazard Mater., **48** (1996), 1–30.
[48] Z. Sapuric, D. Dimitrovski, M. Dimitrovski, F. Ivanovski, *Medical waste incineration in skopje. regulation and standards*, J. Environ. Protect. Ecol., **17** (2016), 805–812.
[49] A. Wu, X: Huang, R.E. Gong, J. Li, Y. Lu, M. Wang, *Effectiveness of immersion disinfectant on medical waste*, Chin. J. Nosoconmiol., **15** (2005), 51-–52.
[50] S. M. Rao, P. Mamatha, R. P. Shanta, B. V. V. Reddy, *Encapsulation of fluoride sludge in stabilised mud blocks*, Proceedings of the Institution of Civil Engineers Waste and Resource Management, R4, (2007), 167–174.
[51] M. Dursun, E.E. Karsak, M.A. Karadayi, *Assessment of health-care waste treatment alternatives using fuzzy multi-criteria decision making approaches*, Resour. Conserv. Recycl., **57** (2011), 98e107.
[52] M. R. Seikh, P. Chatterjee, *Determination of best renewable energy sources in India using SWARA-ARAS in confidence level based interval-valued Fermatean fuzzy environment*, Applied Soft Computing, **155** (2024), 111495.
[53] M. Alrasheedi, A. Mardani, A.R. Mishra, P. Rani, P., L. Nanthakumar, *An extended framework to evaluate sustainable suppliers in manufacturing companies using a new pythagorean fuzzy entropy-SWARA-WASPAS decisionmaking approach*, J. Enterp. Inf. Manag., **35** (2022), 333–357.

Journal of Mathematical Sciences and Modelling, 7(3) (2024) 146-156
Research Article

Journal of Mathematical Sciences and Modelling

Journal Homepage: www.dergipark.gov.tr/jmsm
ISSN: 2636-8692
DOI: https://doi.org/10.33187/jmsm.1475211

Unveiling New Exact Solutions of the Complex-Coupled Kuralay System Using the Generalized Riccati Equation Mapping Method

Bahadır Kopçasız

Department of Computer Engineering, Faculty of Engineering and Architecture, Istanbul Gelisim University, Istanbul, Türkiye

Article Info

Keywords: *Complex-coupled Kuralay system (CCKS), Soliton solutions, The generalized Riccati equation mapping (GREM) method*
2010 AMS: *35C08, 35C09, 35C07, 35A99*
Received: *29 April 2024*
Accepted: *21 December 2024*
Available online: *29 December 2024*

Abstract

This examination analyzes the integrable dynamics of induced curves by utilizing the complex-coupled Kuralay system (CCKS). The significance of the coupled complex Kuralay equation lies in its role as an essential model that contributes to the understanding of intricate physical and mathematical concepts, making it a valuable tool in scientific research and applications. The soliton solutions originating from the Kuralay equations are believed to encapsulate cutting-edge research in various essential domains such as optical fibers, nonlinear optics, and ferromagnetic materials. Analytical procedures are operated to derive traveling wave solutions for this model, given that the Cauchy problem cannot be resolved using the inverse scattering transform. This study uses the generalized Riccati equation mapping (GREM) method to search for analytical solutions. This method observes single and combined wave solutions in the shock, complex solitary shock, shock singular, and periodic singular forms. Rational solutions also emerged during the derivation. In addition to the analytical results, numerical simulations of the solutions are presented to enhance comprehension of the dynamic features of the solutions generated. The study's conclusions could provide insightful information about how to solve other nonlinear partial differential equations (NLPDEs). The soliton solutions found in this work provide valuable information on the complex nonlinear problem under investigation. These results provide a foundation for further investigation, making the solutions helpful, manageable, and trustworthy for the future development of intricate nonlinear issues. This study's methodology is reliable, robust, effective, and applicable to various NLPDEs. The Maple software application is used to verify the correctness of all obtained solutions.

1. Introduction

Partial differential equations (PDEs) play a crucial role in mathematical modeling by serving as a critical mechanism for analyzing and understanding the dynamics of intricate systems across various fields, including physics, engineering, economics, and other disciplines. PDEs offer a robust framework for predicting and interpreting the behavior of diverse phenomena, effectively capturing intricate relationships between variables and their rates of change. These equations elucidate the temporal and spatial evolution of functions with multiple variables. NLPDEs hold significance across various disciplines, such as mathematics, science, and engineering. Contemporary research has unveiled a diverse range of complex nonlinear models, prompting the development of sophisticated mathematical methodologies by numerous scholars to derive exact solutions. Consequently, the exploration of nonlinear phenomena has garnered considerable attention among academics. The construction of soliton structures is progressively gaining importance due to its relevance in multiple scientific domains [1–5].
Furthermore, an emerging application of NLPDEs lies in investigating soliton waves. Soliton waves, characterized by localized wave packets that maintain their shape and velocity as they propagate, are the subject of study in various nonlinear physical models researchers employ to elucidate and forecast their dynamics. Consequently, the significance of soliton waves is progressively growing across diverse

***Email address and ORCID number*: bkopcasiz@gelisim.edu.tr, 0000-0002-6364-3631**
Cite as "B. Kopçasız, *Unveiling new exact solutions of the complex-coupled Kuralay system using the generalized Riccati equation mapping method*, J. Math. Sci. Model., 7(3) (2024), 146-156"

disciplines, including nonlinear optics, optical fibers, and ferromagnetic materials. Recent advancements in understanding soliton waves are comprehensively examined in the literature reference [6–10]. Researchers can advance their knowledge and explore novel applications by enhancing their comprehension of soliton waves. Alongside the advantages of utilizing NLPDEs, numerous methodologies have been devised to address the difficulty of accurately determining analytical solutions for NLPDEs. Recently, there has been a growing interest among scholars in investigating the exact solutions of NLPDEs, particularly concerning nonlinear physical phenomena. Nonlinear critical approaches have been introduced and employed by many physicists and mathematicians, such as the Hirota bilinear method [11], the Painlevé analysis [12], the Bäcklund transformation [13], Lie symmetry analysis and conservation laws [14]. Some more techniques can be found in the literature [15–20].

The Kuralay equation is a mathematical model that has been the subject of a thorough examination by scholars in integrable systems and nonlinear dynamics. Its origins are not attributed to a singular discoverer but have emerged through research endeavors and mathematical inquiries, solidifying its significance as a foundational model in scientific exploration. The Kuralay equation is utilized across diverse disciplines in contemporary scientific studies, notably in analyzing ferromagnetic materials and wave propagation phenomena. This mathematical framework investigates the generation and movement of solitary wave solutions, enhancing comprehension of intricate physical phenomena. Moreover, the Kuralay equation is crucial in examining the integrable dynamics of spatial curves and geometric flows, offering valuable insights into the interactions among curves, multilayer spin systems, and the vector nonlinear Schrödinger equation. The coupled complex Kuralay equation is fundamental in contemporary scientific disciplines because of its integrability and practical implications. This mathematical framework plays a crucial role in examining diverse phenomena and has been subject to thorough investigation for its capacity to depict intricate systems precisely. Scholars have concentrated on deducing exact solutions, examining optical solitons, and delving into innovative soliton solutions through computational modeling techniques centered on the Kuralay equation [21–27].

The primary aim of this study is to utilize the GREM technique on CCKS to investigate novel soliton solutions. For this purpose, we discuss some previous work and our newly obtained results. Researchers have explored various solutions to the complex nonlinear Kuralay-IIA model operating methods, such as the Hirota bilinear procedure [22], simple equation and Paul-Painlevé approaches [23], generalized Kudryashov scheme, extended Sinh Gordon equation expansion scheme, $\exp_\alpha$-function scheme [24], new auxiliary equation scheme [25], modified F-expansion, and new extended auxiliary equation techniques [26]. In this study, we have considered the GREM method. The GREM method is a valuable tool to get the exact solitary wave solutions and control theory, particularly for linear time-invariant systems. Compared to other methods, this method is highly convenient and easy to implement, offers a wide range of solutions, and works efficiently.

The paper is structured as follows: Section 2 presents the mathematical analysis of the model under consideration. Section 3 describes the offered method. Analytical solutions for the model are discussed in Section 4. Section 5 presents a graphical discussion and Section 6 explains the conclusions.

2. Analytical Analysis of the Complex-Coupled Kuralay System (CCKS)

Consider the CCKS as [27]:

$$\begin{cases} i\Phi_t - \Phi_{xt} - \tau\Phi = 0, \\ i\Omega_t + \Omega_{xt} + \tau\Phi = 0, \\ \tau_x + 2R^2(\Omega\Phi)_t = 0, \end{cases}$$

in which $\Phi(x,t)$ is complex function with a complex conjugate as $\Phi^*(x,t)$. Subsequent, τ represents the potential real function, and they depend on the independent spatial and temporal variables x and t, respectively.

By assuming that $R = 1$, $\Omega = \varepsilon\Phi^*$, where $\varepsilon = \pm 1$, the above system of differential equation will become:

$$\begin{cases} i\Phi_t - \Phi_{xt} - \tau\Phi = 0, \\ \tau_x - 2\varepsilon(|\Phi|^2)_t = 0. \end{cases} \tag{2.1}$$

Now, the following complex traveling wave transformation is applied to the complex system of PDEs Eq. (2.1)

$$\Phi(x,t) = \Upsilon(\xi) \times \exp(i(\alpha x + \beta t + \gamma)), \quad \tau(x,t) = \Psi(\xi) \times \exp(i(\alpha x + \beta t + \gamma)), \quad \xi = sx + vt, \tag{2.2}$$

where,

$$\begin{cases} \Phi_t = (v\Upsilon' + \imath\beta\Upsilon) \times \exp(i(\alpha x + \beta t + \gamma)), \\ \Phi_x = (s\Upsilon' + \imath\alpha\Upsilon) \times \exp(i(\alpha x + \beta t + \gamma)), \\ \Phi_{xt} = (vs\Upsilon'' + \imath\beta s\Upsilon' + iv\alpha\Upsilon' + \imath\alpha\beta\Upsilon) \times \exp(i(\alpha x + \beta t + \gamma)), \end{cases} \tag{2.3}$$

and α, β, γ, s, and v are real numbers. The Eq. (2.2) along with Eq. (2.3) is plugging into Eq. (2.1) and gets,

$$\begin{cases} i(v\Upsilon' + i\beta\Upsilon) - (vs\Upsilon'' + i\beta s\Upsilon' + iv\alpha\Upsilon' - \alpha\beta\Upsilon) - \Psi\Upsilon = 0, \\ s\Psi' - 4v\varepsilon\Upsilon\Upsilon' = 0, \end{cases} \tag{2.4}$$

integrating the second part of Eq. (2.4), we attain

$$\Psi = \frac{2\varepsilon v\Upsilon^2}{s} - \frac{v_1}{s}. \tag{2.5}$$

The Eq. (2.5) is putting into the first part of Eq. (2.4):

$$i(v\Upsilon' + i\beta\Upsilon) - (vs\Upsilon'' + i\beta s\Upsilon' + iv\alpha\Upsilon' - \alpha\beta\Upsilon) - \left(\frac{2\varepsilon v\Upsilon^2}{s} - \sigma\right) = 0, \tag{2.6}$$

where $\sigma = \frac{v_1}{s}$.
The real part and imaginary part of Eq. (2.6) are give as, respectively,

$$\Upsilon'' + \frac{(\beta(1-\alpha)-\sigma)}{vs}\Upsilon + \frac{2\varepsilon}{s^2}\Upsilon^3 = 0, \tag{2.7}$$

$$(v - \beta s - v\alpha)\Upsilon' = 0. \tag{2.8}$$

The imaginary part Eq. (2.8) implies

$$s = \frac{v(\alpha-1)}{\beta}. \tag{2.9}$$

The value of s Eq. (2.9) is substituting into Eq. (2.7), and get a nonlinear ordinary differential equation (NLODE)

$$\Upsilon'' + \frac{\beta\,(\beta(1-\alpha)-\sigma)}{v^2(\alpha-1)}\Upsilon + \frac{2\beta^2\varepsilon}{v^2(\alpha-1)^2}\Upsilon^3 = 0. \tag{2.10}$$

3. GREM Method

This section will present the GREM method [28–30].
Consider the following NLPDE:

$$Z(\Phi(x,t), \Phi_x(x,t), \Phi_t(x,t), \Phi_{xx}(x,t), \Phi_{xt}(x,t), \Phi_{tt}(x,t), \ldots) = 0, \tag{3.1}$$

in which Z is generally a polynomial function of its argument, and the subscripts of the dependent variable denote the partial derivatives. By using the Eq. (2.2), Eq. (3.1) can be transformed to an NLODE:

$$W(\Upsilon, \Upsilon', \Upsilon'', \ldots) = 0. \tag{3.2}$$

Suppose that the solution of Eq. (3.2) is in the polynomial form

$$\Upsilon = \sum_{j=0}^{p} A_j \Lambda^j(\xi), \qquad A_p \neq 0, \tag{3.3}$$

in which $A_j (0 \leq j \leq p)$ are arbitrary constants that are determine later, and p is a positive integer that is obtained by the help of the balancing principle in Eq. (3.2). In Eq. (3.3), the function $\Lambda(\xi)$ satisfies the generalized Riccati equation is provided as follows:

$$\Lambda(\xi)' = \theta_0 + \theta_1\Lambda(\xi) + \theta_2\Lambda(\xi)^2, \quad \theta_2 \neq 0, \tag{3.4}$$

in which θ_0, θ_1, and θ_2 are all real constants. Substituting the Eq. (3.3) with Eq. (3.4) into the regarding NLODE and removing all the coefficients of $\Lambda^j(\xi)$ will obtain a system of algebraic equations. Solving the algebraic equations, with the known solutions of Eq. (3.3), one can easily obtain the solutions to the Eq. (3.1). We can obtain the following twenty seven solutions to Eq. (3.2) such as:
Set 1: For $\Delta = \theta_1^2 - 4\theta_0\theta_2 > 0$, and $\theta_1\theta_2 \neq 0$ (or $\theta_0\theta_2 \neq 0$), the solutions of Eq. (3.4) are

$$\Lambda_1(\xi) = -\frac{1}{2\theta_2}\left(\theta_1 + \sqrt{\Delta}\tanh\left(\frac{\sqrt{\Delta}}{2}\xi\right)\right), \tag{3.5}$$

$$\Lambda_2(\xi) = -\frac{1}{2\theta_2}\left(\theta_1 + \sqrt{\Delta}\coth\left(\frac{\sqrt{\Delta}}{2}\xi\right)\right), \tag{3.6}$$

$$\Lambda_3(\xi) = -\frac{1}{2\theta_2}\left(\theta_1 + \sqrt{\Delta}\left(\tanh\left(\sqrt{\Delta}\xi\right) \pm i\,\mathrm{sec}\,h\left(\sqrt{\Delta}\xi\right)\right)\right), \tag{3.7}$$

$$\Lambda_4(\xi) = -\frac{1}{2\theta_2}\left(\theta_1 + \sqrt{\Delta}\left(\coth\left(\sqrt{\Delta}\xi\right) \pm \mathrm{csc}\,h\left(\sqrt{\Delta}\xi\right)\right)\right), \tag{3.8}$$

$$\Lambda_5(\xi) = -\frac{1}{4\theta_2}\left(2\theta_1 + \sqrt{\Delta}\left(\tanh\left(\frac{\sqrt{\Delta}}{4}\xi\right) + \cot h\left(\frac{\sqrt{\Delta}}{4}\xi\right)\right)\right), \tag{3.9}$$

$$\Lambda_6(\xi) = \frac{1}{2\theta_2}\left(-\theta_1 + \frac{\sqrt{\Delta(P^2+Q^2)} - P\sqrt{\Delta}\cosh\left(\sqrt{\Delta}\xi\right)}{P\sinh\left(\sqrt{\Delta}\xi\right) + Q}\right), \tag{3.10}$$

$$\Lambda_7(\xi) = \frac{1}{2\theta_2}\left(-\theta_1 - \frac{\sqrt{\Delta(P^2+Q^2)} + P\sqrt{\Delta}\cosh\left(\sqrt{\Delta}\xi\right)}{P\sinh\left(\sqrt{\Delta}\xi\right) + Q}\right), \tag{3.11}$$

in which P and Q are two non-zero real constants and satisfies $P^2 - Q^2 > 0$.

$$\Lambda_8(\xi) = \frac{2\theta_0 \cosh\left(\frac{\sqrt{\Delta}}{2}\xi\right)}{\sqrt{\Delta}\sinh\left(\frac{\sqrt{\Delta}}{2}\xi\right) - \theta_1 \cosh\left(\frac{\sqrt{\Delta}}{2}\xi\right)}, \tag{3.12}$$

$$\Lambda_9(\xi) = -\frac{2\theta_0 \sinh\left(\frac{\sqrt{\Delta}}{2}\xi\right)}{\theta_1 \sinh\left(\frac{\sqrt{\Delta}}{2}\xi\right) - \sqrt{\Delta}\cosh\left(\frac{\sqrt{\Delta}}{2}\xi\right)}, \tag{3.13}$$

$$\Lambda_{10}(\xi) = \frac{2\theta_0 \cosh\left(\sqrt{\Delta}\xi\right)}{\sqrt{\Delta}\sinh\left(\sqrt{\Delta}\xi\right) - \theta_1 \cosh\left(\sqrt{\Delta}\xi\right) \pm i\sqrt{\Delta}}, \tag{3.14}$$

$$\Lambda_{11}(\xi) = \frac{2\theta_0 \sinh\left(\sqrt{\Delta}\xi\right)}{\sqrt{\Delta}\cosh\left(\sqrt{\Delta}\xi\right) - \theta_1 \sinh\left(\sqrt{\Delta}\xi\right) \pm \sqrt{\Delta}}, \tag{3.15}$$

$$\Lambda_{12}(\xi) = \frac{4\theta_0 \sinh\left(\frac{\sqrt{\Delta}}{4}\xi\right)\cosh\left(\frac{\sqrt{\Delta}}{4}\xi\right)}{2\sqrt{\Delta}\cosh\left(\frac{\sqrt{\Delta}}{4}\xi\right)^2 - 2\theta_1 \sinh\left(\frac{\sqrt{\Delta}}{4}\xi\right)\cosh\left(\frac{\sqrt{\Delta}}{4}\xi\right) - \sqrt{\Delta}}. \tag{3.16}$$

Set 2: For $\Delta = \theta_1^2 - 4\theta_0\theta_2 < 0$, and $\theta_1\theta_2 \neq 0$ (or $\theta_0\theta_2 \neq 0$), the solutions of Eq. (3.4) are

$$\Lambda_{13}(\xi) = \frac{1}{2\theta_2}\left(-\theta_1 + \sqrt{-\Delta}\tan\left(\frac{\sqrt{-\Delta}}{2}\xi\right)\right), \tag{3.17}$$

$$\Lambda_{14}(\xi) = -\frac{1}{2\theta_2}\left(\theta_1 + \sqrt{-\Delta}\cot\left(\frac{\sqrt{-\Delta}}{2}\xi\right)\right), \tag{3.18}$$

$$\Lambda_{15}(\xi) = \frac{1}{2\theta_2}\left(-\theta_1 + \sqrt{-\Delta}\left(\tan\left(\sqrt{-\Delta}\xi\right) \pm \sec\left(\sqrt{-\Delta}\xi\right)\right)\right), \tag{3.19}$$

$$\Lambda_{16}(\xi) = -\frac{1}{2\theta_2}\left(\theta_1 + \sqrt{-\Delta}\left(\cot\left(\sqrt{-\Delta}\xi\right) \pm \csc\left(\sqrt{-\Delta}\xi\right)\right)\right), \tag{3.20}$$

$$\Lambda_{17}(\xi) = \frac{1}{4\theta_2}\left(-2\theta_1 + \sqrt{-\Delta}\left(\tan\left(\frac{\sqrt{-\Delta}}{4}\xi\right) - \cot\left(\frac{\sqrt{-\Delta}}{4}\xi\right)\right)\right), \tag{3.21}$$

$$\Lambda_{18}(\xi) = \frac{1}{2\theta_2}\left(-\theta_1 + \frac{\pm\sqrt{\Delta(-P^2+Q^2)} \mp P\sqrt{-\Delta}\cos\left(\sqrt{-\Delta}\xi\right)}{P\sin\left(\sqrt{-\Delta}\xi\right) + Q}\right), \tag{3.22}$$

in which P and Q are two non-zero real constants and satisfies $P^2 - Q^2 > 0$.

$$\Lambda_{19}(\xi) = -\frac{2\theta_0 \cos\left(\frac{\sqrt{-\Delta}}{2}\xi\right)}{\sqrt{-\Delta}\sin\left(\frac{\sqrt{-\Delta}}{2}\xi\right) + \theta_1 \cos\left(\frac{\sqrt{-\Delta}}{2}\xi\right)}, \tag{3.23}$$

$$\Lambda_{20}(\xi) = \frac{2\theta_0 \sin\left(\frac{\sqrt{-\Delta}}{2}\xi\right)}{\sqrt{-\Delta}\cos\left(\frac{\sqrt{-\Delta}}{2}\xi\right) - \theta_1 \sin\left(\frac{\sqrt{-\Delta}}{2}\xi\right)}, \tag{3.24}$$

$$\Lambda_{21}(\xi) = -\frac{2\theta_0 \cos\left(\sqrt{-\Delta}\xi\right)}{\sqrt{-\Delta}\sin\left(\sqrt{-\Delta}\xi\right) + \theta_1 \cos\left(\sqrt{-\Delta}\xi\right) \pm \sqrt{-\Delta}}, \tag{3.25}$$

$$\Lambda_{22}(\xi) = -\frac{2\theta_0 \sin\left(\sqrt{-\Delta}\xi\right)}{\sqrt{-\Delta}\cos\left(\sqrt{-\Delta}\xi\right) + \theta_1 \sin\left(\sqrt{-\Delta}\xi\right) \pm \sqrt{-\Delta}}, \tag{3.26}$$

$$\Lambda_{23}(\xi) = \frac{4\theta_0 \sin\left(\frac{\sqrt{-\Delta}}{4}\xi\right)\cos\left(\frac{\sqrt{-\Delta}}{4}\xi\right)}{2\sqrt{-\Delta}\cos\left(\frac{\sqrt{-\Delta}}{4}\xi\right)^2 - 2\theta_1 \sin\left(\frac{\sqrt{-\Delta}}{4}\xi\right)\cos\left(\frac{\sqrt{-\Delta}}{4}\xi\right) - \sqrt{-\Delta}}. \tag{3.27}$$

Set 3: For $\theta_0 = 0$, and $\theta_1\theta_2 \neq 0$, the solutions of Eq. (3.4) are

$$\Lambda_{24}(\xi) = -\frac{\theta_1\zeta_0}{\theta_2\left(\zeta_0 + \cosh\left(\theta_1\xi\right) - \sinh\left(\theta_1\xi\right)\right)}, \tag{3.28}$$

$$\Lambda_{25}(\xi) = -\frac{\theta_1\left(\cosh\left(\theta_1\xi\right) - \sinh\left(\theta_1\xi\right)\right)}{\theta_2\left(\zeta_0 + \cosh\left(\theta_1\xi\right) - \sinh\left(\theta_1\xi\right)\right)}, \tag{3.29}$$

$$\Lambda_{26}(\xi) = -\frac{\theta_1\left(\cosh\left(\theta_1\xi\right) + \sinh\left(\theta_1\xi\right)\right)}{\theta_2\left(\zeta_0 + \cosh\left(\theta_1\xi\right) + \sinh\left(\theta_1\xi\right)\right)}, \tag{3.30}$$

in which ζ_0 is any arbitrary constant.
Set 4: For $\theta_0 \neq 0$, and $\theta_1 = \theta_2 = 0$, the solutions of Eq. (3.4) are

$$\Lambda_{27}(\xi) = -\frac{1}{\theta_0 \xi + c_1}, \tag{3.31}$$

in which c_1 is an arbitrary constant.

4. Solving the CCKS Using the Recommended Method

In this part, we explore the analytical solutions of the CCKS by applying the GREM technique. Balancing Φ'' with Φ^3, we get $p = 1$. From Eq. (3.3), the solution is presumed as

$$\Upsilon = K_0 + K_1 \Lambda, \qquad K_1 \neq 0. \tag{4.1}$$

Putting Eq. (4.1) along with Eq. (3.4) into Eq. (2.10), and setting the coefficient of $\Lambda^j(\xi)$ to be zero, which gives a system of algebraic equations. After solving the system of equations, we get the solutions are as follows:

$$K_0 = \mp \frac{\theta_1 v \sigma}{\varepsilon(-4v^2\theta_0\theta_2 + v^2\theta_1^2 + 2\beta^2) \times \sqrt{-\frac{1}{\varepsilon}}}, \quad K_1 = \pm \frac{2\theta_2 v \sigma \sqrt{-\frac{1}{\varepsilon}}}{(-4v^2\theta_0\theta_2 + v^2\theta_1^2 + 2\beta^2)},$$

$$\alpha = \frac{-4v^2\theta_0\theta_2 + v^2\theta_1^2 + 2\beta^2 - 2\beta\sigma}{-4v^2\theta_0\theta_2 + v^2\theta_1^2 + 2\beta^2}. \tag{4.2}$$

By putting constant values Eq. (4.2) along with Eq. (3.5)-Eq. (3.16) in the Eq. (4.1), and by using the wave transformation Eq. (2.2), we get the solutions as follows:

$$\begin{aligned}
\Phi_1(x,t) &= -\frac{\sigma v \sqrt{\Delta} \tanh\left(\frac{\sqrt{\Delta}}{2}(sx+vt)\right)}{\varepsilon(4v^2\theta_0\theta_2 - v^2\theta_1^2 - 2\beta^2) \times \sqrt{-\frac{1}{\varepsilon}}} \\
&\quad \times \exp\left(i\left(\left(\frac{-4v^2\theta_0\theta_2 + v^2\theta_1^2 + 2\beta^2 - 2\beta\sigma}{-4v^2\theta_0\theta_2 + v^2\theta_1^2 + 2\beta^2}\right)x + \beta t + \gamma\right)\right), \\
\Phi_2(x,t) &= -\frac{\sigma v \sqrt{\Delta} \coth\left(\frac{\sqrt{\Delta}}{2}(sx+vt)\right)}{\varepsilon(4v^2\theta_0\theta_2 - v^2\theta_1^2 - 2\beta^2) \times \sqrt{-\frac{1}{\varepsilon}}} \\
&\quad \times \exp\left(i\left(\left(\frac{-4v^2\theta_0\theta_2 + v^2\theta_1^2 + 2\beta^2 - 2\beta\sigma}{-4v^2\theta_0\theta_2 + v^2\theta_1^2 + 2\beta^2}\right)x + \beta t + \gamma\right)\right), \\
\Phi_3(x,t) &= -\frac{\sigma v \sqrt{\Delta}\left(\tanh\left(\sqrt{\Delta}(sx+vt)\right) + i\,\mathrm{sec}\,h\left(\sqrt{\Delta}(sx+vt)\right)\right)}{\varepsilon(4v^2\theta_0\theta_2 - v^2\theta_1^2 - 2\beta^2) \times \sqrt{-\frac{1}{\varepsilon}}} \\
&\quad \times \exp\left(i\left(\left(\frac{-4v^2\theta_0\theta_2 + v^2\theta_1^2 + 2\beta^2 - 2\beta\sigma}{-4v^2\theta_0\theta_2 + v^2\theta_1^2 + 2\beta^2}\right)x + \beta t + \gamma\right)\right), \\
\Phi_4(x,t) &= -\frac{\sigma v \sqrt{\Delta}\left(\coth\left(\sqrt{\Delta}(sx+vt)\right) + \mathrm{csc}\,h\left(\sqrt{\Delta}(sx+vt)\right)\right)}{\varepsilon(4v^2\theta_0\theta_2 - v^2\theta_1^2 - 2\beta^2) \times \sqrt{-\frac{1}{\varepsilon}}} \\
&\quad \times \exp\left(i\left(\left(\frac{-4v^2\theta_0\theta_2 + v^2\theta_1^2 + 2\beta^2 - 2\beta\sigma}{-4v^2\theta_0\theta_2 + v^2\theta_1^2 + 2\beta^2}\right)x + \beta t + \gamma\right)\right), \\
\Phi_5(x,t) &= -\frac{\sigma v \sqrt{\Delta}\left(\tanh\left(\frac{\sqrt{\Delta}}{4}(sx+vt)\right) + \coth\left(\frac{\sqrt{\Delta}}{4}(sx+vt)\right)\right)}{2\varepsilon(4v^2\theta_0\theta_2 - v^2\theta_1^2 - 2\beta^2) \times \sqrt{-\frac{1}{\varepsilon}}} \\
&\quad \times \exp\left(i\left(\left(\frac{-4v^2\theta_0\theta_2 + v^2\theta_1^2 + 2\beta^2 - 2\beta\sigma}{-4v^2\theta_0\theta_2 + v^2\theta_1^2 + 2\beta^2}\right)x + \beta t + \gamma\right)\right),
\end{aligned}$$

$$\Phi_6(x,t) = -\frac{\sigma v\left(P\sqrt{\Delta}\cosh\left(\sqrt{\Delta}(sx+vt)\right)-\sqrt{-(-\Delta)(P^2+Q^2)}\right)}{\varepsilon(4v^2\theta_0\theta_2-v^2\theta_1^2-2\beta^2)(P\sinh\left(\sqrt{\Delta}(sx+vt)\right)+Q)\times\sqrt{-\frac{1}{\varepsilon}}} \times\exp\left(i\left(\left(\frac{-4v^2\theta_0\theta_2+v^2\theta_1^2+2\beta^2-2\beta\sigma}{-4v^2\theta_0\theta_2+v^2\theta_1^2+2\beta^2}\right)x+\beta t+\gamma\right)\right),$$

$$\Phi_7(x,t) = -\frac{\sigma v\sqrt{-(-\Delta)(P^2+Q^2)}+P\sqrt{\Delta}\cosh\left(\sqrt{\Delta}(sx+vt)\right)}{\varepsilon(4v^2\theta_0\theta_2-v^2\theta_1^2-2\beta^2)(P\sinh\left(\sqrt{\Delta}(sx+vt)\right)+Q)\times\sqrt{-\frac{1}{\varepsilon}}} \times\exp\left(i\left(\left(\frac{-4v^2\theta_0\theta_2+v^2\theta_1^2+2\beta^2-2\beta\sigma}{-4v^2\theta_0\theta_2+v^2\theta_1^2+2\beta^2}\right)x+\beta t+\gamma\right)\right),$$

$$\Phi_8(x,t) = -\frac{\sigma v\begin{pmatrix}4\theta_2\theta_0\cosh\left(\frac{\sqrt{\Delta}}{2}(sx+vt)\right)\\-\theta_1^2\cosh\left(\frac{\sqrt{\Delta}}{2}(sx+vt)\right)+\theta_1\sinh\left(\frac{\sqrt{\Delta}}{2}(sx+vt)\right)\sqrt{\Delta}\end{pmatrix}}{\varepsilon(4v^2\theta_0\theta_2-v^2\theta_1^2-2\beta^2)\begin{pmatrix}\theta_1\cosh\left(\frac{\sqrt{\Delta}}{2}(sx+vt)\right)\\-\sqrt{\Delta}\sinh\left(\frac{\sqrt{\Delta}}{2}(sx+vt)\right)\end{pmatrix}\times\sqrt{-\frac{1}{\varepsilon}}} \times\exp\left(i\left(\left(\frac{-4v^2\theta_0\theta_2+v^2\theta_1^2+2\beta^2-2\beta\sigma}{-4v^2\theta_0\theta_2+v^2\theta_1^2+2\beta^2}\right)x+\beta t+\gamma\right)\right),$$

$$\Phi_9(x,t) = -\frac{\sigma v\begin{pmatrix}4\theta_2\theta_0\sinh\left(\frac{\sqrt{\Delta}}{2}(sx+vt)\right)-\theta_1^2\sinh\left(\frac{\sqrt{\Delta}}{2}(sx+vt)\right)\\+\theta_1\cosh\left(\frac{\sqrt{\Delta}}{2}(sx+vt)\right)\sqrt{\Delta}\end{pmatrix}}{\varepsilon(4v^2\theta_0\theta_2-v^2\theta_1^2-2\beta^2)\begin{pmatrix}\theta_1\sinh\left(\frac{\sqrt{\Delta}}{2}(sx+vt)\right)\\-\sqrt{\Delta}\cosh\left(\frac{\sqrt{\Delta}}{2}(sx+vt)\right)\end{pmatrix}\times\sqrt{-\frac{1}{\varepsilon}}} \times\exp\left(i\left(\left(\frac{-4v^2\theta_0\theta_2+v^2\theta_1^2+2\beta^2-2\beta\sigma}{-4v^2\theta_0\theta_2+v^2\theta_1^2+2\beta^2}\right)x+\beta t+\gamma\right)\right),$$

$$\Phi_{10}(x,t) = \frac{\sigma v\begin{pmatrix}4\theta_2\theta_0\cosh\left(\sqrt{\Delta}(sx+vt)\right)+\sqrt{\Delta}\theta_1\sinh\left(\sqrt{\Delta}(sx+vt)\right)\\+i\sqrt{\Delta}\theta_1-\cosh\left(\sqrt{\Delta}(sx+vt)\right)\theta_1^2\end{pmatrix}}{\varepsilon(4v^2\theta_0\theta_2-v^2\theta_1^2-2\beta^2)\begin{pmatrix}\sqrt{\Delta}\sinh\left(\sqrt{\Delta}(sx+vt)\right)\\-\theta_1\cosh\left(\frac{\sqrt{\Delta}}{2}(sx+vt)\right)+i\sqrt{\Delta}\end{pmatrix}\times\sqrt{-\frac{1}{\varepsilon}}} \times\exp\left(i\left(\left(\frac{-4v^2\theta_0\theta_2+v^2\theta_1^2+2\beta^2-2\beta\sigma}{-4v^2\theta_0\theta_2+v^2\theta_1^2+2\beta^2}\right)x+\beta t+\gamma\right)\right),$$

$$\Phi_{11}(x,t) = -\frac{\sigma v\begin{pmatrix}4\theta_2\theta_0\sinh\left(\sqrt{\Delta}(sx+vt)\right)-\theta_1^2\sinh\left(\sqrt{\Delta}(sx+vt)\right)\\+\sqrt{\Delta}\theta_1\cosh\left(\sqrt{\Delta}(sx+vt)\right)+\sqrt{\Delta}\theta_1\end{pmatrix}}{\varepsilon(4v^2\theta_0\theta_2-v^2\theta_1^2-2\beta^2)\begin{pmatrix}\theta_1\sinh\left(\sqrt{\Delta}(sx+vt)\right)\\-\sqrt{\Delta}\cosh\left(\sqrt{\Delta}(sx+vt)\xi\right)-\sqrt{\Delta}\end{pmatrix}\times\sqrt{-\frac{1}{\varepsilon}}} \times\exp\left(i\left(\left(\frac{-4v^2\theta_0\theta_2+v^2\theta_1^2+2\beta^2-2\beta\sigma}{-4v^2\theta_0\theta_2+v^2\theta_1^2+2\beta^2}\right)x+\beta t+\gamma\right)\right),$$

$$\Phi_{12}(x,t) = -\frac{\sigma v\begin{pmatrix}8\theta_2\theta_0\sinh\left(\frac{\sqrt{\Delta}}{4}(sx+vt)\right)\cosh\left(\frac{\sqrt{\Delta}}{4}(sx+vt)\right)\\+2\theta_1\sqrt{\Delta}\cosh\left(\frac{\sqrt{\Delta}}{4}(sx+vt)\right)^2\\-2\theta_1^2\sinh\left(\frac{\sqrt{\Delta}}{4}(sx+vt)\right)\cosh\left(\frac{\sqrt{\Delta}}{4}(sx+vt)\right)-\sqrt{\Delta}\theta_1\end{pmatrix}}{\varepsilon(4v^2\theta_0\theta_2-v^2\theta_1^2-2\beta^2)\begin{pmatrix}2\theta_1\sinh\left(\frac{\sqrt{\Delta}}{4}(sx+vt)\right)\cosh\left(\frac{\sqrt{\Delta}}{4}(sx+vt)\right)\\-2\sqrt{\Delta}\cosh\left(\frac{\sqrt{\Delta}}{4}(sx+vt)\right)^2+\sqrt{\Delta}\end{pmatrix}\times\sqrt{-\frac{1}{\varepsilon}}} \times\exp\left(i\left(\left(\frac{-4v^2\theta_0\theta_2+v^2\theta_1^2+2\beta^2-2\beta\sigma}{-4v^2\theta_0\theta_2+v^2\theta_1^2+2\beta^2}\right)x+\beta t+\gamma\right)\right).$$

By putting constant values Eq. (4.2) along with Eq. (3.17)- Eq. (3.27) in the Eq. (4.1), and by using the wave transformation Eq. (2.2), we obtain the solutions as follows:

$$\Phi_{13}(x,t) = \frac{\sigma v\sqrt{-\Delta}\tan\left(\frac{\sqrt{-\Delta}}{2}(sx+vt)\right)}{\varepsilon(4v^2\theta_0\theta_2-v^2\theta_1^2-2\beta^2)\times\sqrt{-\frac{1}{\varepsilon}}} \times\exp\left(i\left(\left(\frac{-4v^2\theta_0\theta_2+v^2\theta_1^2+2\beta^2-2\beta\sigma}{-4v^2\theta_0\theta_2+v^2\theta_1^2+2\beta^2}\right)x+\beta t+\gamma\right)\right),$$

$$\Phi_{14}(x,t) = -\frac{\sigma v\sqrt{-\Delta}\cot\left(\frac{\sqrt{-\Delta}}{2}(sx+vt)\right)}{\varepsilon(4v^2\theta_0\theta_2-v^2\theta_1^2-2\beta^2)\times\sqrt{-\frac{1}{\varepsilon}}} \times\exp\left(i\left(\left(\frac{-4v^2\theta_0\theta_2+v^2\theta_1^2+2\beta^2-2\beta\sigma}{-4v^2\theta_0\theta_2+v^2\theta_1^2+2\beta^2}\right)x+\beta t+\gamma\right)\right),$$

$$\Phi_{15}(x,t) = \frac{\sigma v\sqrt{-\Delta}\left(\tan\left(\sqrt{-\Delta}(sx+vt)\right)+\sec\left(\sqrt{-\Delta}(sx+vt)\right)\right)}{\varepsilon(4v^2\theta_0\theta_2-v^2\theta_1^2-2\beta^2)\times\sqrt{-\frac{1}{\varepsilon}}} \times\exp\left(i\left(\left(\frac{-4v^2\theta_0\theta_2+v^2\theta_1^2+2\beta^2-2\beta\sigma}{-4v^2\theta_0\theta_2+v^2\theta_1^2+2\beta^2}\right)x+\beta t+\gamma\right)\right),$$

$$\Phi_{16}(x,t) = -\frac{\sigma v\sqrt{-\Delta}\left(\cot\left(\sqrt{-\Delta}(sx+vt)\right)+\csc\left(\sqrt{-\Delta}(sx+vt)\right)\right)}{\varepsilon(4v^2\theta_0\theta_2-v^2\theta_1^2-2\beta^2)\times\sqrt{-\frac{1}{\varepsilon}}} \times\exp\left(i\left(\left(\frac{-4v^2\theta_0\theta_2+v^2\theta_1^2+2\beta^2-2\beta\sigma}{-4v^2\theta_0\theta_2+v^2\theta_1^2+2\beta^2}\right)x+\beta t+\gamma\right)\right),$$

$$\Phi_{17}(x,t) = \frac{\sigma v\sqrt{-\Delta}\left(\tan\left(\frac{\sqrt{-\Delta}}{4}(sx+vt)\right)-\cot\left(\frac{\sqrt{-\Delta}}{4}(sx+vt)\right)\right)}{2\varepsilon(4v^2\theta_0\theta_2-v^2\theta_1^2-2\beta^2)\times\sqrt{-\frac{1}{\varepsilon}}} \times\exp\left(i\left(\left(\frac{-4v^2\theta_0\theta_2+v^2\theta_1^2+2\beta^2-2\beta\sigma}{-4v^2\theta_0\theta_2+v^2\theta_1^2+2\beta^2}\right)x+\beta t+\gamma\right)\right),$$

$$\Phi_{18}(x,t) = \frac{\sigma v\left(\sqrt{(-\Delta)(P-Q)(P+Q)}-P\sqrt{-\Delta}\cos\left(\sqrt{-\Delta}(sx+vt)\right)\right)}{\varepsilon(4v^2\theta_0\theta_2-v^2\theta_1^2-2\beta^2)(P\sin\left(\sqrt{-\Delta}(sx+vt)\right)+Q)\times\sqrt{-\frac{1}{\varepsilon}}} \times\exp\left(i\left(\left(\frac{-4v^2\theta_0\theta_2+v^2\theta_1^2+2\beta^2-2\beta\sigma}{-4v^2\theta_0\theta_2+v^2\theta_1^2+2\beta^2}\right)x+\beta t+\gamma\right)\right),$$

$$\Phi_{19}(x,t) = -\frac{\sigma v\begin{pmatrix}4\theta_2\theta_0\cos\left(\frac{\sqrt{-\Delta}}{2}(sx+vt)\right)-\theta_1^2\cos\left(\frac{\sqrt{-\Delta}}{2}(sx+vt)\right)\\-\theta_1\sin\left(\frac{\sqrt{-\Delta}}{2}(sx+vt)\right)\sqrt{-\Delta}\end{pmatrix}}{\varepsilon(4v^2\theta_0\theta_2-v^2\theta_1^2-2\beta^2)\begin{pmatrix}\sqrt{-\Delta}\sin\left(\frac{\sqrt{-\Delta}}{2}(sx+vt)\right)\\+\theta_1\cos\left(\frac{\sqrt{-\Delta}}{2}(sx+vt)\right)\end{pmatrix}\times\sqrt{-\frac{1}{\varepsilon}}} \times\exp\left(i\left(\left(\frac{-4v^2\theta_0\theta_2+v^2\theta_1^2+2\beta^2-2\beta\sigma}{-4v^2\theta_0\theta_2+v^2\theta_1^2+2\beta^2}\right)x+\beta t+\gamma\right)\right),$$

$$\Phi_{20}(x,t) = -\frac{\sigma v\begin{pmatrix}4\theta_2\theta_0\sin\left(\frac{\sqrt{-\Delta}}{2}(sx+vt)\right)\\-\theta_1^2\sin\left(\frac{\sqrt{-\Delta}}{2}(sx+vt)\right)+\theta_1\cos\left(\frac{\sqrt{-\Delta}}{2}\xi\right)\sqrt{-\Delta}\end{pmatrix}}{\varepsilon(4v^2\theta_0\theta_2-v^2\theta_1^2-2\beta^2)\begin{pmatrix}\theta_1\sin\left(\frac{\sqrt{-\Delta}}{2}(sx+vt)\right)\\-\sqrt{-\Delta}\cos\left(\frac{\sqrt{-\Delta}}{2}(sx+vt)\right)\end{pmatrix}\times\sqrt{-\frac{1}{\varepsilon}}} \times\exp\left(i\left(\left(\frac{-4v^2\theta_0\theta_2+v^2\theta_1^2+2\beta^2-2\beta\sigma}{-4v^2\theta_0\theta_2+v^2\theta_1^2+2\beta^2}\right)x+\beta t+\gamma\right)\right),$$

$$\Phi_{21}(x,t) = -\frac{\sigma v\begin{pmatrix} 4\theta_2\theta_0\cos\left(\sqrt{-\Delta}(sx+vt)\right)-\theta_1^2\cos\left(\sqrt{-\Delta}(sx+vt)\right) \\ -\theta_1\sin\left(\sqrt{-\Delta}(sx+vt)\right)\sqrt{-\Delta}-\theta_1\sqrt{-\Delta}\end{pmatrix}}{\varepsilon(4v^2\theta_0\theta_2-v^2\theta_1^2-2\beta^2)\begin{pmatrix}\sqrt{-\Delta}\sin\left(\sqrt{-\Delta}(sx+vt)\right) \\ +\theta_1\cos\left(\sqrt{-\Delta}(sx+vt)\right)+\sqrt{-\Delta}\end{pmatrix}\times\sqrt{-\frac{1}{\varepsilon}}}$$
$$\times\exp\left(i\left(\left(\frac{-4v^2\theta_0\theta_2+v^2\theta_1^2+2\beta^2-2\beta\sigma}{-4v^2\theta_0\theta_2+v^2\theta_1^2+2\beta^2}\right)x+\beta t+\gamma\right)\right),$$

$$\Phi_{22}(x,t) = -\frac{\sigma v\begin{pmatrix} 4\theta_2\theta_0\sin\left(\sqrt{-\Delta}(sx+vt)\right)-\theta_1^2\sin\left(\sqrt{-\Delta}(sx+vt)\right) \\ -\theta_1\cos\left(\sqrt{-\Delta}(sx+vt)\right)\sqrt{-\Delta}-\theta_1\sqrt{-\Delta}\end{pmatrix}}{\varepsilon(4v^2\theta_0\theta_2-v^2\theta_1^2-2\beta^2)\begin{pmatrix}\sqrt{-\Delta}\cos\left(\sqrt{-\Delta}(sx+vt)\right) \\ +\theta_1\sin\left(\sqrt{-\Delta}(sx+vt)\right)+\sqrt{-\Delta}\end{pmatrix}\times\sqrt{-\frac{1}{\varepsilon}}}$$
$$\times\exp\left(i\left(\left(\frac{-4v^2\theta_0\theta_2+v^2\theta_1^2+2\beta^2-2\beta\sigma}{-4v^2\theta_0\theta_2+v^2\theta_1^2+2\beta^2}\right)x+\beta t+\gamma\right)\right),$$

$$\Phi_{23}(x,t) = -\frac{\sigma v\begin{pmatrix} 8\theta_2\theta_0\sin\left(\frac{\sqrt{-\Delta}}{4}(sx+vt)\right)\cos\left(\frac{\sqrt{-\Delta}}{4}(sx+vt)\right)+2\theta_1\sqrt{-\Delta}\cos\left(\frac{\sqrt{-\Delta}}{4}(sx+vt)\right)^2 \\ -2\theta_1^2\sin\left(\frac{\sqrt{-\Delta}}{4}(sx+vt)\right)\cos\left(\frac{\sqrt{-\Delta}}{4}(sx+vt)\right)-\theta_1\sqrt{-\Delta}\end{pmatrix}}{\varepsilon(4v^2\theta_0\theta_2-v^2\theta_1^2-2\beta^2)\begin{pmatrix}2\theta_1\sin\left(\frac{\sqrt{-\Delta}}{4}(sx+vt)\right)\cos\left(\frac{\sqrt{-\Delta}}{4}(sx+vt)\right) \\ -2\sqrt{-\Delta}\cos\left(\frac{\sqrt{-\Delta}}{4}(sx+vt)\right)^2+\sqrt{-\Delta}\end{pmatrix}\times\sqrt{-\frac{1}{\varepsilon}}}$$
$$\times\exp\left(i\left(\left(\frac{-4v^2\theta_0\theta_2+v^2\theta_1^2+2\beta^2-2\beta\sigma}{-4v^2\theta_0\theta_2+v^2\theta_1^2+2\beta^2}\right)x+\beta t+\gamma\right)\right).$$

By putting constant values Eq. (4.2) along with Eq. (3.28)- Eq. (3.30) in the Eq. (4.1), and by using the wave transformation Eq. (2.2), we reach the solutions as follows:

$$\Phi_{24}(x,t) = \frac{\sigma v\theta_1\begin{pmatrix}-\zeta_0+\cosh(\theta_1(sx+vt)) \\ -\sinh(\theta_1(sx+vt))\end{pmatrix}}{\varepsilon(4v^2\theta_0\theta_2-v^2\theta_1^2-2\beta^2)\begin{pmatrix}\zeta_0+\cosh(\theta_1(sx+vt)) \\ -\sinh(\theta_1(sx+vt))\end{pmatrix}\times\sqrt{-\frac{1}{\varepsilon}}}$$
$$\times\exp\left(i\left(\left(\frac{-4v^2\theta_0\theta_2+v^2\theta_1^2+2\beta^2-2\beta\sigma}{-4v^2\theta_0\theta_2+v^2\theta_1^2+2\beta^2}\right)x+\beta t+\gamma\right)\right),$$

$$\Phi_{25}(x,t) = -\frac{\sigma v\theta_1\begin{pmatrix}\cosh(\theta_1(sx+vt)) \\ -\sinh(\theta_1(sx+vt))-\zeta_0\end{pmatrix}}{\varepsilon(4v^2\theta_0\theta_2-v^2\theta_1^2-2\beta^2)\begin{pmatrix}\zeta_0+\cosh(\theta_1(sx+vt)) \\ -\sinh(\theta_1(sx+vt))\end{pmatrix}\times\sqrt{-\frac{1}{\varepsilon}}}$$
$$\times\exp\left(i\left(\left(\frac{-4v^2\theta_0\theta_2+v^2\theta_1^2+2\beta^2-2\beta\sigma}{-4v^2\theta_0\theta_2+v^2\theta_1^2+2\beta^2}\right)x+\beta t+\gamma\right)\right),$$

$$\Phi_{26}(x,t) = -\frac{\sigma v\theta_1\begin{pmatrix}\cosh(\theta_1(sx+vt)) \\ +\sinh(\theta_1(sx+vt))-\zeta_0\end{pmatrix}}{\varepsilon(4v^2\theta_0\theta_2-v^2\theta_1^2-2\beta^2)\begin{pmatrix}\zeta_0+\cosh(\theta_1(sx+vt)) \\ +\sinh(\theta_1(sx+vt))\end{pmatrix}\times\sqrt{-\frac{1}{\varepsilon}}}$$
$$\times\exp\left(i\left(\left(\frac{-4v^2\theta_0\theta_2+v^2\theta_1^2+2\beta^2-2\beta\sigma}{-4v^2\theta_0\theta_2+v^2\theta_1^2+2\beta^2}\right)x+\beta t+\gamma\right)\right).$$

By putting constant values Eq. (4.2) along with Eq. (3.31) in the Eq. (4.1), and by using the wave transformation Eq. (2.2), we attain the solution as follows:

$$\Phi_{27}(x,t) = \frac{\sigma v(\theta_0\theta_1(sx+vt)+c_1\theta_1-2\theta_2)}{\varepsilon(4v^2\theta_0\theta_2-v^2\theta_1^2-2\beta^2)((sx+vt)\theta_0+c_1)\times\sqrt{-\frac{1}{\varepsilon}}}$$
$$\times\exp\left(i\left(\left(\frac{-4v^2\theta_0\theta_2+v^2\theta_1^2+2\beta^2-2\beta\sigma}{-4v^2\theta_0\theta_2+v^2\theta_1^2+2\beta^2}\right)x+\beta t+\gamma\right)\right).$$

5. Graphical Discussion

In this section, we discuss the graphical behavior of the solutions successfully obtained using the GREM method for the CCKS.

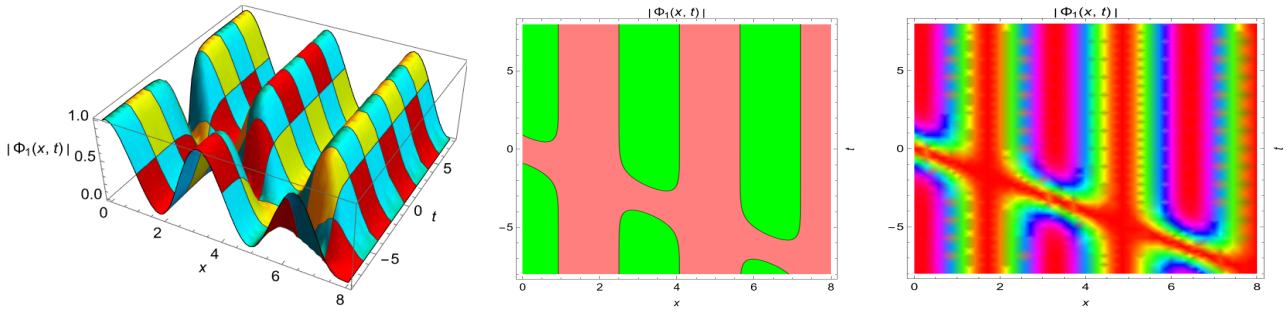

Figure 1. The 3d, contour, and density plots for the solution $|\Phi_1(x,t)|$.

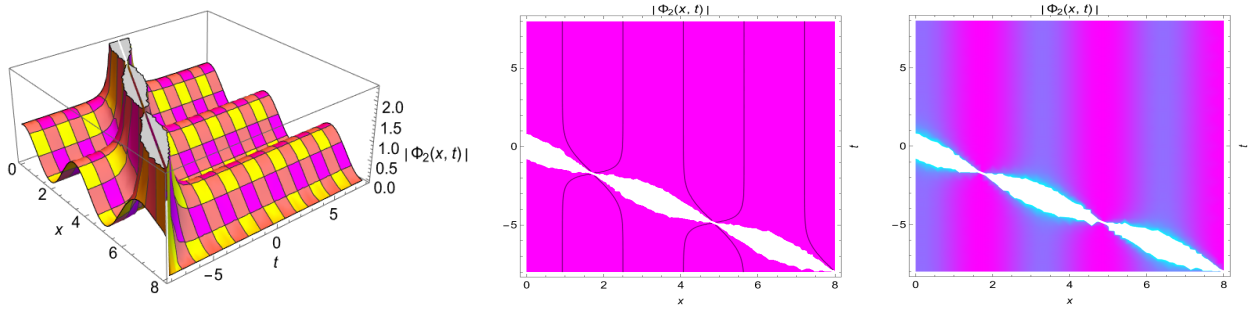

Figure 2. The 3d, contour, and density plots for the solution $|\Phi_2(x,t)|$.

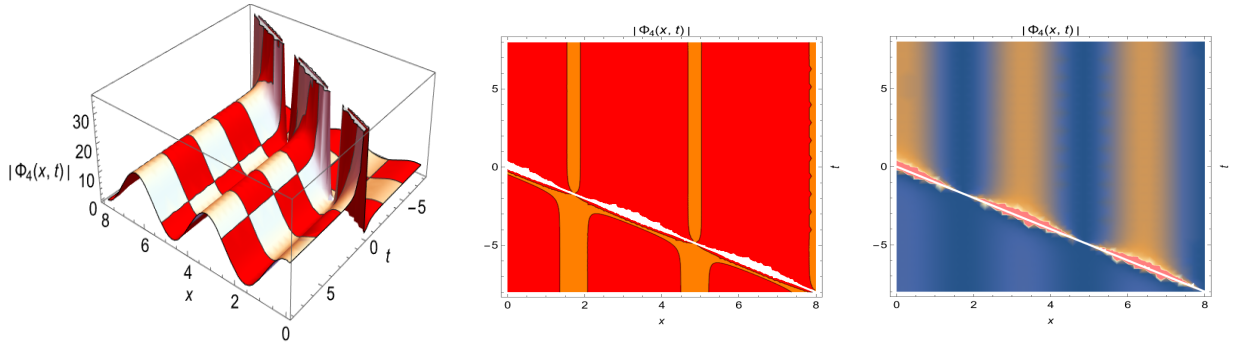

Figure 3. The 3d, contour, and density plots for the solution $|\Phi_4(x,t)|$.

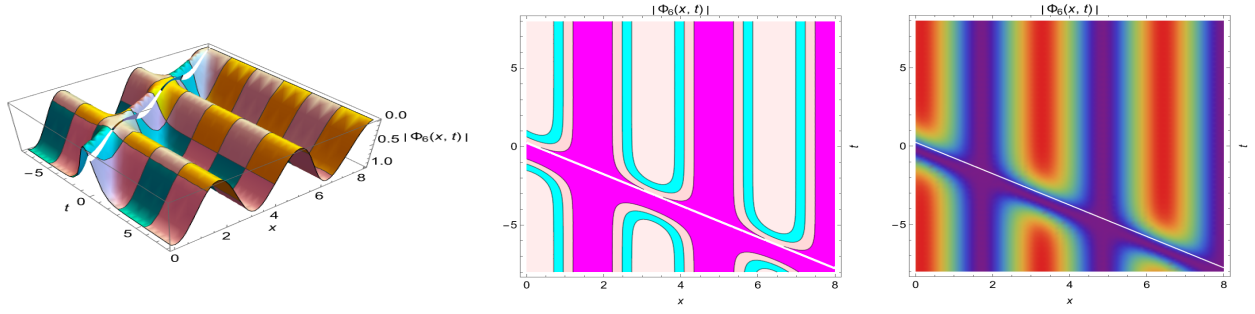

Figure 4. The 3d, contour, and density plots for the solution $|\Phi_6(x,t)|$.

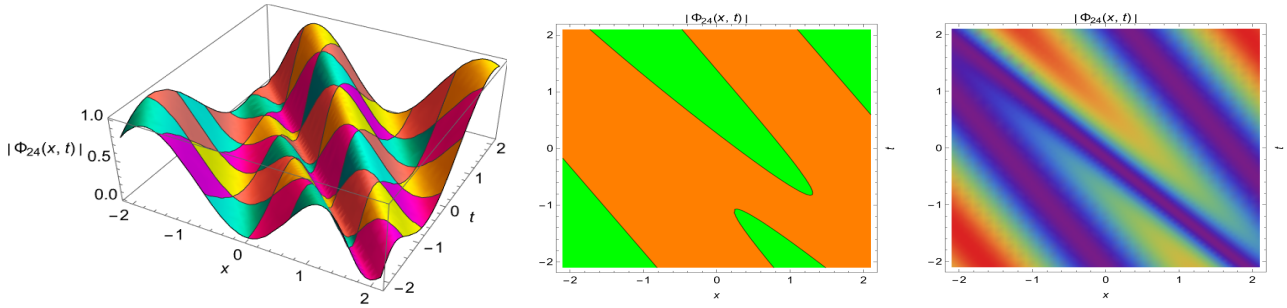

Figure 5. The 3d, contour, and density plots for the solution $|\Phi_{24}(x,t)|$.

Fig.1. The diagram of $|\Phi_1(x,t)|$ when $v=2$, $\beta=1$, $s=2$, $\sigma=3$, $\varepsilon=1$, $\theta_0=1$, $\theta_1=3$, $\theta_2=2$, $\gamma=3$, $\xi=sx+vt$.

Fig.2. The diagram of $|\Phi_2(x,t)|$ when $v=2$, $\beta=1$, $s=2$, $\sigma=3$, $\varepsilon=1$, $\theta_0=1$, $\theta_1=3$, $\theta_2=2$, $\gamma=3$, $\xi=sx+vt$.

Fig.3. The diagram of $|\Phi_4(x,t)|$ when $v=2$, $\beta=1$, $s=2$, $\sigma=3$, $\varepsilon=1$, $\theta_0=1$, $\theta_1=3$, $\theta_2=2$, $\gamma=3$, $\xi=sx+vt$.

Fig.4. The diagram of $|\Phi_6(x,t)|$ when $v=2$, $\beta=1$, $s=2$, $\sigma=3$, $\varepsilon=1$, $\theta_0=1$, $\theta_1=3$, $\theta_2=2$, $\gamma=3$, $P=2$, $Q=-1$, $\xi=sx+vt$.

Fig.5. The diagram of $|\Phi_{24}(x,t)|$ when $v=2$, $\beta=1$, $s=2$, $\sigma=3$, $\varepsilon=1$, $\theta_0=0$, $\theta_1=2$, $\theta_2=3$, $\gamma=3$, $\zeta_0=2$, $\xi=sx+vt$.

6. Conclusion

This examination focused on analyzing the CCKS, which is employed in diverse areas like ferromagnetic materials, nonlinear optics, and optical fibers. The CCKS is significant as it is a crucial model that enhances the understanding of complex physical and mathematical concepts, making it a valuable tool for scientific research and applications. The GREM approach was operated to scrutinize analytical solutions to the considered equation. It is a powerful analytical technique for solving various differential equations, particularly nonlinear ones. Following the application of the method, shock, complex solitary shock, shock singular, and periodic singular wave solutions were seen for both single and mixed wave solutions. The derivation also leads to reasonable solutions. 3D, contour and density graphs were plotted by choosing suitable parameter values via Mathematica to visualize the graphical representation of the acquired soliton solutions. These solutions we obtained using the GREM method can be extended to the analytical examination of various other types of NLPDEs in fields such as mathematical physics, plasma physics, applied sciences, nonlinear dynamics, and engineering. The accuracy of the results was verified by utilizing Maple to substitute the solutions back into the initial equation.

Article Information

Acknowledgements: The author would like to express his sincere thanks to the editor and the anonymous reviewers for their helpful comments and suggestions.

Supporting/Supporting organizations: No grants were received from any public, private or non-profit organizations for this research.

Ethical approval and participant consent: It is declared that during the preparation process of this study, scientific and ethical principles were followed and all the studies benefited from are stated in the bibliography.

Plagiarism statement: This article was scanned by the plagiarism program.

References

[1] E. Yaşar, Y. Yıldırım, A. R. Adem, *Perturbed optical solitons with spatio-temporal dispersion in (2+1)-dimensions by extended Kudryashov method*, Optik, **158** (2018), 1-14.

[2] M. Şenol, *Abundant solitary wave solutions to the new extended (3+ 1)-dimensional nonlinear evolution equation arising in fluid dynamics*, Mod. Phys. Lett. B., (2024) 2450475.

[3] A.R. Seadawy, N. Nasreen, S. Althobaiti, S. Sayed, A. Biswas, *Soliton solutions of Sasa–Satsuma nonlinear Schrödinger model and construction of modulation instability analysis*, Opt. Quantum Electron., **53** (2021), 1-15.

[4] C. M. Khalique, O. D. Adeyemo, *Soliton solutions, travelling wave solutions and conserved quantities for a three-dimensional soliton equation in plasma physics*, Commun. Theor. Phys., **73**(12) (2021), 125003.

[5] M. Bilal, U. Younas, J. Ren, *Dynamics of exact soliton solutions to the coupled nonlinear system using reliable analytical mathematical approaches*, Commun. Theor. Phys., **73**(8) (2021), 085005.

[6] S. Arshed, G. Akram, M. Sadaf, M. Irfan, M. Inc, *Extraction of exact soliton solutions of (2+ 1)-dimensional Chaffee-Infante equation using two exact integration techniques*, Opt. Quantum Electron., **56**(6) (2024), 1-15.

[7] M. A. Ullah, K. Rehan, Z. Perveen, M. Sadaf, G. Akram, *Soliton dynamics of the KdV-mKdV equation using three distinct exact methods in nonlinear phenomena*, Nonlinear Eng., **13**(1) (2024), 20220318.

[8] M. Bilal, H. Haris, A. Waheed, M. Faheem, *The analysis of exact solitons solutions in monomode optical fibers to the generalized nonlinear Schrödinger system by the compatible techniques*, Int. J. Math. Comput. Eng., **1**(2) (2023), 149-170.

[9] A. Ali, J. Ahmad, S. Javed, *Exact soliton solutions and stability analysis to (3+1)-dimensional nonlinear Schrödinger model,* Alex. Eng. J., **76** (2023), 747-756.

[10] E. H. Zahran, H. Ahmad, M. Rahaman, R. A. Ibrahim, *Soliton solutions in (2+1)-dimensional integrable spin systems: an investigation of the Myrzakulov–Lakshmanan equation-II*, Opt. Quantum Electron., **56**(5) (2024), 895.

[11] W. Ma, S. Bilige, *Novel interaction solutions to the (3+1)-dimensional Hirota bilinear equation by bilinear neural network method*, Mod. Phys. Lett. B., (2024) 2450240.

[12] A. M. Wazwaz, L. Kaur, *New integrable Boussinesq equations of distinct dimensions with diverse variety of soliton solutions*, Nonlinear Dyn., **97** (2019), 83-94.

[13] D. Wang, Y. T. Gao, X. Yu, G. F. Deng, F. Y. Liu, *Painlevé Analysis, Bäcklund Transformation, Lax Pair, Periodic-and Travelling-Wave Solutions for a Generalized (2+ 1)-Dimensional Hirota–Satsuma–Ito Equation in Fluid Mechanics*, Qual. Theory Dyn. Syst., **23**(1) (2024) 12.

[14] C. M. Khalique, M. Y. T. Lephoko, *Conserved vectors and symmetry solutions of the Landau-Ginzburg-Higgs equation of theoretical physics,* Commun. Theor. Phys., **76**(4) (2024), 045006.

[15] A. H. Arnous, A. Biswas, Y. Yildirim, A. J. M. Jawad, L. Moraru, S. Moldovanu, A. S. Alshomrani, *Optical solitons for the concatenation model with differential group delay having multiplicate white noise*, Ukr. J. Phys. Opt., **25**(1) (2024).

[16] A. Jawad, A. Biswas, *Solutions of resonant nonlinear Schrödinger's equation with exotic non-Kerr law nonlinearities*, Al-Rafidain J. Eng. Sci., (2024) 43-50.

[17] E. M. Zayed, K. A. Alurrfi, M. Elshater, Y. Yildirim, *Dispersive optical solitons with Stochastic Radhakrishnan-Kundu-Lakshmanan equation in Magneto-Optic Waveguides having power law nonlinearity and multiplicative white noise,* Ukr. J. Phys. Opt., **25**(5) (2024), S1086-S1112.

[18] M. A. U. Khan, G. Akram, M. Sadaf, *Dynamics of novel exact soliton solutions of concatenation model using effective techniques*, Opt. Quantum Electron., **56**(3) (2024), 385.

[19] M. A. Ullah, K. Rehan, Z. Perveen, M. Sadaf, G. Akram, *Soliton dynamics of the KdV–mKdV equation using three distinct exact methods in nonlinear phenomena*, Nonlinear Eng., **13**(1) (2024), 20220318.

[20] G. Akram, M. Sadaf, M.A.U. Khan, *Dynamics investigation of the (4+ 1)-dimensional Fokas equation using two effective techniques*, Results Phys., **42** (2022) 105994.

[21] M. Raheel, A. Zafar, M. R. Ali, Z. Myrzakulova, A. Bekir, R. Myrzakulov, *New analytical wave solutions to the M-fractional Kuralay-II equations based on three distinct schemes*, (2023).

[22] Z. Sagidullayeva, G. Nugmanova, R. Myrzakulov, N. Serikbayev, *Integrable Kuralay equations: geometry, solutions and generalizations*, Symmetry, **14**(7) (2022) 1374.

[23] E. H. M. Zahran, Z. Umurzakhova A. Bekir, R. A. Ibrahim, R. Myrzakulov, *New diverse types of the soliton arising from the integrable Kuralay equations against its numerical solutions,* The Europ. Phys. Journal Plus, **139**(11) (2023), 1-18.

[24] A. Zafar, M. Raheel, M. R. Ali, Z. Myrzakulova, A. Bekir, R. Myrzakulov, *Exact solutions of M-fractional Kuralay equation via three analytical schemes*, Symmetry, **15**(10) (2023), 1862.

[25] W. A. Faridi, M. A. Bakar, Z. Myrzakulova, R. Myrzakulov, A. Akgül, S. M. El Din, *The formation of solitary wave solutions and their propagation for Kuralay equation*, Results Phys., **52** (2023) 106774.

[26] T. Mathanaranjan, *Optical soliton, linear stability analysis and conservation laws via multipliers to the integrable Kuralay equation*, Optik, **290** (2023), 171266.

[27] S. Ali, A. Ullah, S. F. Aldosary, S. Ahmad, S. Ahmad, *Construction of optical solitary wave solutions and their propagation for Kuralay system using tanh-coth and energy balance method*, Results Phys., **59** (2024), 107556.

[28] S. D. Zhu, *The generalizing Riccati equation mapping method in non-linear evolution equation: application to (2+ 1)-dimensional Boiti-Leon-Pempinelle equation,* Chaos, Solitons & Fractals, **37**(5) (2008), 1335-1342.

[29] N. Ahmed, M. Z. Baber, M. S. Iqbal, A. Annum, S. M. Ali, M. Ali, A. Akgül, S. M. El Din, *Analytical study of reaction diffusion Lengyel-Epstein system by generalized Riccati equation mapping method,* Scientific Reports, **13**(1) (2023), 20033.

[30] S. Kumar, M. Niwas, *Abundant soliton solutions and different dynamical behaviors of various waveforms to a new (3+1)-dimensional Schrödinger equation in optical fibers,* Opt. Quantum Electron., **55**(6) (2023), 531.

Journal of Mathematical Sciences and Modelling, 7(3) (2024) 157-167
Research Article

Journal of Mathematical Sciences and Modelling

Journal Homepage: www.dergipark.gov.tr/jmsm
ISSN: 2636-8692
DOI: https://doi.org/10.33187/jmsm.1595276

Numerical Solution of Nonlinear Advection Equation Using Reproducing Kernel Method

Onur Saldır

Department of Mathematics, Faculty of Science, Van Yuzuncu Yıl University, Van, Türkiye

Article Info

Keywords: *Advection equation, Convergence, Iterative solution, Numerical solution, Reproducing kernel method*
2010 AMS: *46E22, 47B32, 65M99*
Received: *2 December 2024*
Accepted: *31 December 2024*
Available online: *31 December 2024*

Abstract

In this study, an iterative approximation is proposed by using the reproducing kernel method (RKM) for the nonlinear advection equation. To apply the iterative RKM, specific reproducing kernel spaces are defined and their kernel functions are presented. The proposed method requires homogenising the initial or boundary conditions of the problem under consideration. After homogenising the initial condition of the advection equation, a linear operator selection is made, and then the approximate solution is constructed using orthonormal basis functions in serial form. Convergence analysis of the approximate solution is demonstrated through the lemma and theorem. Numerical outcomes are provided in the form of graphics and tables to show the efficiency and accuracy of the presented method.

1. Introduction

In this paper, an iterative reproducing kernel approximation is presented for obtaining a serial solution of the nonlinear advection equation as follows [1]:

$$y_\kappa(\zeta,\kappa)+y(\zeta,\kappa)y_\zeta(\zeta,\kappa)=f(\zeta,\kappa), \tag{1.1}$$

$$0\le\zeta\le 1, 0\le\kappa\le 1,$$

$$y(\zeta,0)=h(\zeta). \tag{1.2}$$

Here, $f(\zeta,\kappa)$ is a continuous function.

In environmental sciences, advection is transporting chemical or biological material by bulk motion. The advection equation has significant importance in meteorology and oceanography [2]. Various analytical and numerical methods have been proposed in the literature to obtain solutions to the advection equation. For instance, Khan and Wu proposed the homotopy perturbation transform method for the advection equation in [3], the Fourier series method is applied by Sanugi and Evans in [4], Wazwaz employed the Adomian decomposition method for the advection equation in [5], the finite difference method is presented by Molenkamp in [6], the Laplace decomposition method is employed in [7]. Nisar et al. [8] suggested a numerical technique for the nonlinear advection equation using the Padé approximation. The explicit finite difference scheme is used to obtain a numerical solution of the advection diffusion equation by Ara et al. [9]. Cosgun and Sari [10] employed the reversed fixed point iteration for advection-diffusion processes. The homotopy analaysis method is implemented for the fractional advection equation by Alkan [11]. Mirza et al. [12] proposed an analytical solution to the fractional advection diffusion equation. Mirzaee et al. [13] suggested the finite difference and spline approximation for stochastic the advection-diffusion equation with fractional order.
The origin of the reproducing kernel method goes back to Zaremba's researches at the beginning of last century. He focused on boundary value problems with Dirichlet conditions in [14]. This concept is improved as theoretically in [15] and [16]. Also, some specific reproducing kernel spaces that have trigonometric and polynomial kernels are presented in [17]. The reproducing kernel method is applied to many model problems. For instance, Bagley-Torvik and Painlevé equations [18], fractional order systems [19], Fredholm integro-differential

***Email address and ORCID number*: onursaldir@gmail.com, 0000-0002-5292-9458 (O. Saldır),**
Cite as "O. Saldır, *Numerical solution of nonlinear advection equation using reproducing kernel method*, J. Math. Sci. Model., 7(3) (2024), 157-167"

equations [20], integro-differential equations with Fredholm operator [21], eighth order boundary value problems [22], fractional Riccati differential equations [23], sine-Gordon equation [24], nonlinear system of PDEs [25], fractional advection-dispersion equation [26], time fractional telegraph equation [27], nonlinear hyperbolic telegraph equation [28], reaction-diffusion equations [29], time fractional partial integro-differential equations [30], class of fractional partial differential equation [31], time fractional Tricomi and Keldysh equations [32], and so on [33]-[38].

This paper is arranged as follows: Section 2 presents some specific reproducing kernel spaces and basic definitions. Section 3 provides a detailed explanation of the linear operator selection and the construction of the approximate solution for the nonlinear advection equation. In Section 4, a theorem and lemma show the convergence of the constructed approximate solution. In Section 5, the proposed method is tested on two equations, and the numerical outcomes are presented with tables and graphs to demonstrate the effectiveness of the method. Section 6 gives a brief conclusion.

Symbols and nomenclature

Notation	Meaning
κ	Time variable
ζ	Space variable
$W_2^{(2,2)}$	Special Hilbert space
Δ	$[0,1]\times[0,1]$
$T_{(t,x)}(\zeta,\kappa)$	Reproducing kernel function
AC	Absolutely continuous
L	Linear operator
CC	Completely continuous
$\omega(\zeta,\kappa)$	Exact solution
$\omega_n(\zeta,\kappa)$	Approximate solution
$\mathbb{C}$	Complex numbers
$L^2[0,1]$	Squared integrable Lebesgue space in $[0,1]$

2. Preliminaries

This section introduces the special one- and two-variable Hilbert spaces used in the construction of the approximate solution and the reproducing kernel functions of these spaces.

Definition 2.1. *Let $\Theta\neq\emptyset$ an abstract set, H be a Hilbert space and B is defined as $B:\Theta\times\Theta\to\mathbb{C}$.*

$$i.B(.,r)\in H,\ \ \forall r\in\Theta,$$
$$ii.\langle\mu(.),B(.,r)\rangle=\mu(r)\ \ \forall r\in\Theta,\ \forall\mu\in H.$$

If the above conditions are satisfied, then B and H are called reproducing kernel function and reproducing kernel Hilbert space, respectively.

Before the construction of the representation solution, some specific reproducing kernel spaces and their kernel functions will be given to solve the advection equation. The procedure for obtaining the reproducing kernels can be found in [36].

$W_2^1[0,1]$ Hilbert space

$$W_2^1[0,1]=\{\tau(\zeta)\ |\ \tau\text{ is AC function},\ \ \tau'\in L^2[0,1]\}.$$

The inner product, norm and kernel function for the space $W_2^1[0,1]$ are given as follows.

1. The inner product:

$$\langle\tau(\zeta),\omega(\zeta)\rangle_{W_2^1}=\tau(0)\,\omega(0)+\int_0^1\tau'(\zeta)\,\omega'(\zeta)\,d\zeta.$$

2. The norm:

$$\|\tau\|^2_{W_2^1}=\langle\tau,\tau\rangle_{W_2^1},\ \ \tau,\omega\in W_2^1[0,1].$$

3. The kernel function:

$$R_t^{\{1\}}(\zeta)=\begin{cases}1+\zeta,\ \ \zeta\le t,\\ 1+t,\ \ t>\zeta.\end{cases}$$

$W_2^2[0,1]$ Hilbert space

$$W_2^2[0,1]=\{\tau(\zeta)|\tau,\ \tau'\text{are AC functions},\tau''\in L^2[0,1]\}$$

The inner product, norm and kernel function for the space $W_2^2[0,1]$ are given as follows.

1. The inner product:

$$\langle\tau(\zeta),\omega(\zeta)\rangle_{W_2^2}=\tau(0)\,\omega(0)+\tau'(0)\,\omega'(0)+\int_0^1\tau''(\zeta)\,\omega''(\zeta)\,d\zeta.$$

2. The norm:

$$\|\tau\|^2_{W_2^2} = \langle \tau, \tau \rangle_{W_2^2},\ \omega, \tau \in W_2^2[0,1].$$

3. The kernel function:

$$R_t^{\{2\}}(\zeta) = \begin{cases} 1+\zeta t+\frac{1}{2}t\zeta^2-\frac{1}{6}\zeta^3,\ \zeta \le t, \\ 1-\frac{1}{6}t^3+\frac{1}{2}\zeta t^2+t\zeta,\ \zeta > t. \end{cases}$$

In a similar manner to the above, namely under same inner product and norm, the following closed subspace of $W_2^2[0,1]$ can be defined as

$$W_2^2[0,1] = \{\tau(\zeta) | \tau, \tau' \text{are AC functions}, \tau'' \in L^2[0,1], \tau(0) = 0\},$$

and its kernel function is

$$R_x^{\{2\}}(\kappa) = \begin{cases} \kappa x+\frac{1}{2}x\kappa^2-\frac{1}{6}\kappa^3,\ \kappa \le x, \\ -\frac{1}{6}x^3+\frac{1}{2}\kappa x^2+x\kappa,\ \kappa > x. \end{cases}$$

$\mathbf{W_2^{(2,2)}}(\Delta)$ Hilbert space

Let be $\Delta = [0,1]\times[0,1]$. $W_2^{(2,2)}(\Delta)$ should be defined for obtain representation solution of model problem (1.1) subject to initial condition (1.2).

$$W_2^{(2,2)}(\Delta) = \{\omega(\zeta,\kappa) | \frac{\partial^2\omega}{\partial\zeta\partial\kappa} \text{ is completely continuous in } \Delta, \frac{\partial^4\omega}{\partial\zeta^2\partial\kappa^2} \in L^2(\Delta), \omega(\zeta,0) = 0\}.$$

The inner product and norm for the space $W_2^{(2,2)}(\Delta)$ are given as follows.
1. The inner product :

$$\begin{aligned} \langle \omega(\zeta,\kappa), u(\zeta,\kappa)\rangle_{W_2^{(2,2)}} &= \sum_{i=0}^{1}\int_0^1 [\frac{\partial^2}{\partial\kappa^2}\frac{\partial^i}{\partial\zeta^i}\omega(0,\kappa)\frac{\partial^2}{\partial\kappa^2}\frac{\partial^i}{\partial\zeta^i}u(0,\kappa)]d\kappa + \sum_{j=0}^{1}\langle \frac{\partial^j}{\partial\kappa^j}\omega(\zeta,0), \frac{\partial^j}{\partial\kappa^j}u(\zeta,0)\rangle_{W_2^2} \\ &+ \int_0^1\int_0^1 [\frac{\partial^2}{\partial\zeta^2}\frac{\partial^2}{\partial\kappa^2}\omega(\zeta,\kappa)\frac{\partial^2}{\partial\zeta^2}\frac{\partial^2}{\partial\kappa^2}u(\zeta,\kappa)]d\zeta d\kappa,\ \omega, u \in W_2^{(2,2)}(\Delta). \end{aligned}$$

2. The norm:

$$\|\omega\|^2_{W_2^{(2,2)}} = \langle \omega, \omega \rangle_{W_2^{(2,2)}},\ \omega \in W_2^{(2,2)}(\Delta).$$

The following basic theorem of reproducing kernel theory shows that the kernel function of $W_2^{(2,2)}(\Delta)$ is derived as multiplying of kernel functions of $W_2^2[0,1]$ for ζ and κ variables.

Theorem 2.2. *[36] Let $T_{(t,x)}(\zeta,\kappa)$ be a kernel function of $W_2^{(2,2)}(\Delta)$. So, it can be written that*

$$T_{(t,x)}(\zeta,\kappa) = R_t^{\{2\}}(\zeta)R_x^{\{2\}}(\kappa),$$

where $R_t^{\{2\}}(\zeta)$ and $R_x^{\{2\}}(\kappa)$ are reproducing kernel functions of $W_2^2[0,1]$. For any $\omega(\zeta,\kappa) \in W_2^{(2,2)}(\Delta)$

$$\omega(t,x) = \langle \omega(\zeta,\kappa), T_{(t,x)}(\zeta,\kappa)\rangle_{W_2^{(2,2)}}$$

and

$$T_{(\zeta,\kappa)}(t,x) = T_{(t,x)}(\zeta,\kappa).$$

$\mathbf{W_2^{(1,1)}}(\Delta)$ Hilbert space

$$W_2^{(1,1)}(\Delta) = \{\omega(\zeta,\kappa) |\ \omega \text{ is CC function in } \Delta, \frac{\partial^2\omega}{\partial\zeta\partial\kappa} \in L^2(\Delta)\}.$$

The inner product, norm and kernel function for the space $W_2^{(1,1)}(\Delta)$ are given as follows.
1. The inner product:

$$\begin{aligned} \langle \omega(\zeta,\kappa), u(\zeta,\kappa)\rangle_{W_2^{(1,1)}} &= \int_0^1 [\frac{\partial}{\partial\kappa}\omega(0,\kappa)\frac{\partial}{\partial\kappa}u(0,\kappa)]d\kappa + \langle \omega(\zeta,0), u(\zeta,0)\rangle_{W_2^1} \\ &+ \int_0^1\int_0^1 [\frac{\partial}{\partial\zeta}\frac{\partial}{\partial\kappa}\omega(\zeta,\kappa)\frac{\partial}{\partial\zeta}\frac{\partial}{\partial\kappa}u(\zeta,\kappa)]d\zeta d\kappa,\ \omega, u \in W_2^{(1,1)}(\Delta). \end{aligned}$$

2. The norm:

$$\|\omega\|^2_{W_2^{(1,1)}} = \langle \omega, \omega \rangle_{W_2^{(1,1)}},\ \omega \in W_2^{(1,1)}(\Delta).$$

3. The kernel function:

$$\tilde{T}_{(t,x)}(\zeta,\kappa) = R_t^{\{1\}}(\zeta)R_x^{\{1\}}(\kappa).$$

3. Iterative Solution for Eqs. (1)-(2) in Space $W_2^{(2,2)}(\Delta)$

This section will explain how to construct an iterative solution for the nonlinear advection equation and provide the necessary theoretical information. First, the initial condition of Eq. (1.1) is homogenised, and then the linear operator selection is made. After the homogenisation process, the selection of the linear operator L is as follows:

$$L : W_2^{(2,2)}(\Delta) \to W_2^{(1,1)}(\Delta),$$

$$L\omega(\zeta,\kappa) = \omega_\kappa(\zeta,\kappa) + h(\zeta)\omega_\zeta(\zeta,\kappa) + h^{'}(\zeta)\omega(\zeta,\kappa). \tag{3.1}$$

The Eq. (3.1) can be expressed as:

$$\begin{cases} L\omega(\zeta,\kappa) = F(\zeta,\kappa,\omega(\zeta,\kappa),\omega_\zeta(\zeta,\kappa)), \quad \zeta,\kappa \in [0,1], \\ \omega(\zeta,0) = 0. \end{cases} \tag{3.2}$$

Here, $F(\zeta,\kappa,\omega(\zeta,\kappa),\omega_\zeta(\zeta,\kappa)) = f(\zeta,\kappa) - h^{'}(\zeta)h(\zeta) - \omega(\zeta,\kappa)\omega_\zeta(\zeta,\kappa)$.

If $\{(\zeta_i,\kappa_i)\}_{i=1}^{\infty}$ is a countable dense subset in Δ, then $\Psi_i(\zeta,\kappa)$ is defined as:

$$\begin{aligned} \Psi_i(\zeta,\kappa) &= L_{(t,x)}T_{(t,x)}(\zeta,\kappa)|_{(t,x)=(\zeta_i,\kappa_i)} \\ &= \{\frac{\partial}{\partial x}T_{(t,x)}(\zeta,\kappa) + h(t)\frac{\partial}{\partial t}T_{(t,x)}(\zeta,\kappa) + h^{'}(t)T_{(t,x)}(\zeta,\kappa)\}|_{(t,x)=(\zeta_i,\kappa_i)} \\ &= \frac{\partial}{\partial\kappa}T_{(\zeta_i,\kappa_i)}(\zeta,\kappa) + h(\zeta_i)\frac{\partial}{\partial t}T_{(\zeta_i,\kappa_i)}(\zeta,\kappa) + h^{'}(\zeta_i)T_{(\zeta_i,\kappa_i)}(\zeta,\kappa). \end{aligned} \tag{3.3}$$

The following theorem shows that $\Psi_i(\zeta,\kappa)$ is completely continuous and linear operator L is bounded.

Theorem 3.1. $\Psi_i(\zeta,\kappa) \in W_2^{(2,2)}(\Delta), i = 1,2,...$

Proof. The following conditions should be provide to prove this theorem.
1. $\frac{\partial^4\Psi_i(\zeta,\kappa)}{\partial\zeta^2\partial\kappa^2} \in L^2(\Delta)$
2. $\frac{\partial^2\Psi_i(\zeta,\kappa)}{\partial\zeta\partial\kappa}$ is completely continuous function
3. $\Psi_i(\zeta,\kappa)$ satisfies the initial condition.

One can show that any elements of $W_2^{(2,2)}(\Delta)$ satisfies the above conditions 1-3.
Now, from the kernel function property, the following equation can be written

$$\partial^5_{t\zeta^2\kappa^2}T_{(t,x)}(\zeta,\kappa) = \partial^3_{t\zeta^2}R_t^{\{2\}}(\zeta)\partial^2_{\kappa^2}R_x^{\{2\}}(\kappa).$$

The $\partial^3_{t\zeta^2}R_t^{\{2\}}(\zeta)$ and $\partial^2_{\kappa^2}R_x^{\{2\}}(\kappa)$ functions are bounded in $[0,1]$ due to their continuity in $[0,1]$. Therefore, the following inequality can be expressed:

$$|\partial^5_{t\zeta^2\kappa^2}T_{(t,x)}(\zeta,\kappa)| \le M_1.$$

The following inequalities can be written by the same way of above:

$$\begin{aligned} |\partial^5_{x\zeta^2\kappa^2}T_{(t,x)}(\zeta,\kappa)| &\le M_2, \\ |\partial^4_{\zeta^2\kappa^2}T_{(t,x)}(\zeta,\kappa)| &\le M_3. \end{aligned}$$

Here, M_1, M_2 and M_3 are positive constants. From (3.3),

$$\begin{aligned} |\frac{\partial^4\Psi_i(\zeta,\kappa)}{\partial\zeta^2\partial\kappa^2}| &\le |M_2 + h(\zeta_i)M_1 + h^{'}(\zeta_i)M_3| \\ &\le M_2 + |h(\zeta_i)|M_1 + |h^{'}(\zeta_i)|M_3. \end{aligned}$$

Therefore, $\frac{\partial^4\Psi_i(\zeta,\kappa)}{\partial\zeta^2\partial\kappa^2} \in L^2(\Delta)$. Noting that Δ is closed, thus, $\frac{\partial^2\Psi_i(\zeta,\kappa)}{\partial\zeta\partial\kappa}$ is completely continuous in Δ. And also, $\Psi_i(\zeta,\kappa)$ satisfies the initial condition because $T_{(t,x)}(\zeta,0) = 0$. Thus $\Psi_i(\zeta,\kappa) \in W_2^{(2,2)}(\Delta)$.

Theorem 3.2. *$\{\Psi_i(\zeta,\kappa)\}_{i=1}^{\infty}$ is a complete system of $W_2^{(2,2)}(\Delta)$, for $i = 1,2,....$*

Proof. We have

$$\begin{aligned} \Psi_i(\zeta,\kappa) &= (L^*\Phi_i)(\zeta,\kappa) = \langle (L^*\Phi_i)(t,x), T_{(\zeta,\kappa)}(t,x)\rangle_{W_2^{(2,2)}} \\ &= \langle \Phi_i(t,x), L_{(t,x)}T_{(\zeta,\kappa)}(t,x)\rangle_{W_2^{(1,1)}} = L_{(t,x)}T_{(\zeta,\kappa)}(t,x)|_{(t,x)=(\zeta_i,\kappa_i)} \\ &= L_{(t,x)}T_{(t,x)}(\zeta,\kappa)|_{(t,x)=(\zeta_i,\kappa_i)}. \end{aligned}$$

Clearly, $\Psi_i(\zeta,\kappa) \in W_2^{(2,2)}(\Delta)$, for each fixed $\omega(\zeta,\kappa) \in W_2^{(2,2)}(\Delta)$, if $\langle \omega(\zeta,\kappa), \Psi_i(\zeta,\kappa)\rangle_{W_2^{(2,2)}} = 0$.
Namely,

$$\langle \omega(\zeta,\kappa), (L^*\Phi_i)(\zeta,\kappa)\rangle_{W_2^{(2,2)}} = \langle L\omega(\zeta,\kappa), \Phi_i(\zeta,\kappa)\rangle_{W_2^{(1,1)}} = (L\omega)(\zeta_i,\kappa_i) = 0, \;\; i = 1,2,... \tag{3.4}$$

$(L\omega)(\zeta,\kappa) = 0$ since $\{(\zeta_i,\kappa_i)\}_{i=1}^{\infty}$ is dense in Δ. When the inverse operator L^{-1} is used in Eq.(3.4), it can be clearly seen that $\omega = 0$.

The orthonormal system $\{\overline{\Psi}_i(\zeta,\kappa)\}_{i=1}^{\infty}$ can be attained by the Gram-Schmidt orthogonalization of $\{\Psi_i(\zeta,\kappa)\}_{i=1}^{\infty}$ as

$$\overline{\Psi}_i(\zeta,\kappa) = \sum_{k=1}^{i} \beta_{ik}\Psi_k(\zeta,\kappa).$$

The orthogonalization process is given by formula as follow:

$$\beta_{11} = \frac{1}{\|\Psi_1\|}, \;\; \beta_{ik} = \frac{1}{d_{ik}}, \;\; \beta_{ij} = -\frac{1}{d_{ik}}\sum_{k=j}^{i-1} c_{ik}\beta_{kj} \;\text{ for }\; j < i,$$

and also

$$d_{ik} = \sqrt{\|\Psi_i\|^2 - \sum_{k=1}^{i-1} c_{ik}^2}, \;\; c_{ik} = \langle \Psi_i, \overline{\Psi_k}\rangle_{W_2^{(2,2)}}.$$

Theorem 3.3. *Let $\{(\zeta_i,\kappa_i)\}_{i=1}^{\infty}$ be dense in Δ, then the iterative solution of Eq. (3.2) is*

$$\omega(\zeta,\kappa) = \sum_{i=1}^{\infty}\sum_{k=1}^{i} \beta_{ik}F(\zeta_k,\kappa_k,\omega(\zeta_k,\kappa_k),\partial_\zeta\omega(\zeta_k,\kappa_k))\overline{\Psi}_i(\zeta,\kappa). \tag{3.5}$$

Proof. $\{\Psi_i(\zeta,\kappa)\}_{i=1}^{\infty}$ is a complete system of $W_2^{(2,2)}(\Delta)$. Therefore, it can be written

$$\begin{aligned}
\omega(\zeta,\kappa) &= \sum_{i=1}^{\infty}\langle \omega(\zeta,\kappa), \overline{\Psi}_i(\zeta,\kappa)\rangle_{W_2^{(2,2)}}\overline{\Psi}_i(\zeta,\kappa) = \sum_{i=1}^{\infty}\sum_{k=1}^{i}\beta_{ik}\langle \omega(\zeta,\kappa), \Psi_k(\zeta,\kappa)\rangle_{W_2^{(2,2)}}\overline{\Psi}_i(\zeta,\kappa) \\
&= \sum_{i=1}^{\infty}\sum_{k=1}^{i}\beta_{ik}\langle \omega(\zeta,\kappa), L^*\Phi_k(\zeta,\kappa)\rangle_{W_2^{(2,2)}}\overline{\Psi}_i(\zeta,\kappa) = \sum_{i=1}^{\infty}\sum_{k=1}^{i}\beta_{ik}\langle L\omega(\zeta,\kappa), \Phi_k(\zeta,\kappa)\rangle_{W_2^{(1,1)}}\overline{\Psi}_i(\zeta,\kappa) \\
&= \sum_{i=1}^{\infty}\sum_{k=1}^{i}\beta_{ik}\langle L\omega(\zeta,\kappa), \tilde{T}_{(\zeta_k,\kappa_k)}(\zeta,\kappa)\rangle_{W_2^{(1,1)}}\overline{\Psi}_i(\zeta,\kappa) = \sum_{i=1}^{\infty}\sum_{k=1}^{i}\beta_{ik}L\omega(\zeta_k,\kappa_k)\overline{\Psi}_i(\zeta,\kappa) \\
&= \sum_{i=1}^{\infty}\sum_{k=1}^{i}\beta_{ik}F(\zeta_k,\kappa_k,\omega(\zeta_k,\kappa_k),\partial_\zeta\omega(\zeta_k,\kappa_k))\overline{\Psi}_i(\zeta,\kappa).
\end{aligned} \tag{3.6}$$

The proof is completed.
When finite n-terms are taken in Eq.(3.6), the approximate solution $\omega_n(\zeta,\kappa)$ is expressed as follows:

$$\omega_n(\zeta,\kappa) = \sum_{i=1}^{n}\sum_{k=1}^{i}\beta_{ik}F(\zeta_k,\kappa_k,\omega(\zeta_k,\kappa_k),\partial_\zeta\omega(\zeta_k,\kappa_k))\overline{\Psi}_i(\zeta,\kappa).$$

The convergence of approximate solution will be presented in the next section.

4. Convergence Analysis

Here, it will be shown that the iterative approximate solution is uniformly convergent. Taking A_i as:

$$A_i = \sum_{k=1}^{i}\beta_{ik}F(\zeta_k,\kappa_k,\omega(\zeta_k,\kappa_k),\partial_\zeta\omega(\zeta_k,\kappa_k)),$$

then Eq.(3.5) can be written as

$$(\zeta,\kappa) = \sum_{i=1}^{\infty}A_i\overline{\Psi}_i(\zeta,\kappa).$$

Now from the initial conditions of Eq. (3.2), if taking $(\zeta_1,\kappa_1) = 0$, $\omega(\zeta_1,\kappa_1)$ can be calculated. When $\omega_0(\zeta_1,\kappa_1) = \omega(\zeta_1,\kappa_1)$ is taked, then the n-term approximation of $\omega(\zeta,\kappa)$ can be given as follow:

$$\omega_n(\zeta,\kappa) = \sum_{i=1}^{n}B_i\overline{\Psi}_i(\zeta,\kappa), \tag{4.1}$$

here

$$B_i = \sum_{k=1}^{i}\beta_{ik}F(\zeta_k,\kappa_k,\omega_{k-1}(\zeta_k,\kappa_k),\partial_\zeta\omega_{k-1}(\zeta_k,\kappa_k)). \tag{4.2}$$

Now, the uniform convergence of the approximate solution $\omega_n(\zeta,\kappa)$ will be shown. Therefore the following lemma should be given.

Lemma 4.1. *If $F(\zeta,\kappa,\omega(\zeta,\kappa),\omega_\zeta(\zeta,\kappa))$ is continuous and $\omega_n \to \hat{\omega}$ for $(\zeta_n,\kappa_n)\to(t,x)$, then*

$$F(\zeta_n,\kappa_n,\omega_{n-1}(\zeta_n,\kappa_n),\partial_\zeta\omega_{n-1}(\zeta_n,\kappa_n)) \to F(t,x,\hat{\omega}(t,x),\partial_\zeta\hat{\omega}(t,x)).$$

Proof. Since

$$\begin{aligned}|\omega_{n-1}(\zeta_n,\kappa_n)-\hat{\omega}(t,x)| &= |\omega_{n-1}(\zeta_n,\kappa_n)-\omega_{n-1}(t,x)+\omega_{n-1}(t,x)-\hat{\omega}(t,x)|\\ &\le |\omega_{n-1}(\zeta_n,\kappa_n)-\omega_{n-1}(t,x)|+|\omega_{n-1}(t,x)-\hat{\omega}(t,x)|.\end{aligned}$$

By using the reproducing kernel feature, it can be said that

$$\omega_{n-1}(\zeta_n,\kappa_n)=\langle\omega_{n-1}(\zeta,\kappa),T_{(\zeta_n,\kappa_n)}(\zeta,\kappa)\rangle_{W_2^{(2,2)}},\quad \omega_{n-1}(t,x)=\langle\omega_{n-1}(\zeta,\kappa),T_{(t,x)}(\zeta,\kappa)\rangle_{W_2^{(2,2)}}.$$

It follows that

$$|\omega_{n-1}(\zeta_n,\kappa_n)-\omega_{n-1}(t,x)|=|\langle\omega_{n-1}(\zeta,\kappa),T_{(\zeta_n,\kappa_n)}(\zeta,\kappa)-T_{(t,x)}(\zeta,\kappa)\rangle|.$$

It is known that there exists a constant M from the convergence of $\omega_{n-1}(\zeta,\kappa)$, such that

$$\|\omega_{n-1}(\zeta,\kappa)\|_{W_2^{(2,2)}} \le M\|\hat{\omega}(t,x)\|_{W_2^{(2,2)}},\ \text{as } n\ge M.$$

Also, it can be proven that

$$\|T_{(\zeta_n,\kappa_n)}(\zeta,\kappa)-T_{(t,x)}(\zeta,\kappa)\|_{W_2^{(2,2)}}\to 0,\ \text{for } n\to\infty$$

by using Theorem 2.2. So,

$$\omega_{n-1}(\zeta_n,\kappa_n)\to\hat{\omega}(t,x),\ \text{as } (\zeta_n,\kappa_n)\to(t,x).$$

Similarly, the following expression can be written

$$\partial_\zeta\omega_{n-1}(\zeta_n,\kappa_n)\to\partial_\zeta\hat{\omega}(t,x),\ \text{as } (\zeta_n,\kappa_n)\to(t,x).$$

Therefore,

$$F(\zeta_n,\kappa_n,\omega_{n-1}(\zeta_n,\kappa_n),\partial_\zeta\omega_{n-1}(\zeta_n,\kappa_n)) \to F(t,x,\hat{\omega}(t,x),\partial_\zeta\hat{\omega}(t,x)).$$

So, the proof is completed.

Theorem 4.2. *Let $\{(\zeta_i,\kappa_i)\}_{i=1}^{\infty}$ be dense in Δ. Assume that $\|\omega_n\|$ is a bounded, and the Eq. (4.1) has a unique solution. Then, $\omega_n(\zeta,\kappa)\to\omega(\zeta,\kappa)$ and*

$$\omega(\zeta,\kappa)=\sum_{i=1}^{\infty}B_i\overline{\Psi}_i(\zeta,\kappa).$$

Proof. It will be shown that the convergence of $\omega_n(\zeta,\kappa)$. From the Eq. (4.1), it can be easily seen that

$$\omega_{n+1}(\zeta,\kappa)=\omega_n(\zeta,\kappa)+B_{n+1}\overline{\Psi}_{n+1}(\zeta,\kappa).$$

By using of $\{\overline{\Psi}_i\}_{i=1}^{\infty}$, the following equation can be written:

$$\|\omega_{n+1}\|^2=\|\omega_n\|^2+B_{n+1}^2=\sum_{i=1}^{n+1}B_i^2. \tag{4.3}$$

Therefore, from Eq. (4.3), it can be seen that $\|\omega_{n+1}\|>\|\omega_n\|$. By the using boundedness of $\|\omega_n\|$, it can be easily seen that $\|\omega_n\|$ is convergent. And also there exists a constant c such that

$$\sum_{i=1}^{\infty}B_i^2=c. \tag{4.4}$$

So, Eq. (4.4) shows that $\{B_i\}_{i=1}^{\infty}\in l^2$. If $m>n$, then

$$\begin{aligned}\|\omega_m-\omega_n\|^2 &= \|\omega_m-\omega_{m-1}+\omega_{m-1}-\omega_{m-2}+\cdots+\omega_{n+1}-\omega_n\|^2\\ &= \|\omega_m-\omega_{m-1}\|^2+\|\omega_{m-1}-\omega_{m-2}\|^2+\cdots+\|\omega_{n+1}-\omega_n\|^2.\end{aligned}$$

On account of

$$\|\omega_m-\omega_{m-1}\|^2=B_m^2,$$

consequently

$$\|\omega_m-\omega_n\|^2=\sum_{l=n+1}^{m}B_l^2\to 0,\ \text{as } n\to\infty.$$

From the completeness of $W_2^{(2,2)}(\Delta)$, it can be expressed that $\omega_n \to \hat{\omega}$ as $n \to \infty$. Now, it will be shown that $\hat{\omega}$ is the solution of Eq. (3.2). Taking limits in Eq. (4.1) we get

$$\hat{\omega}(\zeta,\kappa) = \sum_{i=1}^{\infty} B_i \overline{\Psi}_i(\zeta,\kappa).$$

Note that

$$(L\hat{\omega})(\zeta,\kappa) = \sum_{i=1}^{\infty} B_i L\overline{\Psi}_i(\zeta,\kappa),$$

$$\begin{aligned}(L\hat{\omega})(\zeta_l,\kappa_l) &= \sum_{i=1}^{\infty} B_i L\overline{\Psi}_i(\zeta_l,\kappa_l) = \sum_{i=1}^{\infty} B_i \langle L\overline{\Psi}_i(\zeta,\kappa), \Phi_l(\zeta,\kappa)\rangle_{W_2^{(1,1)}} \\ &= \sum_{i=1}^{\infty} B_i \langle \overline{\Psi}_i(\zeta,\kappa), L^*\Phi_l(\zeta,\kappa)\rangle_{W_2^{(2,2)}} = \sum_{i=1}^{\infty} B_i \langle \overline{\Psi}_i(\zeta,\kappa), \Psi_l(\zeta,\kappa)\rangle_{W_2^{(2,2)}}.\end{aligned}$$

Therefore,

$$\begin{aligned}\sum_{l=1}^{i} \beta_{il}(L\hat{\omega})(\zeta_l,\kappa_l) &= \sum_{i=1}^{\infty} B_i \langle \overline{\Psi}_i(\zeta,\kappa), \sum_{l=1}^{i} \beta_{il}\Psi_l(\zeta,\kappa)\rangle_{W_2^{(2,2)}} \\ &= \sum_{i=1}^{\infty} B_i \langle \overline{\Psi}_i(\zeta,\kappa), \overline{\Psi}_l(\zeta,\kappa)\rangle_{W_2^{(2,2)}} = B_l.\end{aligned}$$

From Eq. (4.2), we have

$$L\hat{\omega}(\zeta_l,\kappa_l) = F(\zeta_l,\kappa_l,\omega_{l-1}(\zeta_l,\kappa_l),\partial_\zeta\omega_{l-1}(\zeta_l,\kappa_l)).$$

Since $\{(\zeta_i,\kappa_i)\}_{i=1}^{\infty}$ is dense in Δ, there exists a subsequence $\{(\zeta_{n_j},\kappa_{n_j})\}_{j=1}^{\infty}$ such that $(\zeta_{n_j},\kappa_{n_j}) \to (t,x)$, for each $(t,x) \in \Delta$, $(j \to \infty)$. It can be expressed that

$$L\hat{\omega}(\zeta_{n_j},\kappa_{n_j}) = F(\zeta_{n_j},\kappa_{n_j},\omega_{n_{j-1}}(\zeta_{n_j},\kappa_{n_j}),\partial_\zeta\omega_{n_{j-1}}(\zeta_{n_j},\kappa_{n_j})).$$

Using Lemma 4.1 and the continuity of F, it can be written that

$$(L\hat{\omega})(t,x) = F(t,x,\hat{\omega}(t,x),\partial_\zeta\hat{\omega}(t,x)), \text{ for } j \to \infty. \tag{4.5}$$

The Eq. (4.5) demonstrates that $\hat{\omega}(\zeta,\kappa)$ provides Eq. (3.2). The proof is completed.

5. Numerical Outcomes

In this section, the iterative reproducing kernel method is tested on two nonlinear advection equations. When calculating numerical results, $\zeta_i = \frac{i}{q}$, $i = 0,1,\ldots,q$, $\kappa_i = \frac{i}{p}$, $i = 0,1,\ldots,p$ and $n = q \times p$ are selected. The numerical results obtained for different values of p and q are shown in tables and graphs. Also, the algorithm process of the method is presented as follows.

5.1. Algorithm of method

The iterative RKM process is presented as follow:

Step 1. Choose iteration number as $n = q \times p$ discrete point in the $[0,1] \times [0,1]$.
Step 2. Enter $\Psi_i(\zeta,\kappa) = L_{(t,x)}T_{(t,x)}(\zeta,\kappa)|_{(t,x)=(\zeta_i,\kappa_i)}$.
Step 3. Attain β_{ik} orthogonalization coefficients.
Step 4. For $i = 1,2,...,n$, set $\overline{\Psi}_i(\zeta,\kappa) = \sum_{k=1}^{i} \beta_{ik}\Psi_k(\zeta,\kappa)$.
Step 5. Enter initial approximation $\omega_0(\zeta_i,\kappa_i)$.
Step 6. For $i = 1,2,...,n$, evaluate $B_i = \sum_{k=1}^{i} \beta_{ik}F(\zeta_k,\kappa_k,\omega_{k-1}(\zeta_k,\kappa_k),\partial_\zeta\omega_{k-1}(\zeta_k,\kappa_k))$.
Step 7. For $i = 1,2,...,n$, evaluate $\omega_i(\zeta,\kappa) = \sum_{k=1}^{i} B_k\overline{\Psi}_k(\zeta_k,\kappa_k)$.

5.2. Examples

Example 5.1. *The following nonlinear advection equation is considered:*

$$y_\kappa(\zeta,\kappa) + y(\zeta,\kappa)y_\zeta(\zeta,\kappa) = f(\zeta,\kappa), \quad \zeta,\kappa \in [0,1]. \tag{5.1}$$

The exact solution of Eq. (5.1) is

$$y(\zeta,\kappa) = \zeta^2(\kappa+2),$$

and the initial condition of problem is

$$y(\zeta,0)=2\zeta^2.$$

After the homogenisation of initial condition, Eq.(5.1) turns into the following form:

$$\omega_\kappa(\zeta,\kappa)+2\zeta^2\omega_\zeta(\zeta,\kappa)+4\zeta\omega(\zeta,\kappa)+\omega(\zeta,\kappa)\omega_\zeta(\zeta,\kappa)+8\zeta^3=f(\zeta,\kappa). \tag{5.2}$$

The initial condition of Eq.(5.2) is

$$\omega(\zeta,0)=0,$$

and the exact solution of Eq.(5.2) is

$$\omega(\zeta,\kappa)=\zeta^2\kappa.$$

In Eq.(5.2),

$$f(\zeta,\kappa)=2\kappa^2\zeta^3+8\kappa\zeta^3+8\zeta^3+\zeta^2.$$

The absolute error values are computed for $n=225$ in Table 5.1 and $n=400$ in Table 5.2. The graphics of approximate solution, absolute error and exact solution are presented in Figure 1 for $n=400$ $(q=p=20)$.

ζ/κ	0.1	0.2	0.3	0.4	0.5	0.6	0.7	0.8	0.9
0.1	6.96×10^{-6}	4.26×10^{-6}	6.39×10^{-6}	8.48×10^{-6}	1.02×10^{-5}	1.14×10^{-5}	1.21×10^{-5}	1.71×10^{-5}	5.42×10^{-5}
0.2	1.30×10^{-5}	6.77×10^{-6}	9.18×10^{-6}	1.09×10^{-5}	1.19×10^{-5}	1.05×10^{-5}	7.08×10^{-6}	1.48×10^{-5}	1.03×10^{-4}
0.3	1.90×10^{-5}	7.81×10^{-6}	1.03×10^{-5}	1.08×10^{-5}	1.05×10^{-5}	5.78×10^{-6}	3.51×10^{-6}	4.59×10^{-6}	1.42×10^{-4}
0.4	2.48×10^{-5}	8.25×10^{-6}	1.19×10^{-5}	1.15×10^{-5}	1.03×10^{-5}	2.90×10^{-6}	1.16×10^{-5}	2.95×10^{-6}	1.84×10^{-4}
0.5	3.05×10^{-5}	7.68×10^{-6}	1.32×10^{-5}	1.23×10^{-5}	1.03×10^{-5}	4.60×10^{-7}	1.91×10^{-5}	9.59×10^{-6}	2.26×10^{-4}
0.6	3.60×10^{-5}	6.03×10^{-6}	1.42×10^{-5}	1.30×10^{-5}	1.02×10^{-5}	2.08×10^{-6}	2.65×10^{-5}	1.61×10^{-5}	2.69×10^{-4}
0.7	4.13×10^{-5}	3.18×10^{-6}	1.45×10^{-5}	1.33×10^{-5}	9.83×10^{-6}	4.95×10^{-6}	3.43×10^{-5}	2.29×10^{-5}	3.12×10^{-4}
0.8	4.62×10^{-5}	6.95×10^{-7}	1.42×10^{-5}	1.34×10^{-5}	9.36×10^{-6}	7.82×10^{-6}	4.20×10^{-5}	2.97×10^{-5}	3.54×10^{-4}
0.9	5.07×10^{-5}	5.55×10^{-6}	1.32×10^{-5}	1.32×10^{-5}	8.87×10^{-6}	1.06×10^{-5}	4.96×10^{-5}	3.63×10^{-5}	3.97×10^{-4}

Table 5.1: The absolute error values of Example 5.1 for $p=15$ and $q=15$.

ζ/κ	0.1	0.2	0.3	0.4	0.5	0.6	0.7	0.8	0.9
0.1	7.56×10^{-7}	1.72×10^{-6}	2.45×10^{-6}	3.23×10^{-6}	4.03×10^{-6}	4.51×10^{-6}	4.07×10^{-6}	4.88×10^{-6}	1.85×10^{-5}
0.2	1.59×10^{-6}	3.06×10^{-6}	3.52×10^{-6}	4.13×10^{-6}	4.80×10^{-6}	4.55×10^{-6}	1.44×10^{-6}	6.04×10^{-7}	3.15×10^{-5}
0.3	1.93×10^{-6}	4.09×10^{-6}	4.04×10^{-6}	4.37×10^{-6}	4.90×10^{-6}	3.98×10^{-6}	1.95×10^{-6}	5.13×10^{-6}	4.18×10^{-5}
0.4	1.85×10^{-6}	5.02×10^{-6}	4.39×10^{-6}	4.47×10^{-6}	4.99×10^{-6}	3.56×10^{-6}	5.03×10^{-6}	1.05×10^{-5}	5.23×10^{-5}
0.5	1.38×10^{-6}	5.83×10^{-6}	4.65×10^{-6}	4.46×10^{-6}	5.04×10^{-6}	3.19×10^{-6}	7.95×10^{-6}	1.56×10^{-5}	6.32×10^{-5}
0.6	5.51×10^{-7}	6.48×10^{-6}	4.82×10^{-6}	4.33×10^{-6}	5.00×10^{-6}	2.79×10^{-6}	1.08×10^{-5}	2.06×10^{-5}	7.42×10^{-5}
0.7	6.02×10^{-7}	6.90×10^{-6}	4.93×10^{-6}	4.10×10^{-6}	4.87×10^{-6}	2.33×10^{-6}	1.37×10^{-5}	2.55×10^{-5}	8.52×10^{-5}
0.8	2.04×10^{-6}	7.06×10^{-6}	4.99×10^{-6}	3.78×10^{-6}	4.64×10^{-6}	1.78×10^{-6}	1.67×10^{-5}	3.06×10^{-5}	9.62×10^{-5}
0.9	3.71×10^{-6}	6.89×10^{-6}	4.99×10^{-6}	3.40×10^{-6}	4.32×10^{-6}	1.16×10^{-6}	1.97×10^{-5}	3.56×10^{-5}	1.07×10^{-4}

Table 5.2: The absolute error values of Example 5.1 for $p=20$ and $q=20$.

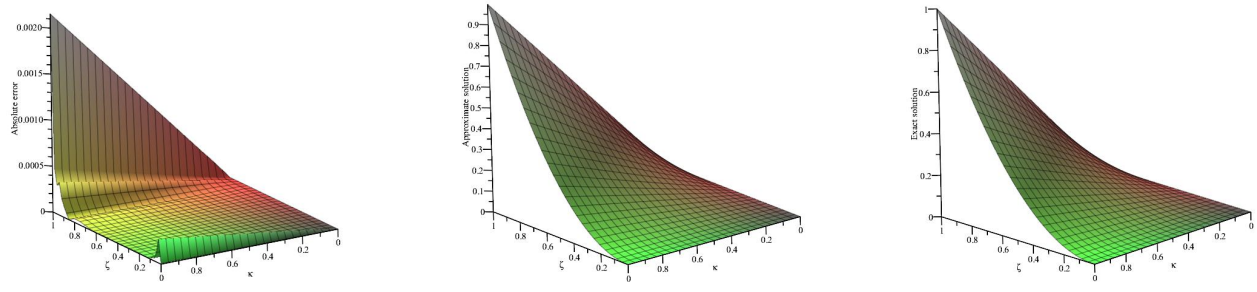

Figure 5.1: The graphs of the absolute error, approximate solution and exact solution for $p=20$ and $q=20$ in Example 5.1.

Example 5.2. *The following nonlinear advection equation is considered:*

$$y_\kappa(\zeta,\kappa)+y(\zeta,\kappa)y_\zeta(\zeta,\kappa)=f(\zeta,\kappa),\ 0\le\zeta,\kappa\le 1. \tag{5.3}$$

The exact solution of problem is

$$y(\zeta,\kappa)=\zeta(\frac{\kappa^2}{2}+1),$$

and the initial condition of problem is

$$y(\zeta,0)=\zeta.$$

After the homogenisation of initial condition, Eq.(5.3) turns into the following form:

$$\omega_\kappa(\zeta,\kappa)+\zeta\omega_\zeta(\zeta,\kappa)+\omega(\zeta,\kappa)+\omega_\zeta(\zeta,\kappa)\omega(\zeta,\kappa)+\zeta=f(\zeta,\kappa). \tag{5.4}$$

The initial condition of Eq. (5.4) is

$$\omega(\zeta,0)=0,$$

and the exact solution of Eq. (5.4) is

$$\omega(\zeta,\kappa)=\zeta\frac{\kappa^2}{2}.$$

In Eq. (5.4),

$$f(\zeta,\kappa)=\kappa\zeta+\kappa^2\zeta+\frac{1}{4}\zeta\kappa^4+\zeta.$$

The absolute error values are computed for $n=225$ in Table 5.3 and $n=400$ in Table 5.4. The graphics of approximate solution, absolute error and exact solution are presented in Figure 2 for $n=400$ $(q=p=20)$.

ζ/κ	0.1	0.2	0.3	0.4	0.5	0.6	0.7	0.8	0.9
0.1	6.03×10^{-6}	2.73×10^{-6}	3.36×10^{-6}	4.54×10^{-6}	5.75×10^{-6}	6.91×10^{-6}	8.06×10^{-6}	9.21×10^{-6}	1.03×10^{-5}
0.2	1.16×10^{-5}	6.49×10^{-6}	6.72×10^{-6}	8.93×10^{-6}	1.14×10^{-5}	1.38×10^{-5}	1.61×10^{-5}	1.84×10^{-5}	2.07×10^{-5}
0.3	1.65×10^{-5}	1.15×10^{-5}	1.05×10^{-5}	1.35×10^{-5}	1.74×10^{-5}	2.12×10^{-5}	2.48×10^{-5}	2.83×10^{-5}	3.18×10^{-5}
0.4	2.01×10^{-5}	1.79×10^{-5}	1.49×10^{-5}	1.81×10^{-5}	2.34×10^{-5}	2.87×10^{-5}	3.37×10^{-5}	3.85×10^{-5}	4.32×10^{-5}
0.5	2.20×10^{-5}	2.57×10^{-5}	2.06×10^{-5}	2.35×10^{-5}	3.02×10^{-5}	3.71×10^{-5}	4.37×10^{-5}	5.00×10^{-5}	5.62×10^{-5}
0.6	2.16×10^{-5}	3.45×10^{-5}	2.75×10^{-5}	2.96×10^{-5}	3.73×10^{-5}	4.59×10^{-5}	5.43×10^{-5}	6.22×10^{-5}	7.00×10^{-5}
0.7	1.84×10^{-5}	4.47×10^{-5}	3.66×10^{-5}	3.76×10^{-5}	4.61×10^{-5}	5.66×10^{-5}	6.70×10^{-5}	7.70×10^{-5}	8.67×10^{-5}
0.8	1.14×10^{-5}	5.54×10^{-5}	4.76×10^{-5}	4.75×10^{-5}	5.65×10^{-5}	6.87×10^{-5}	8.13×10^{-5}	9.35×10^{-5}	1.05×10^{-4}
0.9	2.59×10^{-7}	6.69×10^{-5}	6.15×10^{-5}	6.08×10^{-5}	7.06×10^{-5}	8.46×10^{-5}	9.97×10^{-5}	1.14×10^{-4}	1.29×10^{-4}

Table 5.3: The absolute error values of Example 5.2 for $p=15$ and $q=15$.

ζ/κ	0.1	0.2	0.3	0.4	0.5	0.6	0.7	0.8	0.9
0.1	9.78×10^{-7}	1.26×10^{-6}	1.82×10^{-6}	2.47×10^{-6}	3.10×10^{-6}	3.72×10^{-6}	4.33×10^{-6}	4.95×10^{-6}	5.57×10^{-6}
0.2	2.52×10^{-6}	2.71×10^{-6}	3.61×10^{-6}	4.99×10^{-6}	6.29×10^{-6}	7.54×10^{-6}	8.78×10^{-6}	1.00×10^{-5}	1.12×10^{-5}
0.3	4.42×10^{-6}	4.51×10^{-6}	5.41×10^{-6}	7.57×10^{-6}	9.60×10^{-6}	1.15×10^{-5}	1.34×10^{-5}	1.53×10^{-5}	1.72×10^{-5}
0.4	6.41×10^{-6}	6.83×10^{-6}	7.27×10^{-6}	1.02×10^{-5}	1.30×10^{-5}	1.57×10^{-5}	1.83×10^{-5}	2.09×10^{-5}	2.35×10^{-5}
0.5	8.24×10^{-6}	9.85×10^{-6}	9.36×10^{-6}	1.30×10^{-5}	1.68×10^{-5}	2.03×10^{-5}	2.36×10^{-5}	2.70×10^{-5}	3.03×10^{-5}
0.6	9.60×10^{-6}	1.37×10^{-5}	1.18×10^{-5}	1.61×10^{-5}	2.09×10^{-5}	2.53×10^{-5}	2.95×10^{-5}	3.37×10^{-5}	3.79×10^{-5}
0.7	1.01×10^{-5}	1.84×10^{-5}	1.51×10^{-5}	1.97×10^{-5}	2.56×10^{-5}	3.11×10^{-5}	3.63×10^{-5}	4.41×10^{-5}	4.67×10^{-5}
0.8	9.45×10^{-6}	2.41×10^{-5}	1.94×10^{-5}	2.41×10^{-5}	3.11×10^{-5}	3.79×10^{-5}	4.44×10^{-5}	5.07×10^{-5}	5.71×10^{-5}
0.9	7.12×10^{-6}	3.08×10^{-5}	2.52×10^{-5}	2.99×10^{-5}	3.78×10^{-5}	4.60×10^{-5}	5.41×10^{-5}	6.19×10^{-5}	6.97×10^{-5}

Table 5.4: The absolute error values of Example 5.2 for $p=20$ and $q=20$.

6. Conclusion

In this study, a numerical approach is proposed for the nonlinear advection equation. This approach is based on the reproducing kernel function obtained from special Hilbert spaces and the selection of a linear operator. The approximate solution is constructed by the basis function obtained by applying the reproducing kernel function to the selected linear operator. The convergence analysis of the proposed approach is given in detail. To demonstrate the validity of the method, the RKM is applied to two different nonlinear advection equations. The obtained results verify the effectiveness of the method. It is thought that the proposed method will contribute to the literature. The proposed method can be applied to integral differential equations with nonhomogeneous initial or boundary conditions by improving it.

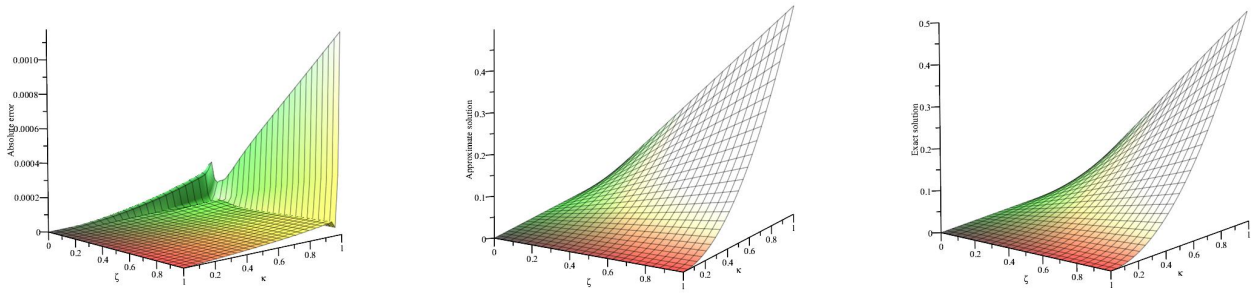

Figure 5.2: The graphs of the absolute error, approximate solution and exact solution for $p = 20$ and $q = 20$ in Example 5.2.

Article Information

Acknowledgements: The author expresses his sincere thanks to the editor and anonymous referees for their helpful comments and suggestions.

Author's contributions: The author has read and approved the final manuscript.

Conflict of interest disclosure: No potential conflict of interest was declared by the author.

Supporting/Supporting organizations: No grants were received from any public, private or non-profit organizations for this research.

Ethical approval and participant consent: It is declared that during the preparation process of this study, scientific and ethical principles were followed and all the studies benefited from are stated in the bibliography.

Plagiarism statement: This article was scanned by the plagiarism program.

References

[1] A. M. Wazwaz, *Partial Differential Equations and Solitary Waves Theory*, Springer, New York, 2009.
[2] L. I. Pitarbarg, A. G. Ostrovskii, *Advection and Diffusion in Random Media*, Springer, New York, 1997.
[3] Y. Khan, Q. Wu, *Homotopy perturbation transform method for nonlinear equations using He's polynomials*, Comput. Math. Appl., **61**(8) (2011), 1963-1967.
[4] B. B. Sanugi, D. J. Evans, *A Fourier series method for the numerical solution of the nonlinear advection problem*, Appl. Math. Lett., **1**(4) (1988), 385-389.
[5] A. M. Wazwaz, *A new approach to the nonlinear advection problem: An application of the decomposition method*, Appl. Math. Comput., **72**(2-3) (1995), 175-181.
[6] C. R. Molenkamp, *Accuracy of finite-difference methods applied to the advection equation*, J. Appl. Meteor. Climatol., **7** (1968), 160-167.
[7] Y. Khan, F. Austin, *Application of the Laplace decomposition method to nonlinear homogeneous and non-homogenous advection equations*, Zeitschrift für Naturforschung A, **65**(10) (2010), 849-853.
[8] K. S. Nisar, J. Ali, M. K. Mahmood, D. Ahmad, S. Ali, *Hybrid evolutionary padé approximation approach for numerical treatment of nonlinear partial differential equations*, Alexandria Engineering Journal, **60**(5) (2021), 4411-4421.
[9] K. N. I. Ara, Md. M. Rahaman, Md. S. Alam, *Numerical solution of advection diffusion equation using semi-discretization scheme*, Appl. Math., **12** (2021), 1236-1247.
[10] T. Cosgun, M. Sari, *A novel method to investigate nonlinear advection-diffusion processes*, J. Comput. Appl. Math., **425** (2023), 115057.
[11] A. Alkan, *Analysis of fractional advection equation with improved homotopy analysis method*, OKU Journal of The Institute of Science and Technology, **7**(3) (2024), 1215-1229.
[12] I. A. Mirza, M. S. Akram, N. A. Shah, W. Imtiaz, J. D. Chung, *Analytical solutions to the advection-diffusion equation with Atangana-Baleanu time-fractional derivative and a concentrated loading*, Alexandria Engineering Journal, **60**(1) (2021), 1199-1208.
[13] F. Mirzaee, K. Sayevand, S. Rezaei, N. Samadyar, *Finite difference and spline approximation for solving fractional stochastic advection-diffusion equation*, Iran. J. Sci. Technol. Trans. A Sci., **45** (2021), 607-617.
[14] S. Zaremba, *Sur le calcul numérique des fonctions demandées dans le probléme de Dirichlet et le problème hydrodynamique*, Bulletin International de l'Académie des Sciences de Cracovie, **908** (1908), 125-195.
[15] N. Aronszajn, *Theory of reproducing kernels*, Trans. Am. Math. Soc., **68** (1950), 337-404.
[16] L. Schwartz, *Sous-espaces hilbertiens d'espaces vectoriels topologiques et noyaux associés (noyaux reproduisants)*, J. Anal. Math., **13** (1964), 115-256.
[17] S. Saitoh, Y. Sawano, *Theory of Reproducing Kernels and Applications*, Springer, Singapore, 2016.
[18] O. A. Arqub, M. A. Smadi, *Atangana-Baleanu fractional approach to the solutions of Bagley-Torvik and Painlevé equations in Hilbert space*, Chaos Solitons Fractals, **117** (2018), 161-167.
[19] O. A. Arqub, *Numerical algorithm for the solutions of fractional order systems of Dirichlet function types with comparative analysis*, Fund. Inform., **166**(2) (2019), 111-137.
[20] O. A. Arqub, M. Smadi, N. Shawagfeh, *Solving Fredholm integro-differential equations using reproducing kernel Hilbert space method*, Appl. Math. Comput., **219**(17) (2013), 8938-8948.
[21] O. A. Arqub, B. Maayah, *Numerical solutions of integro differential equations of Fredholm operator type in the sense of the Atangana-Baleanu fractional operator*, Chaos Solitons Fractals, **117** (2018), 117-124.
[22] G. Akram, H. Rehman, *Numerical solution of eighth order boundary value problems in reproducing kernel space*, Numer. Algorithms, **62** (2013), 527-540.
[23] M. G., Sakar, A. Akgül, D. Baleanu, *On solutions of fractional Riccati differential equations*, Adv. Difference Equ., **39** (2017), 1-10.
[24] A. Akgül, M. Inc, A. Kilicman, D. Baleanu, *A new approach for one-dimensional sine-Gordon equation*, Adv. Difference Equ., **8** (2016), 1-20.

[25] M. Mohammadi, R. Mokhtari, *A reproducing kernel method for solving a class of nonlinear systems of PDEs*, Math. Model. Anal., **19**(2) (2014), 180-198.
[26] W. Jiang, Y. Lin, *Approximate solution of the fractional advection-dispersion equation*, Comput. Phys. Commun., **181**(3) (2010), 557-561.
[27] W. Jiang, Y. Lin, *Representation of exact solution for the time-fractional telegraph equation in the reproducing kernel space*, Commun. Nonlinear Sci. Numer. Simul., **16**(9) (2011), 3639-3645.
[28] H. Yao, *Reproducing kernel method for the solution of nonlinear hyperbolic telegraph equation with an integral condition*, Numer. Methods Partial Differential Equations, **27**(4) (2011), 867-886.
[29] Y. Lin, Y. Zhou, *Solving the reaction-diffusion equations with nonlocal boundary conditions based on reproducing kernel space*, Numer. Methods Partial Differential Equations, **25**(6) (2004), 1468-1481.
[30] O. A. Arqub, M. A. Smadi, *Numerical algorithm for solving time-fractional partial integro differential equations subject to initial and Dirichlet boundary conditions*, Numer. Methods Partial Differential Equations, **34**(5) (2018), 1577-1597.
[31] Y. Wang, M. Du, F. Tan, Z. Li, T. Nie, *Using reproducing kernel for solving a class of fractional partial differential equation with non-classical conditions*, Appl. Math. Comput., **219**(11) (2013), 5918–5925.
[32] O. A. Arqub, *Solutions of time-fractional Tricomi and Keldysh equations of Dirichlet functions types in Hilbert space*, Numer. Methods Partial Differential Equations, **34**(5) (2018), 1759-1780.
[33] M. G. Sakar, O. Saldır, A. Akgül, *A novel technique for fractional Bagley–Torvik equation*, Proc. Nat. Acad. Sci. India Sect. A, **89** (2019), 539-545.
[34] M. Mohammadi, F. S. Zafarghandi, E. Babolian, S. Jvadi, *A local reproducing kernel method accompanied by some different edge improvement techniques: Application to the Burgers' equation*, Iran. J. Sci. Technol. Trans. A Sci., **42** (2018), 857-871.
[35] D. Baleanu, A. Fernandez, *On some new properties of fractional derivatives with Mittag-Leffler kernel*, Commun. Nonlinear Sci. Numer. Simul., **59** (2018), 444-462.
[36] M. G. Cui, Y. Z. Lin, *Nonlinear Numerical Analysis in the Reproducing Kernel Space*, Nova Science Publisher, New York, 2009.
[37] M. G. Sakar, O. Saldır, F. Erdogan, *An iterative approximation for time-fractional Cahn-Allen equation with reproducing kernel method*, Comput. Appl. Math., **37** (2018), 5951-5964.
[38] M. G. Sakar, O. Saldır, A. Akgül, *Numerical solution of fractional Bratu type equations with Legendre reproducing kernel method*, Int. J. Appl. Comput. Math., **4**(126) (2018), 1-14.